Kinetics and Mechanisms of Formation and Reactivity of Non-heme Iron Oxygen Intermediates

Sergey V. Kryatov and Elena V. Rybak-Akimova*

Department of Chemistry, Tufts University, Medford, Massachusetts 02155

Siegfried Schindler*

Institut für Anorganische und Analytische Chemie, Justus-Liebig-Universität Giessen, Heinrich-Buff-Ring 58, 35392 Giessen, Germany

Received October 6, 2004

Contents

* To whom correspondence should be addressed. E-mail: elena.rybak-akimova@tufts.edu (E.V.R.-A.); siegfried.schindler@anorg.chemie.uni-giessen.de (S.S.).

1. Introduction

Understanding the mechanisms of dioxygen activation at the metal centers is important for unraveling the mechanisms of metal-containing oxidases and oxygenases, synthesizing new selective oxidation catalysts and new drugs analogous to bleomycin, and suppressing free radical pathways of oxidative damage in biological systems. Dioxygen and, to a lesser extent, hydrogen peroxide are ideal oxidants for the chemical industry, because they are readily available and environmentally clean. While selective activation of these small molecules still represents a challenge for the chemists, nature developed numerous metalloprotein systems for the utilization of dioxygen. The

10.1021/cr030709z CCC: $53.50
Published on Web 05/21/2005

Sergey V. Kryatov was born in Kiev region (Ukraine) in 1969. He became interested in chemistry early, was a winner of the Ukraine and USSR Chemistry Olympiads during 1983–86, and in 1986 won a silver medal at the 18th International Chemistry Olympiad in Leiden (The Netherlands). He received a Diploma in Chemistry (M.S.) from Kiev State University in 1991 and his Ph.D. from the Institute of Physical Chemistry of the Ukrainian Academy of Sciences in 1997 for a work on mixed-ligand complex formation from solid metal complexes and gaseous ligands and the application of such reactions in sensors (under the guidance of Lev I. Budarin and Vitaliy V. Pavlishchuk). In 1998 he joined the group of Elena V. Rybak-Akimova at Tufts University and studied kinetics and mechanisms of small molecule binding and activation by metal complexes in solution.

Elena V. Rybak-Akimova was born and grew up in Kiev, Ukraine. She received her M.S. in Chemistry from Kiev State University (1983) and her Ph.D. in Bioinorganic Chemistry from the Institute of Physical Chemistry of the Ukrainian Academy of Sciences (1987), working with transition metal macrocyclic complexes under the guidance of Konstantin B. Yatsimirskii. She then worked as a staff scientist at the Institute of Physical Chemistry, investigating oscillating chemical reactions and membrane transport of transition metals, and later, she spent several enjoyable and productive years (1993–1997) at the University of Kansas as a postdoctoral associate with Daryle H. Busch, studying synthetic oxygen carriers and magnetically coupled polynuclear complexes. In 1997, she joined the faculty of Tufts University, where she is currently an Associate Professor. Her research interests are in coordination, bioinorganic, and supramolecular chemistry. Current projects focus on understanding the mechanisms of small molecule (O_2, N_2) activation with biomimetic transition metal complexes, and designing selective metal-containing receptors, reagents, and catalysts.

major role in dioxygen transport and activation in biology is played by proteins containing copper, heme iron, and non-heme iron centers.[1,2] Understanding of these metalloproteins was facilitated by the structural, spectroscopic, and mechanistic investigations of synthetic inorganic model complexes. A recent special issue of *Chemical Reviews* (February 2004) on biomimetic inorganic chemistry provided excellent reviews on the dioxygen activation by synthetic model complexes.[3−7]

Siegfried Schindler was born in Toledo, Ohio, in 1959 and grew up in Germany near Frankfurt, Main. He studied chemistry at the Technical University in Darmstadt and then did graduate work with Professor Horst Elias. Following a postdoctoral appointment with Dr. Carol Creutz at Brookhaven National Laboratory, New York, he began his Habilitation in the group of Professor Rudi van Eldik at the Private University of Witten/Herdecke, Germany, in 1993. In 1994 he moved to the University of Erlangen-Nürnberg, Germany, where he completed his Habilitation in 1997. After visiting professorships at the University of Southern Denmark, Odense, in 1997 and the University of Vienna, Austria, in 1999, he had a temporary position as Professor at the University of Erlangen-Nürnberg till 2003. He then joined the Justus-Liebig-University in Giessen, where he is currently a Professor of Inorganic Chemistry. His research interests focus on the mechanisms (kinetics) of dioxygen activation of copper and iron complexes and the design and synthesis of model complexes that mimic the function of copper and iron enzymes, leading to new oxidation catalysts for substrate oxidation with air.

For a complete understanding of dioxygen binding at the metal centers and the subsequent reactions of metal−dioxygen adducts, it is necessary to investigate the mechanisms of these reactions by detailed kinetic measurements. Compared to the cases of the copper systems[5,6,8−14] and heme iron systems,[15−19] there has been much less knowledge available on the kinetics of the reactions of dioxygen with non-heme iron complexes until recently. The main purpose of this review is to summarize the data on the kinetic and mechanistic aspects of dioxygen binding and activation with non-heme iron model complexes published within the past decade. Several excellent reviews of earlier literature are available.[20−22] Various aspects of non-heme synthetic iron model complexes (their geometric and electronic structure, spectroscopy, and, to a lesser extent, reactivity with oxidants and substrates) have been reviewed recently[3,4,23−30] and will not be covered in detail in the current article. The structural, electronic, and spectroscopic properties will only be considered in order to illustrate their impact on the rates and mechanisms of dioxygen binding and activation.

The reactions between non-heme iron(II) complexes and dioxygen that generate observable iron−oxygen intermediates are of primary interest for this review (iron−oxygen intermediates here imply iron complexes with dioxygen, superoxide, and peroxide, and also high-valent iron complexes with oxo and hydroxo ligands derived from the dioxygen species). The mechanisms and kinetics of these reactions are described, and the available kinetic parameters are tabulated. In some cases, reactions with "O_2 surrogates" (CO, NO) provide additional information on

the mechanisms of oxygenation; these reactions are briefly considered, as appropriate. The general aspects of metal−dioxygen interaction have been described before[18,21,31−33] and will not be covered here. Next, the "peroxide shunt" pathway of generating iron−oxygen intermediates (the reaction of iron(III) complexes with hydrogen peroxide) will be considered. Other oxygen donors (superoxide, alkyl hydroperoxides, peroxoacids, iodosobenzene, etc.), which are often used in generating iron−oxygen intermediates, will only be treated if kinetic or mechanistic information on their reactions with iron complexes is available. Finally, the reactivity of iron−oxygen intermediates will be discussed. This includes transformation of superoxo or peroxo intermediates into high-valent species, self-decomposition of the intermediates, and their reactions with substrates. Kinetic data on the reactivity of synthetic non-heme iron−oxygen intermediates are limited.

Catalytic oxidations with iron complexes will not be covered in this review, unless iron−oxygen intermediates were directly observed or there is other strong evidence of their active participation. In the synthetic catalytic systems, oxygen-centered radicals (such as •OH) were more often identified as the active oxidizing species, and the degree of involvement of iron−oxygen intermediates is still under debate.[34−46] This situation is in contrast to the identification of iron(III)−peroxo and iron(IV)−oxo intermediates in the cycles of non-heme dioxygen-activating enzymes.[23,24,29,47−53]

Dioxygen-binding and -activating biomolecules with non-heme iron centers include a unique glycopeptide antibiotic bleomycin and numerous proteins, which are generally grouped into two large families: mononuclear (having only one iron at the active site) and dinuclear (having two proximate irons connected by bridging ligands at the active site). Bleomycin and non-heme iron enzymes will be briefly introduced in the next section of this review. The only non-heme iron dioxygen carrier, hemerythrin, will be considered in some detail. Then, general aspects of model chemistry will be introduced, followed by detailed sections on the kinetics and mechanisms of dioxygen binding and activation with mono- and dinuclear non-heme iron complexes and related reactions. The last section of this review is devoted to issues of kinetic methodology specific for dioxygen-binding studies.

2. Dioxygen-Binding and -Activating Non-heme Iron Biocomplexes

The chemistry of non-heme iron dioxygen activation with mononuclear[3,24,29,51,52,54−56] or dinuclear[4,23,27,29,53,57−61] biocomplexes has become a very active area of research in recent years, with several reaction intermediates characterized by spectroscopic methods.[3,4,29,53] The lack of a porphyrin ligand was previously believed to create significant challenges for non-heme complexes. The investigation of metalloporphyrins was greatly facilitated by characteristic spectroscopic signatures that are sensitive to the coordination environment and oxidation state of the metal. Additionally, the electronic structure of hemes is well suited for the stabilization of high-valent

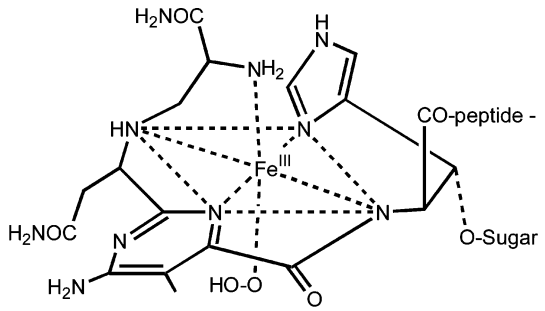

Figure 1. Iron coordination sphere in "activated bleomycin".

intermediates. Recent developments in non-heme iron chemistry, including the crystallization and spectroscopic characterization of an Fe^{IV}=O complex supported by tetramethylcyclam,[62,63] suggest greater similarities in the dioxygen activation pathways of heme- and non-heme systems, which may share many common intermediates.

The mechanisms of iron dioxygen-activating enzymes depend on the number of metal centers. The dinuclear systems, such as the extensively studied methane monooxygenase, which utilizes an Fe^{IV}_2/Fe^{III}_2 redox couple for a formally two-electron oxidation of methane with an intermediate Q of its hydroxylase component, take advantage of both iron centers in catalysis.[49,61,64] In addition to partial electron and charge delocalization over two irons that stabilize high-valent intermediates, the second metal ion can also be important for substrate coordination at the dinuclear center. The mononuclear non-heme iron complexes do not have either the porphyrin ligand or the second metal center in order to facilitate formation of reactive intermediates in dioxygen activation. Therefore, many mononuclear iron oxygenases require a reducing cofactor (pterin or α-keto acid) for dioxygen activation.[3,29] The mechanisms of mononuclear iron hydroxylases are considered in detail in a review by Abu-Omar published in this issue of *Chemical Reviews*.[47] Here, we will only mention a very important recent finding of an Fe(IV)−oxo intermediate that is kinetically competent to oxidize the substrate in the enzymatic cycle of taurine/α-ketoglutarate dioxygenase (TauD).[65,66] Another remarkable result is the crystallographic characterization of a dioxygen adduct with naphthalene dioxygenase, which revealed a side-on binding mode of the O_2 molecule coordinated to an iron active site.[67]

2.1. Iron Bleomycin

A relatively simple mononuclear system, iron bleomycin (FeBlm), attracted significant attention and inspired numerous attempts to prepare simple synthetic models of this biomolecule (Figure 1, Scheme 1). Bleomycins are a family of natural antibiotics and clinically used anticancer drugs, which are active only in the presence of transition metals, especially iron.[68−73] The dioxygen activation at the iron center in FeBlm is the key step in single- and double-strand sequence-specific DNA cleavage, which is considered to be responsible for the anticancer activity of the drug.[74] The sequence of events at the iron center in FeBlm leading to DNA cleavage (Scheme 1) includes

Scheme 1. Redox Chemistry of Iron Bleomycin

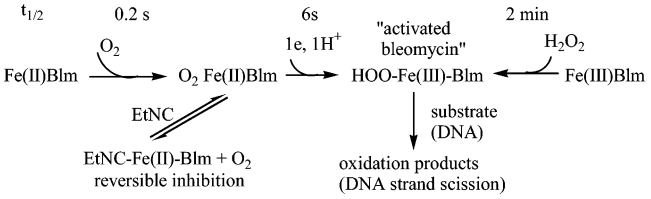

O_2 binding to the Fe(II) center, one-electron reduction of the dioxygen adduct with the formation of a so-called "activated bleomycin", and an interaction of "activated bleomycin" with the substrate (in the case of DNA cleavage, the 4′-hydrogen abstraction from the sugar occurs).[69,75] The peroxide activation of Fe(III)Blm ("peroxide shunt") is also possible. While the "activated bleomycin" was shown to be an Fe(III)−OOH hydroperoxo species,[75−78] the mechanism of its reaction with the substrates is still unknown and may involve a homo- or heterolytic O−O bond cleavage[79] or a direct reaction between the hydroperoxo intermediate and the substrate.[80] Some other features of the Fe(II)Blm chemistry resemble the reactivity of heme proteins.[81,82] The chemistry of bleomycin has been recently reviewed.[83] Many mononuclear iron model complexes resemble iron bleomycin in their ability to react directly with O_2 (starting from the +2 oxidation state of the metal) or with H_2O_2 (starting from either the +2 or +3 oxidation state of the metal), yielding peroxo intermediates. The mechanistic studies on these mononuclear iron model complexes are described in section 4.

2.2. Hemerythrin

Dinuclear iron proteins provide the only example of a non-heme iron dioxygen carrier, hemerythrin. The chemistry of hemerythrin, with particular emphasis on the kinetics of O_2 binding, is described below.

Hemerythrin is a non-heme iron-containing dioxygen carrier that features a dinuclear active site. Unlike hemoglobin and hemocyanin, which are present in numerous living organisms, hemerythrin was found in a limited number of marine organisms (marine invertebrate phyla of Sipuncula, Priapulida, Brachiopoda, and an Annelida worm, *Magelona papillicornis*).[84] Because of its low abundance, hemerythrin may be a dead end of evolution and was even called a Cinderella in the family of dioxygen carriers.[85] The beautiful chemistry of this metalloprotein, however, was extensively studied and provided an important structural, spectroscopic, and mechanistic benchmark for understanding other, more complex diiron systems. Several excellent reviews describe the biochemistry and coordination chemistry of hemerythrins in detail,[84−86] often in the context of other dioxygen carriers[60,87] or diiron proteins and their synthetic models.[21,23,29,59]

Hemerythrins (Hr) from different organisms have very similar structures (although not necessarily very high sequence homology). Hemerythins exist as stable oligomers, most often as an octamer of identical subunits of ∼13.5 kDa, although tetramers, trimers, and dimers, as well as octamers of nonidentical subunits ($\alpha_4\beta_4$), are also known.[60,84,86] The monomeric analogue of hemerythrin, myohemerythrin (MHr), was isolated from the retractor muscles of marine worms; it relates to hemerythrin as myoglobin (a dioxygen storage heme protein found in muscles) relates to hemoglobin (a dioxygen carrier).[60,84]

2.2.1. Reactions with O_2

The reaction normally carried out by hemerythrins appears to be very simple:

$$\mathrm{Hr} + \mathrm{O_2} \underset{k_{\mathrm{off}}}{\overset{k_{\mathrm{on}}}{\rightleftharpoons}} \mathrm{Hr(O_2)}, \quad K_{\mathrm{eq}} = \frac{k_{\mathrm{on}}}{k_{\mathrm{off}}} \qquad (1)$$

Everyone who ever handled iron(II) compounds, however, appreciates the challenges associated with reversible dioxygen binding. In most hemerythrins, dioxygen binding is noncooperative, and each monomeric subunit displays the same chemistry as an oligomeric protein. Although examples of weakly cooperative hemerythrins are known among the oligomeric proteins that consist of nonidentical subunits (e.g., $\alpha_4\beta_4$),[21,60] their structure, the mechanisms of dioxygen binding, and the origins of cooperativity were not firmly established and will not be discussed here.

The active site of hemerythrins, buried in a four-helix bundle, contains two nonequivalent iron(II)

Scheme 2. Dioxygen Binding at the Hemerythrin Active Site

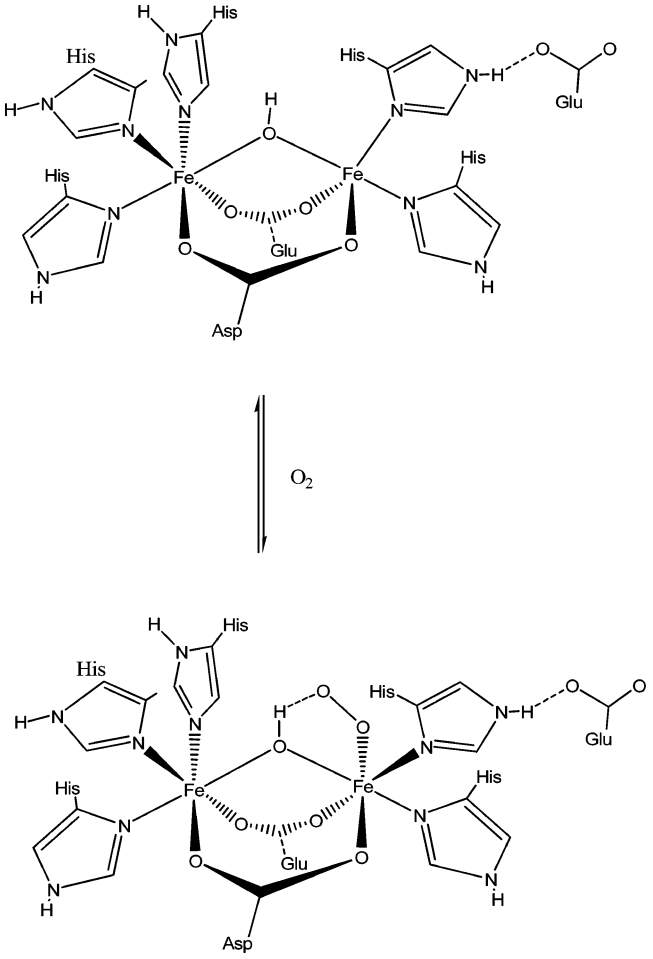

Scheme 3. Reduction Potential Diagram (vs NHE) for Octameric Hemerythrin from *T. zostericola*[a]

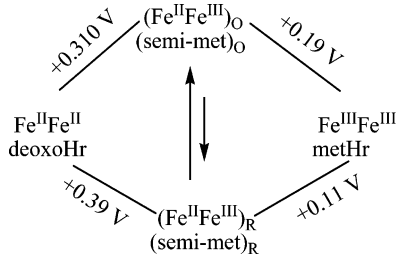

[a] $(\text{Semi-met})_O$ is a product of 1e-oxidation of deoxyHr; $(\text{semi-met})_R$ is a product of 1e-reduction of met-Hr; these two forms slowly interconvert, $K = [(\text{semi-met})_O]/[(\text{semi-met})_R] = 20$ (ref 90).

centers bridged by two carboxylates (one from aspartate and one from glutamate) and one hydroxide anion.[86] The two high-spin iron(II) centers are antiferromagnetically coupled ($J = -14$ cm^{-1}, $\mathbf{H} = -2J\mathbf{S_1S_2}$, as measured by SQUID magnetometry).[88] The coordination sphere at one of the iron(II) centers is completed to six ligands by three hystidine nitrogens; the other iron(II) center, however, is bound to only two histidines and remains coordinatively unsaturated, as established by X-ray crystallography[89] and spectroscopy[29] (Scheme 2). The histidine-rich environment of the iron centers in Hr is different from the carboxylate-rich coordination sphere of diiron oxidative enzymes and presumably helps prevent overstabilization of high oxidation states of iron, thus favoring reversible dioxygen binding (see Scheme 3 for the redox potential values).[90] The presence of only one vacant coordination site in Hr is very important for reversible, end-on O_2 binding to a single iron center, as opposed to the bridging between both iron centers in dioxygen-activating diiron enzymes (e.g., MMO, RNR-R2, or Δ9D).[29]

Another distinct structural feature of hemerythrins is the hydrophobic character of the dioxygen-binding site: except for the residues shown in Scheme 2, the binding pocket is formed by the amino acids with hydrocarbon side chains.[60,86]

The structure of oxyhemerythrin (oxyHr) was established with a number of spectroscopic techniques,[29,60,86] and one X-ray structure is also available.[89] In oxyHr, a dioxygen molecule is formally reduced to an end-on bound peroxide, while both irons are oxidized to the +3 state. Only one iron atom (initially five-coordinate) directly interacts with O_2; the second, six-coordinate iron serves as a charge reservoir. The proton from the hydroxo bridge is transferred to the noncoordinating oxygen atom of the O_2 moiety, and a resulting −OOH unit is hydrogen bonded to an oxo bridge (Scheme 4). Therefore, the reaction between Hr and O_2 proceeds through a number of elementary steps, including dioxygen diffusion through solvent and through protein toward the diiron active site, the Fe−O bond formation with a concomitant electron transfer, another one-electron transfer, and a proton transfer (or a proton-coupled electron transfer). Additionally, spin changes occur as the O_2 diradical interacts with the weakly antiferromagnetically coupled diiron(II) center, yielding a strongly antiferromagnetically coupled ($J = -77$ cm^{-1}, $\mathbf{H} = -2J\mathbf{S_1S_2}$) diiron(III)−peroxo species.[91] Detailed kinetic and mechanistic studies were performed in order to determine the mechanism of dioxygen binding to hemerythrin at the molecular level. In addition to the experimental investigations described below, recent quantum chemical and QM/MM calculations[91−93] provided additional insight into the nature of elementary steps in oxygenation of the diiron site in hemerythrin.

Scheme 4. Proposed Mechanism of Dioxygen Binding by Hemerythrin

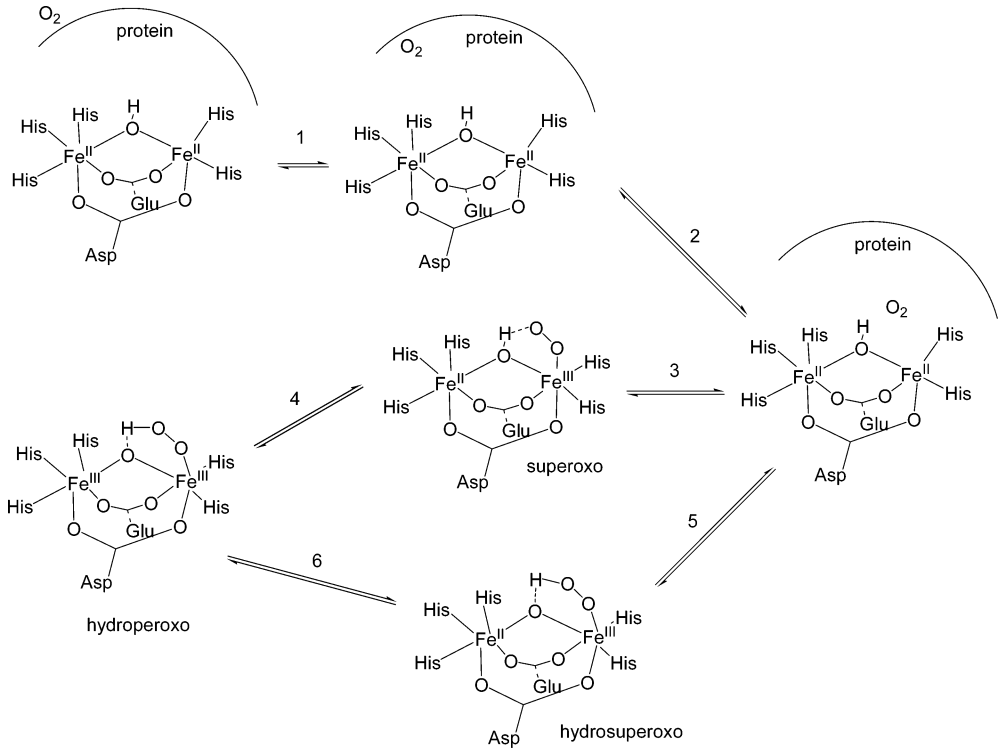

Table 1. Kinetic Parameters[a] of Dioxygen Binding to Noncooperative Hemerythrins

species[b]	k_{on}	$\Delta H^{\ddagger}_{on}$	$\Delta S^{\ddagger}_{on}$	$\Delta V^{\ddagger}_{on}$	k_{off}	$\Delta H^{\ddagger}_{off}$	$\Delta S^{\ddagger}_{off}$	$\Delta V^{\ddagger}_{off}$	K_{eq}	$t_{1/2}$[c]	ref
T. zostericola (MHr, monomer)	78[d]	16[j]	−46[j]		315	70.5	38		1.5×10^5 [h] 2.5×10^5 [i]		96
T. zostericola (Hr, octamer)	7.5[d,g]				82				1.3×10^5 [h]		96
T. zostericola (Hr, octamer)	7.6[a]			+14	40 (23 °C, 5 mPa)			+52	9.7×10^4 [i,o]		97
T. zostericola (MHr, monomer), wild-type, recombinant	1.4[f]	1.3	−122	+8.4	209	92	117	+28	$6.7(1) \times 10^3$ [i] $2.5(5) \times 10^5$ [h]	19 h[r]	101, 104
T. zostericola (MHr, monomer), L103V mutant	oxy-form is not observed due to rapid autoxidation									7 s	104
T. zostericola (MHr, monomer), L103N mutant	oxy-form is not observed due to rapid autoxidation									500 s	104
P. gouldii (synonym: *Golfingia Gouldii)* (octamer)	7.4[e]	34	4.2		51[p]	86	80		1.5×10^5 [i]		98
P. gouldii (octamer)	12[d]				43.1 (35.0 in D_2O)				2.8×10^5 [i]		99
P. gouldii (octamer), wild-type, recombinant	3.3[e]	13	−147		51	122	197		$P_{50} = 4.8$ Torr[h] ($K = 1.3 \times 10^5$ M^{-1})[n]	20 h	100
P. gouldii (octamer), L98V	2.0[e]	8.4	−176		53	101	122		$P_{50} = 5.8$ Torr[h] ($K = 1.1 \times 10^5$ M^{-1})[n]	3.7 h	100
P. gouldii (octamer), L98F	1.0[e]	8.4	−176		52	92	105		$P_{50} = 15$ Torr[h] ($K = 4.1 \times 10^5$ M^{-1})[n]	2 h	100
P. gouldii (octamer), L98Y	1.7[e]	13	−159		0.30	101	80		$P_{50} = 0.32$ Torr[h] ($K = 1.9 \times 10^6$ M^{-1})[n]	~40 h	100
P. gouldii (octamer), L98T	2.7[e]	21	−134		54	109	159		5×10^4 [i]	30 min	100
P. gouldii (octamer), L98W	0.07[e]	25	−143							0.07 s	100
P. gouldii (octamer), L98A	2.3[e]	8.4	−172							0.2 s	100
P. gouldii (octamer), L98N	1.2[e]	17	−151							0.8 s	100
P. gouldii (octamer), L98D	3.3[e]	17	−147							1.1 s	100
P. gouldii (MHr, monomer; wild-type, recombinant)	>70[e]				240 (190 in D_2O)	85.6	84		$P_{50} = 2.2$ Torr[h] ($K = 2.8 \times 10^5$ M^{-1})[n]	10 h	102
P. gouldii (MHr, monomer); L104V	>70[e]				130 (110 in D_2O)	79	59		$P_{50} = 2.6$ Torr[h] ($K = 2.4 \times 10^5$ M^{-1})[n]	3 h	102
P. gouldii (MHr, monomer); L104F	0.7[e]	17	−155		1.8 (1.6 in D_2O)	122	168		1.5 Torr[h] ($K = 4.1 \times 10^5$ M^{-1})[n]	5.5 h	102
P. gouldii (MHr, monomer); L104Y	0.36[e]	29	−113		0.58 (0.45 in D_2O)	122	143		1.2 Torr[h] ($K = 5.1 \times 10^5$ M^{-1})[n]	11 h	102
P. gouldii (MHr, monomer); L104N										1.2 s	102
P. gouldii (MHr, monomer); L104T										<2 ms	102
P. gouldii (MHr, monomer); F56Y										6 s	102
P. gouldii (MHr, monomer); W103A										<2 ms	102
P. gouldii (MHr, monomer); W103F	>70[e]				292	84	84			0.5 h	102
S. nudus (octamer)	13[d,k]	10	−75[q]		120[l]	53 (E_a)	−27[q]		1.0×10;[5 h] 1.1×10^5 [i]		95
S. nudus (octamer)	29[f,m]	18 (E_a)	−125[q]								94
S. cumanese (trimer)	11.3[d]				9.1				3.4 $Torr^{-1}$ [h] (1.8×10^5 M^{-1})[h,n] 1.24×10^6 M^{-1} [i]		106

[a] Units: k_{on}, $\times 10^{-6}$ M^{-1} s^{-1}; $\Delta H^{\ddagger}_{on}$, kJ mol^{-1}; $\Delta S^{\ddagger}_{on}$, J mol^{-1} K^{-1}; $\Delta V^{\ddagger}_{on}$, cm^3 mol^{-1}; K_{off}, s^{-1}; $\Delta H^{\ddagger}_{off}$, kJ mol^{-1}; $\Delta S^{\ddagger}_{off}$, J mol^{-1} K^{-1}; $\Delta V^{\ddagger}_{off}$, cm^3 mol^{-1}; $\Delta V^{\ddagger}_{off}$, cm^3 mol^{-1}; K_{eq}, M^{-1}. [b] *T.*, *Themiste*; *P.*, *Phascolopsis; S.*, *Siphonosoma*. [c] Autoxidation. [d] T-jump. [e] Stopped-flow. [f] Flash photolysis. [g] k_{on} increases 2−4-fold in the presence of ClO_4^-, Cl^-, Mg^{2+}, or Ca^{2+}. [h] K_{eq} determined from dioxygen titrations or spectrophotometric tonometry. [i] K_{eq} determined from k_{on}/k_{off}. [j] Calculated from ΔH (−55 kJ/mol), ΔS (−84 J K^{-1} mol^{-1}), $\Delta H^{\ddagger}_{off}$, and $\Delta S^{\ddagger}_{off}$. [k] A value of 2.6×10^7 M^{-1} s^{-1} was calculated under an assumption that both iron atoms are involved in O_2 binding (which was later shown to be incorrect); the value in the table was obtained with an assumption of O_2 binding to only one iron atom in each Hr molecule. [l] Initial fragment of kinetic curve, reaction slowed with time. [m] At higher viscosities, a second rapid, concentration-independent process (corresponding to a geminant recombination) is also observed. [n] Calculated from $P_{1/2}$ and O_2 solubility in water (1.234 mM at 760 Torr). [o] Value quoted in ref 97; calculation gives a slightly different value of 1.9×10^5 M^{-1}. [p] k_{off} increases 3-fold in the presence of ClO_4^-; k_{on} did not change. [q] Calculated from the expression $\Delta S^{\ddagger}/R = \ln(k/T) + \Delta H^{\ddagger}/RT - 23.76$. [r] Decreases in the presence of N_3^- [$k = 0.04[N_3^-]/(0.5 + [N_3]^-)$].

Despite the multistep nature of hemerythrin oxygenation, the kinetics of dioxygen binding to this diiron(II) protein is remarkably simple and quite similar to the oxygenation of other classes of dioxygen carriers (myoglobin and hemocyanin). In most studies (Table 1), one-exponential growth of the oxo-Hr was observed under excess O_2. The dioxygen binding is a fairly rapid second-order reaction (first order in Hr, and first order in O_2), with rate constants (at room temperature) ranging from 10^6 to 10^8 M^{-1} s^{-1}.

These rates are at the limit of conventional stopped-flow instruments; therefore, temperature jump and laser flash photolysis methods were also widely used in studying the kinetics of dioxygen binding to

hemerythrins. In these methods, oxyHr partially dissociates upon pulse heating (temperature jump) or the illumination with visible light (flash photolysis) and then re-forms in a relaxation process that is followed by spectrophotometry. In several cases, good agreement between the rate constants obtained by different methods was observed.[94−100] In one flash photolysis study,[101] however, oxygenation of myohemerythrin (from *Themiste zostericola)* appeared to be at least 60 times slower than dioxygen binding to the same protein measured by the T-jump technique[96] or the oxygenation of another monomeric MHr (from *Phascolopsis gouldii*) estimated by a direct stopped-flow method.[102] The reasons for this discrepancy are unclear. It is possible that, in some cases, photochemical processes other than reversible dissociation of oxyHr could occur upon irradiation with intense laser light.

Flash photolysis sometimes allowed for the observation of an additional, very rapid reaction phase corresponding to a geminant recombination-type process.[94] Geminant recombination was clearly seen in water−glycerol mixtures with high viscosity (50−200 times greater than the viscosity of water), where biphasic relaxation consisted of a concentration-dependent process essentially identical to dioxygen binding in water, and a 3 orders of magnitude faster, concentration-independent relaxation process.[94] These results indicate that high viscosity "freezes" protein dynamics and prevents the escape of the unbound O_2 molecule from the protein "cage" into solvent.

The oxygenation of hemerythrins is reversible, as required by their function as dioxygen carriers. The equilibrium constants of O_2 binding can be determined directly by spectrophotometric dioxygen titrations or by dioxygen pressure measurements (often referred to as tonometry in original publications). Alternatively, the thermodynamic equilibrium implies that the equilibrium constant of dioxygen binding equals the ratio of the rate constants for dioxygen binding to Hr and dioxygen dissociation from oxyHr (eq 1, Table 1). Under the ambient conditions of temperature and dioxygen partial pressure, the equilibrium is shifted toward dioxygen adduct formation. In this situation, one cannot accurately determine the dissociation rate constants (k_{off}) from the observed dependencies of the oxygenation rates on dioxygen concentration. For an equilibrium process, the plots of k_{obs} vs dioxygen concentration should yield straight lines with slopes equal to k_{on} and intercepts equal to k_{off} (eq 2).[103]

$$k_{obs} = k_{on}[O_2] + k_{off} \quad (2)$$

Similarly, in relaxation measurements (e.g., T-jump), straight lines are obtained when τ^{-1} is plotted vs ([Hr] + [O_2]) (eq 3).

$$\tau^{-1} = k_{on}([Hr] + [O_2]) + k_{off} \quad (3)$$

If the intercepts are small, the accuracy of k_{off} is low. Fortunately, the dioxygen dissociation rates can be measured independently. The common method utilizes dithionite, $S_2O_4^{2-}$, as a dioxygen scavenger. The solution of oxyHr is mixed with an excess $S_2O_4^{2-}$, which rapidly reacts with free O_2, preventing the association of Hr and O_2. Thus, the dissociation of HrO_2 can be conveniently followed by the stopped-flow method. When HrO_2 dissociation is the rate-limiting step, the overall reaction rate does not depend on the concentration of $S_2O_4^{2-}$. This condition should always be tested experimentally in the measurements of dioxygen dissociation rates with the help of dioxygen scavengers. The O_2-scavenging stopped-flow methodology is convenient, and dioxygen dissociation rates can usually be determined with high accuracy for natural dioxygen carriers. The dioxygen adducts studied by this method should be stable toward autoxidation (condition always met by natural dioxygen carriers selected by evolution, but not necessarily by their mutants or by the synthetic models of their active sites).

Even though kinetic data on hemerythrin oxygenation do not explicitly reveal individual reaction steps, detailed studies of activation parameters and media effects uncovered the most likely sequence of events in dioxygen binding and dissociation. Recent site-directed mutagenesis results[100,102,104] also revealed the role of a leucine amino acid residue at the entrance into the Hr active site.

The rates of O_2 binding are high, and the k_{on} values ($\sim 10^6-10^8$ M^{-1} s^{-1}) (Table 1) approach the diffusion-controlled limit ($\sim 10^9$ M^{-1} s^{-1}). Activation enthalpies for dioxygen binding to Hr are relatively small (15−20 kJ mol^{-1}), while the activation entropies are negative. The second-order kinetics of the oxygenation reaction, along with the negative values of activation entropy, suggests an associative nature of the process. The small value of the activation enthalpy was interpreted as an indication of the rate-limiting dioxygen diffusion to the diiron center (step 1 and/or 2, Scheme 4), rather than the Fe−O_2 bond formation (step 3 or 5, Scheme 4). This argument alone, however, is insufficient to discount a rate-limiting Fe−O_2 bond formation step, because similarly low (or even lower) values of activation enthalpy were found for the oxygenation of synthetic diiron complexes (see section 5 for details).

Another argument in favor of a multistep oxygenation (with diffusion being the rate-limiting process in O_2 binding, and the Fe−O bond breaking being rate-limiting in O_2 dissociation) was proposed on the basis of nonequal values of K_{eq} determined by kinetic flash photolysis measurements and by independent equilibrium constant measurement studies.[101] This result, however, should be considered with caution, as other studies yielded excellent agreement between the "kinetic" and "equilibrium" K_{eq} values (Table 1), which is expected for an equilibrium process, regardless of the exact rate-limiting steps for the forward and reverse reactions. Relatively low k_{on} values reported in this laser flash photolysis study[101] should also be noted.

Compelling evidence in favor of dioxygen diffusion through protein playing an important role in the rate-limiting oxygenation event was obtained in pressure-dependent studies.[97,101] A small, but definitely positive activation volume of dioxygen binding is incompatible with the Fe−O_2 bond formation, which should be accompanied by volume decrease. An

experimentally observed volume increase in the transition state was attributed to protein "expansion" in order to allow for the O_2 access to the active site.

To distinguish between dioxygen diffusion through solvent and dioxygen diffusion through protein, the viscosity of solutions was varied by adding ethylene glycol or other cosolvent to an aqueous buffer. In some studies, a strong viscosity dependence of k_{on} was observed in the presence of ethylene glycol, and sometimes kinetics even became biphasic.[94] This result, however, does not contradict the rate-limiting O_2 diffusion through protein, because protein dynamics may also be effected (at least in some cases) by the viscosity of the solvent and by the solvation with ethylene glycol. More recent studies demonstrated that viscosity dependence, which was observed with ethylene glycol and other small molecular weight compounds as cosolvents, disappeared in the presence of large molecular weight compounds ($M > 100$ kDa).[105] It was concluded that small molecular weight cosolvents might be involved in protein−solvent interactions and change protein dynamics. The k_{on} values were found to be independent of viscosity, thus ruling out dioxygen diffusion through solvent (which would be modulated by the viscosity of the reaction media).[105] The second, very rapid reaction phase, which was observed at high ethylene glycol concentration,[94] corresponds to the geminant recombination of a trapped O_2 molecule.

Interestingly, the oxygenation rates of an octameric form of hemerythrin were found to be an order of magnitude smaller as compared to those of an analogous monomeric MHr (Table 1). It is unclear whether dioxygen binding sites become less accessible in the octamer. The reasons for this difference in oxygenation rates were not investigated.

The rate constants of dioxygen binding to hemerythrins are independent of pH (at least in the pH interval from 6 to 9)[98,99] and of the H_2O/D_2O substitution.[99,101] This strongly implies intramolecular, post-rate-limiting proton transfer. A computational study (DFT) proposed that the initial Fe−O_2 binding event involves a proton-coupled electron-transfer yielding an end-on protonated superoxide coordinated to an Fe(III)Fe(II) center; this intermediate undergoes a second electron transfer, giving the oxyHr product (reactions 5 and 6, Scheme 4).[91] If proton tunneling is indeed coupled to the Fe−O_2 bond formation, the lack of a H/D kinetic isotope effect in the oxygenation of Hr supports the idea of the rate-limiting dioxygen diffusion through the protein matrix (as opposed to the rate-limiting Fe−O_2 bond formation, which would display an H/D isotope effect for a proton-coupled electron-transfer reaction). Another computational approach (large scale QM/MM), however, indicated the possibility of a somewhat different scenario: an incoming O_2 may initially approach the bridging hydroxo group and initiate an outer-sphere electron transfer from the six-coordinated iron site yielding a superoxo species, which then reacts with the second iron from the mixed-valent intermediate.[93] The details of the intimate mechanism of hemerythrin oxygenation are still under active investigation.

Dioxygen dissociation from oxyHr is characterized by a fairly large activation enthalpy and large positive activation entropy and activation volume. This is typical of the reactions that are limited by a bond-breaking event (in this case, the Fe−O bond breaking). A noticeable (although not very large) H/D kinetic isotope effect was observed: k_{off} for *P. gouldii* oxyHr decreases from 54.1 s^{-1} in H_2O to 35.0 s^{-1} in D_2O ($k_H/k_D = 1.55$);[99] similarly, $k_H/k_D = 1.6$ was found for *T. zostericola* oxyMHr,[101] and $k_H/k_D = 1.3$ for *P. gouldii* oxyMHr.[102] The H/D kinetic isotope effect suggests that proton transfer and/or disruption of hydrogen bonding is involved in the rate-limiting step. The dioxygen dissociation rate, however, was found to be insensitive to pH.[98,106] Therefore, proton transfer in O_2 dissociation from oxyHr is likely to be an intramolecular process.

The autoxidation of oxyhemerythrin is rather slow: the half-life of oxyHr was reported by Wilkins and co-workers to be 18.5 h at 25 °C and pH 7,[107] and very similar results were obtained in several recent studies.[100,104] The products of oxyhemerythrin autoxidation are metHr (Fe^{III}_2 form) and hydrogen peroxide. Given that the formal oxidation state of both iron centers in oxyHr is also +3 and that "coordinated O_2" in oxyHr is present as a hydroperoxide, no further electron transfer occurs in the autoxidation process, which is essentially a ligand substitution reaction:

$$Fe^{III}(\mu\text{-}O)Fe^{III}(OOH) + H_2O \rightarrow Fe^{III}(\mu\text{-}O)Fe^{III}(OH) + H_2O_2 \quad (4)$$

An alternative, proton-assisted autoxidation pathway is inconsistent with an increase in autoxidation rate as pH increases.[107] Therefore, the incoming water molecule facilitates the dissociation of hydroperoxide from oxyHr. The high kinetic stability of oxyHr can be attributed to a hydrophobic nature of the dioxygen binding pocket, which is largely inaccessible for accommodating an additional water molecule. The oxyHr autoxidation rates increase greatly in the presence of cyanate or azide anions that promote ligand substitution better than a water molecule does.[107]

For a trimeric hemerythrin from *Siphonosoma cumanese*, autoxidation is greatly facilitated by protein dissociation into monomeric subunits, which can be induced by modification of the SH groups of cysteines (k_{autox} increases from 5×10^{-5} s^{-1} to 5.6×10^{-4} s^{-1} upon increasing the concentration of SH modifier, *p*-chloromercuriphenylsulfonic acid, from 0.3 mM to 3 mM).[108] Therefore, it is likely that the physiological importance of the oligomerization of hemerythrins, which in most cases does not result in cooperativity of dioxygen binding, is related to suppressing autoxidation of their dioxygen adducts.

The role of individual amino acid residues in the dioxygen binding pocket of Hr was not studied until recently, when two groups began site-directed mutagenesis experiments on recombinant proteins (*T. zostericola*[104,109] and *P. gouldii*[100,102]). The conserved leucine residue (L98 in *P. gouldii* hemerythrin, L104 in *P. gouldii* myohemerythrin, and L103 in *T.*

zostericola myohemerythrin) was considered as a possible "gate" into the O_2-binding pocket, because of the position of this residue at the entrance into the active site and the close proximity of the alkyl group of Leu to the bound ligand (O_2 or N_3^-). The coordinated O_2 was found to be within van der Waals contact (3.6 Å) of the methyl groups of Leu.[89] As discussed above, the activation parameters of dioxygen binding (especially small activation enthalpy and positive activation volume) suggest that some protein motion occurs in the rate-limiting step. Laser flash photolysis experiments indicated the possibility of O_2 binding and release being controlled by "opening" the gate to the diiron site.[94] Experiments with hemerythrin mutants were designed in order to test this "gating" hypothesis.

The results of site-directed mutagenesis studies were perhaps unexpected, but unambiguous: the leucine residue does not interfere with the process of dioxygen binding to the diiron site in Hr. Instead, this residue protects the oxyHr from autoxidation.

Neither of the two mutants of *T. zostericola* MHr, L103V or L103N, formed an oxygenated protein; both mutants rapidly reacted with O_2, yielding metMHr.[109] Remarkably, decreasing the size of Leu-103 by just one methylene group increases the autoxidation rate of the L103V mutant by a factor of 10^5.[104] Autoxidation was shown to be an associative process, in which an oxyHr reacts with either a water molecule or small anions (such as N_3^-).[104] Therefore, it was proposed that side chains smaller than Leu will not prevent an entrance of these nucleophiles into the active site, thus dramatically increasing the autoxidation rate.[104]

A series of mutants of *P. gouldii* Hr and MHr retained the ability of a wild-type protein to form dioxygen adducts, although the autoxidation rate of mutant oxyHr or oxyMHr was much higher than that of a native Hr.[100,102] The steric effects on O_2-binding rates, which could result from substitutions of Leu98 in octameric Hr for smaller or bulkier residues, were found to be surprisingly small (Table 1). The only exception, L98W, reacted with O_2 about 50 times slower than the native protein, but the spectral changes in the course of this reaction were also different from those for the usual formation of oxyHr and suggested the formation of an unusual intermediate (possibly, a mixed-valent $Fe^{II}Fe^{III}$ species or a μ-1,2-peroxo species). Very rapid autoxidation of this mutant did not allow for detailed mechanistic studies.[100] Dioxygen binding to a monomeric MHr, which was significantly faster than oxygenation of an octameric Hr, was modulated by L104X mutations.[102] Importantly, an ~100-fold rate deceleration was observed, when bulky aromatic residues were incorporated in place of Leu. Replacing Leu with a smaller valine residue in either monomeric MHr or octameric Hr, however, had no effect on the oxygenation rates.[100,102] This implies that the Leu side chain does not shield the dioxygen-binding site in the native protein and does not function as a gate for the O_2 entrance into the binding pocket.

Steric effects of most L104X (MHr) or L98X (Hr) mutations on the dioxygen affinity of these proteins were negligible (Table 1), because changes in the O_2-binding rates were compensated by the corresponding changes in the dissociation rates.[100,102] These results are consistent with additional steric hindrance introduced at the entrance into the O_2-binding pocket rather than inside the pocket. In the former case, the "gate" installed by Leu mutations would equally hinder the O_2 access to the diiron center and the O_2 escape from the binding center. In the latter case, the bulky residues inside of the binding pocket would prevent rapid oxygenation but would also be expected to facilitate dioxygen release (due to the steric repulsion between bound O_2 and bulky substituents of the amino acid side chains).

While replacing a leucine residue with a tyrosine causes similar changes in both k_{on} and k_{off} for the monomeric MHr,[102] the same mutation selectively alters the dioxygen dissociation rate for the octameric Hr, thus increasing significantly the dioxygen affinity of the L98Y Hr.[100] This effect was attributed to a new hydrogen bond between bound O_2 and the OH group of tyrosine. The significance of the hydrogen bond breaking in dioxygen dissociation was confirmed by a large H/D kinetic isotope effect in k_{off} (~4, as compared to 1.2 for the wild-type protein). Simultaneously with the thermodynamic and kinetic stabilization of the dioxygen adduct with L98Y Hr, the stability of the oxyHr toward autoxidation also greatly increased (Table 1).[100] X-ray crystallographic data for the L98Y MetHr showed a hydrogen bond between the OH group of tyrosine and a terminal hydroxo/aqua ligand in one of the iron(III) atoms.[110] A similar geometry is possible for a dioxygen adduct, where the usual hydrogen bond between the coordinated O_2 and a bridging hydroxide is replaced by a new hydrogen bond from coordinated −OOH to Tyr−O(H). This interaction would lead to the stabilization of a dioxygen adduct.[110] Interestingly, the experimental evidence in favor of a hydrogen bonding between coordinated O_2 and an amino acid side chain also supports the proposal of this type of H-bonding being responsible for the allosteric effects and cooperativity in hemerythrin from *Lingula unguis* (a rare example of cooperative octameric hemerythrins).[21,111]

As mentioned above, leucine mutations have a profound effect on the oxyHr autoxidation rates. With the sole exception of L98Y, which is stabilized by a hydrogen bond to a coordinated O_2, hemerythrin mutants are far more susceptible to autoxidation than the wild-type proteins.[100,102,104,109] Systematic studies by Kurtz and co-workers demonstrated that, in the absence of a specific H bond to O_2, polar, hydrophilic amino acid side chains promote autoxidation of oxyHr to a greater extent than the nonpolar, hydrophobic residues do (Table 1).[100,102] Smaller side chains are less effective in protecting the oxyHr from autoxidation than native Leu, while larger residues do not change significantly the autoxidation rate.[100,102,104,109] The site-directed mutagenesis studies strongly suggest that the role of the leucine residue is to protect the hemerythrin active site from the entrance of water, which promotes autoxidation.[100,102] It is understandable that hydrophobic amino acids prevent water entrance into the active site, while hydrophilic residues allow for an easier access of

water. The polarity effect is greater than the size effect for *P. gouldii* Hr and MHr.[100,102] The size effect itself, however, is dramatic for *T. zostericola* Hr, where replacing Leu with Val causes a 10^5-fold acceleration of autoxidation.[109] Ligand substitution reactions, such as reaction of MetMHr with N_3^- (azide anation), are also facilitated by mutating Leu to a smaller Val, although to a lesser extent than was observed for autoxidation.[109] It is clear from the first mutagenesis studies on hemerythrins that the second coordination sphere is critically important in regulating dioxygen binding, release, and autoxidation of dioxygen carriers. The second coordination sphere effects are very difficult to reproduce accurately in synthetic models. It is becoming increasingly apparent that the next generation of metalloprotein models will have to mimic the surrounding of the metal−ligand core, in addition to the first coordination sphere of the metal ion(s).

2.2.2. Reactions with NO

Even though two iron(II) centers are present in hemerythrin, only one molecule of NO binds to the active site, apparently coordinating to the vacant dioxygen binding site.[112] Stopped-flow measurements of the reaction between Hr (octamer from *P. gouldii*) and NO yielded the following kinetic parameters: $k_{on} = 4.2 \times 10^6$ M^{-1} s^{-1} (23.6 °C), $\Delta H^{\ddagger}_{on} = 44.3$ kJ mol^{-1}, $\Delta S^{\ddagger}_{on} = 30$ J K^{-1} mol^{-1}. The NO binding rate constant at room temperature is only slightly lower than the oxygenation rate (Table 1). The activation enthalpy for NO binding is somewhat higher than the activation enthalpy for the oxygenation, while the activation entropy is more favorable for the former process. The similarity in the on-rates for O_2 and NO suggests that small molecule binding to Hr is not limited by an outer-sphere electron transfer, which was independently shown to follow Marcus linear free energy relationship[113] and would have depended strongly on the redox potentials of the incoming small molecule.

Oxyhemerythrin undergoes a substitution reaction with NO (eq 5).

$$Hr(O_2) + NO \rightleftharpoons Hr(NO) + O_2 \qquad (5)$$

The rate constant for this process agrees well with the dioxygen dissociation from oxyHr, suggesting a dissociative mechanism for the substitution reaction. In contrast to the cases of heme dioxygen carriers, which rapidly form nitrate and a met-form of the protein upon reacting oxymyoglobin or oxyhemoglobin with NO, no irreversible oxidation of oxyHr with NO was observed.[112]

The NO dissociation, which was studied by the stopped-flow method using several different NO scavengers, is slower than NO binding and has a much higher activation barrier ($k_{off} = 0.84$ s^{-1}, $\Delta H^{\ddagger}_{off} = 95.6$ kJ mol^{-1}, $\Delta S^{\ddagger}_{off} = 74$ J K^{-1} mol^{-1}). Similar to the cases of many other iron complexes, the Hr affinity for NO ($K_{eq} = 5.0 \times 10^6$ M^{-1}) exceeds its dioxygen affinity (Table 1) due to slower NO dissociation rates.

2.2.3. Reactions with H_2O_2

The treatment of Hr with hydrogen peroxide yields a diiron(III) form of hemerythrin that contains an OH anion coordinated to one of the iron centers (hydroxymetHr).[114] This is different from the oxidations of Hr with other oxidants, which usually produce semi-metHr ($Fe^{II}Fe^{III}$ form).[85] The reaction (investigated in detail for octameric Hr from *T. zostericola)* is pH-independent between pH 6.3 and 9.5. The reaction of Hr with H_2O_2 is much slower than oxygenation and is characterized by a higher activation barrier (reported kinetic parameters: $k = 5.5$ M^{-1} s^{-1}, $\Delta H^{\ddagger} = 31.9$ kJ mol^{-1}, $\Delta S^{\ddagger} = -12$ J K^{-1} mol^{-1}).[114] An order of magnitude higher rate of the reaction with H_2O_2 ($k = 97$ M^{-1} s^{-1}) was reported for a monomeric Hr.[115,116] Semi-metHr ($Fe^{II}Fe^{III}$) also reacts with H_2O_2, producing another $Fe^{III}Fe^{III}$ form of Hr, with the rate of the $(semi\text{-}met)_R$ oxidation ($k = 2.6$ M^{-1} s^{-1}) being somewhat slower than that of the corresponding reaction of deoxyHr ($k = 15$ M^{-1} s^{-1} for Hr from *P. gouldii*, pH 9).[84,85] The regular diiron(III) form, metHr, reacts with H_2O_2 very slowly ($k = 3 \times 10^{-3}$ M^{-1} s^{-1}), yielding an unidentified product with a visible spectrum similar to that of an oxyHr.[84,116] It is not surprising that formation of a diiron−peroxo species (oxyHr) from a diiron(III) precursor (metHr), if it occurs, is much slower than oxygenation of an Fe(II)Fe(II) protein: in the former case, the reaction would have to involve slow dissociation of an anionic ligand (usually OH^-) from coordinatively saturated iron(III), while, in the latter case, dioxygen binding at a vacant site of five-coordinated iron(II) proceeds with a very low activation barrier.

2.3. Dinuclear Non-heme Iron Enzymes

Dinuclear non-heme iron enzymes constitute an emerging family of metalloproteins that catalyze oxidation of different organic substrates with dioxygen at an active site containing two proximate iron atoms bridged by carboxylates and/or water-derived ligands (H_2O, OH^-, O^{2-}).[23,29,53,57] The best studied examples now include soluble methane monooxygenase (MMO),[49,53,61] class I ribonucleotide reductase (RNR),[50] and stearoyl-ACP Δ^9 desaturase (Δ9D).[48,117] The hydroxylase component of the MMO system catalyzes the formation of methanol from methane and O_2, the R2 subunit of RNR oxidizes a tyrosyl residue into a tyrosyl radical that is necessary for the catalytic conversion of ribonucleotides into deoxyribonuceotides, and Δ9D catalyzes the dehydrogenation of the stearoyl residue that introduces a C=C bond between positions 9 and 10 of the hydrocarbon chain. Other enzymes of this family have been discovered and are under intense investigation, e.g., toluene monoxygenase,[118] alkane ω-hydoxylase,[119] and others.

It has been proved for MMO and RNR and suggested for other non-heme diiron enzymes that high-valent ($Fe^{IV}Fe^{IV}$ or $Fe^{IV}Fe^{III}$) intermediates formed from diiron(II) precursors and dioxygen are responsible for the oxidation of organic substrates.[23,29] The diiron active sites of these enzymes are significantly more carboxylate-rich than the active site of hemerythrin (Scheme 5). Negatively charged carboxylate residues are better electron donors than neutral nitrogen atoms from histidine and stabilize high

Scheme 5. Active Sites of Non-heme Diiron Enzymes

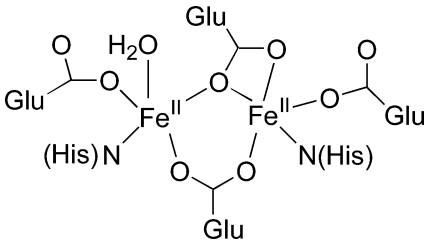

MMO

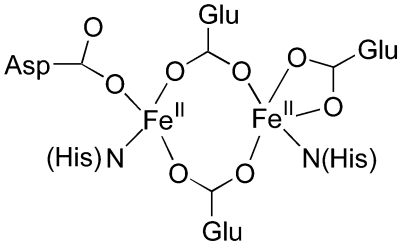

RNR

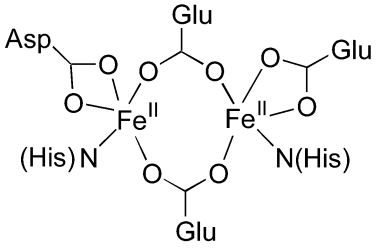

Δ^9D

oxidation states of iron, thus facilitating the redox catalysis.

Extensive recent studies are beginning to shed light on the details of substrate oxidation with the dinuclear iron enzymes.[23,29,49,61,64] Ongoing kinetic and mechanistic investigations in several laboratories are extremely helpful in developing a clear picture of dioxygen and peroxide activation at dinuclear iron sites. Particularly extensive studies were undertaken for methane monooxygenase,[120−132] ribonucleotide reductase and its mutants,[133−147] and fatty acid desaturase.[148−151] Mechanistic studies regarding the intermediate formation from ferritin,[152−154] superoxide reductase,[155,156] and toluene 4-monooxygenase[157] are also available. The mechanistic implications of these studies were extensively reviewed recently. In addition to general reviews on diiron oxygen-activating proteins,[23,29,53,57−61] more specialized review articles on the chemistry of MMO,[49,61,158] RNR,[50] and fatty acid desaturases[48,117,159] are also available. Instead of duplicating these excellent publications, we will only summarize the main features of the enzymatic mechanisms that are relevant to our discussion of synthetic model chemistry (section 5).

Scheme 6. Dioxygen-Activating Cycle of the Hydroxylase Component of Soluble MMO

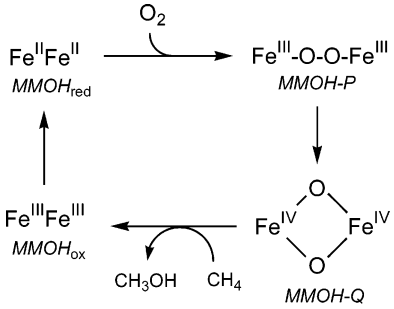

Scheme 7. Dioxygen-Activating Cycle of RNR R2

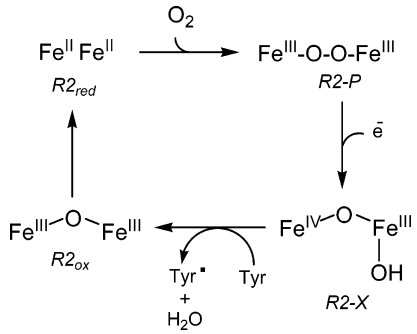

The catalytic cycles of MMO hydroxylase and the RNR R2 subunit are chosen as examples.

The diiron(II) form of MMO reacts with O_2, yielding a peroxo−diiron(III) species P as the first spectroscopically observable intermediate (Scheme 6). Although intermediate P itself does not react with a native substrate of MMO (methane), there is some evidence of its ability to transfer an oxygen atom to olefins.[129] Intermediate P undergoes further transformation into a high-valent diiron(IV) species, which most likely has an $Fe^{IV}_2(\mu\text{-}O)_2$ core.[64] This high-valent intermediate, termed intermediate Q, is a kinetically competent oxidant for methane.[125−127,129,131,132]

The catalytic cycle of the R2 RNR protein (Scheme 7)[23,29,50,53] is in many respects similar to that of MMO. A diiron(II) form of the enzyme reacts with O_2, forming a diiron(III)−peroxo intermediate, which in this case was observed clearly only for RNR mutants. For the native enzyme, this peroxo species rapidly decomposes into an observable high-valent intermediate X. Unlike intermediate Q of MMO, intermediate X contains an $Fe^{III}(\mu\text{-}O)Fe^{IV}$ core, with only one iron center being oxidized to the +4 state. Intermediate X oxidizes a phenol group from the

Scheme 8. Reactive Iron Oxygen Intermediates

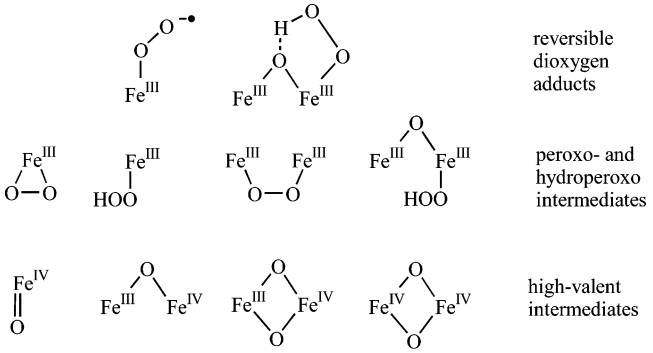

Scheme 9. Structural Formula of Ligands Supporting Iron Oxygen Intermediates

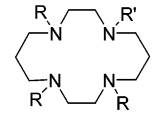

Cyclam: R = R' = H,
TMC: R = R' = Me
Cyclam-acetato: R = H, R' = CH_2CO_2H

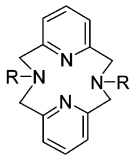

LN_4R_2

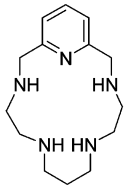

Pyan5

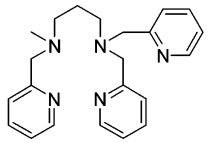

Metppn

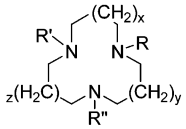

TACN, R = R' = R'' =H, x = y = z = 0
[11]aneN_3MePy_2, R = R' = CH_2-Py, R'' = CH_3, x = 0, y = z = 1
[12]aneN_3MePy_2, R = R' = CH_2-Py, R'' = CH_3, x = y = z = 1
TPC R = R' = R'' = CH_2-Py, x = y = z = 0
DPC R = R' = CH_2-Py, R'' =H, x = y = z = 0

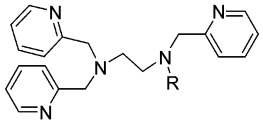

Rtpen

Metpen, R = CH_3
Ettpen, R = CH_2CH_3
Bztpen, R = $CH_2C_6H_5$

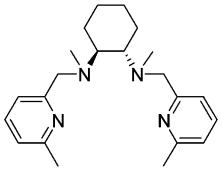

6-Me_2-bpmcn

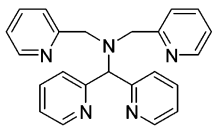

N4Py

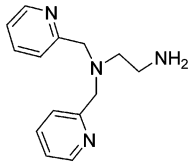

uns-penp

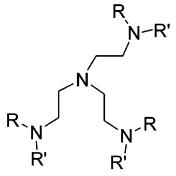

Tren, R = R' = H
Trenur, R = H, R' =$CONH^tBu$

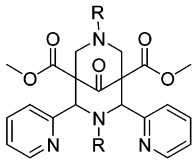

Bispidine

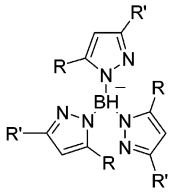

$HB(3,5\text{-}R_2pz)_3$

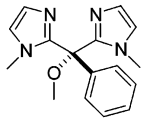

BIPhMe

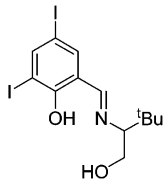

Sbl

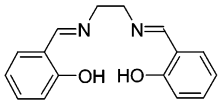

H_2Salen

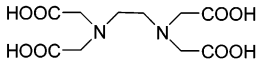

H_4EDTA

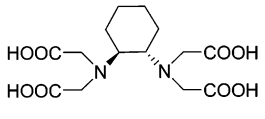

H_4CDTA

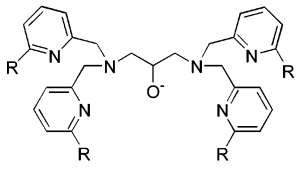

HPTP: R = H
HPTMP: R = Me

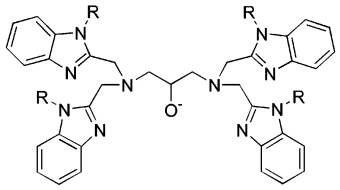

HPTB: R = H
Et-HPTB: R = Et
EtOH-HPTB: R = CH_2CH_2OH

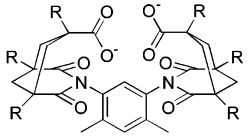

XDK: R = Me
PXDK: R = Pr
BXDK: R = CH_2Ph

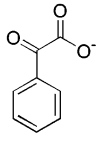

BF

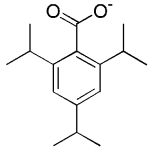

O_2CAr^{iPr3}

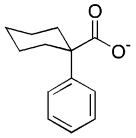

O_2CPhCy

Scheme 9 (Continued)

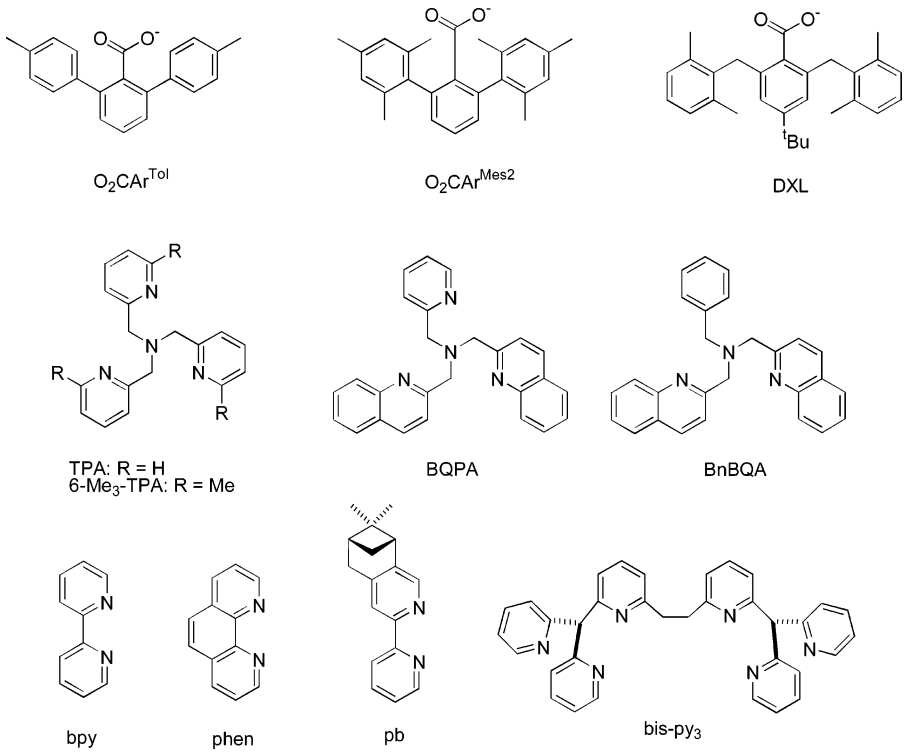

tyrosine residue, yielding a catalytically important tyrosyl radical.

The key intermediates in the catalytic cycles of the non-heme diiron enzymes include diiron(III)−peroxo complexes and high-valent iron-oxo species (either $Fe^{IV}Fe^{IV}$ or $Fe^{III}Fe^{IV}$). Understanding the mechanisms of formation and reactivity of these intermediates is an important goal of synthetic model chemistry.

3. General Aspects of Model Chemistry of Non-heme Iron Biocomplexes

Preparing coordination compounds that resemble the composition and geometry of the metal-containing active sites of biomolecules (structural modeling) or participate in reactions that are carried our by the biomolecules (functional modeling) is a challenging but rewarding task for bioinorganic chemistry. Ideally, an accurate structural model of an enzyme should also display the enzyme-like catalytic activity. Excellent recent reviews describe successes and challenges in modeling non-heme iron dioxygen-activating enzymes.[3,4,21,23,25−29,52,160−165]

The mechanistic emphasis of this review defines our focus on functional modeling of dioxygen activation chemistry. There are, however, very few synthetic complexes that model full cycles of dioxygen-activating enzymes. Therefore, "partial" functional models that mimic some reaction steps from the enzymatic cycles are also considered in the following sections. In particular, reactions that generate intermediates similar to those observed in the enzymatic processes (Scheme 8) will be included. Many of these intermediates were introduced in section 2; here, we will briefly summarize the current state of knowledge regarding the iron−oxygen intermediates in model complexes. The structural formulas of the ligands that provide nitrogen and/or oxygen donors to the iron center(s) in biomimetic complexes included in this review are summarized in Scheme 9.

Reversible dioxygen binding to mononuclear complexes yields end-on (η^1) dioxygen adducts that resemble oxygenated myoglobin. These species are usually best formulated as Fe(III)−superoxo compounds. Compared to the case of porphyrin chemistry, relatively few non-heme Fe(η^1-O_2) complexes have been characterized; they are stabilized by lacunar ligands.[166] Coordinated superoxide is well suited for reversible dioxygen binding; it does not easily oxidize substrates.

Recently, a number of mononuclear and dinuclear iron(III) peroxo complexes in synthetic model systems were spectroscopically and structurally characterized.[3,4,23,29,167−181] Typically, end-on (η^1) hydroperoxide or side-on (η^2) peroxide is coordinated to the iron(III) in the mononuclear complexes, and bridging peroxide (μ-1,2) is coordinated to both iron(III) centers in dinuclear complexes (Scheme 8). To the extent of our knowledge, the only example of an end-on dioxygen adduct in dinuclear iron systems is oxyhemerythrin (section 2.2).

The mechanistic data obtained for catalytic substrate oxidations, combined with quantum chemical calculations on iron(III) peroxo complexes,[29,52] suggest that the coordination mode of the peroxo ligand is very important for its reactivity (Scheme 8). Deprotonated side-on peroxide displays nucleophilic reactivity, while protonated end-on peroxide is activated toward the O−O bond cleavage and substrate oxidation.[182−186] The nucleophilic reactivity of side-on peroxide in heme complexes has been confirmed recently in direct stopped-flow experiments, indicating that these intermediates are responsible for

aldehyde deformylation.[187] Similarly, bridging peroxo ligand displays nucleophilic reactivity but is inactive in substrate oxidation.[178] Recent experiments, however, provided evidence of productive inner-sphere substrate oxidations, when an oxygen atom transfer from coordinated peroxide occurs to a substrate coordinated to the same active site.[188,189] It is also becoming clear that multiple intermediates are involved in catalytic oxidation of the substrates. Even with the same catalyst, different substrates may select a particular intermediate to react with. A precedent was established for methane monooxygenase, where peroxo intermediate P appears to be active in olefin epoxidation, while high-valent diamond core intermediate Q is responsible for alkane hydroxylation.[129] Thus, establishing the reactivity profiles of individual intermediates of different structure is very important for design of selective reagents and catalysts.

While iron(III)−peroxo species have been known for quite some time, ferryl(IV) in non-heme systems became readily available and well-characterized only very recently, when the X-ray structure of one Fe^{IV}=O complex was determined[62] and several similar complexes were identified spectroscopically.[63,190−194] This recent breakthrough provides access to an entirely new class of intermediates in mononuclear non-heme iron systems that will allow for meaningful comparisons with high-valent iron−oxo heme species, on one hand, and peroxo complexes in non-heme complexes, on the other hand.

The definitive proof of the existence and relative stability of the iron(IV)−oxo species energized the search for high-valent intermediates in dinuclear systems. Earlier reports on Fe(III)Fe(IV) complexes with the tripodal ligand TPA and its derivatives[195−197] were significantly expanded,[27] and the electronic structure of these species was investigated in detail by spectroscopic and computational methods.[198,199] Initial reports on the Fe(III)Fe(IV) intermediates generated from diiron(II) complexes with sterically hindered carboxylates[200] also gave rise to a family of high-valent species.[4,201] Furthermore, relatively stable valence-localized Fe(III)Fe(IV) compounds were prepared by one-electron oxidation of oxo−carboxylato-bridged diiron(III) complexes containing tridentate capping ligands (derivatives of triazacyclononane, TACN, or tris(pyrazolyl)borates, $HB(3,5\text{-}R_2pz)_3$).[202] Remarkably, nonsymmetric complexes, with one iron capped with Me_3TACN and the other iron capped with a tris(pyrazolyl)borate ligand, were also synthesized.[202] Nonsymmetric diiron(III, IV) complexes, along with similar heterodinuclear complexes, will be extremely valuable in uncovering the role of each metal center in substrate oxidation processes. An obvious (although extremely difficult) next step would be the characterization of diiron(IV) complexes similar to the intermediate Q of methane monooxygenase. One encouraging result in this area is the report of a μ-nitrido Fe(IV)Fe(IV) species.[203] A preliminary report on a bis(μ-oxo)diiron(IV) complex with an aminopyridine ligand,[204] supported by electronic structure calculations on the $Fe^{IV}_2O_2$ core,[205] suggests that dinuclear high-valent iron complexes can be trapped in relatively simple synthetic systems. Very recently, stable (μ-oxo)diiron(IV) complexes with tetraamidato N_4-macrocyclic ligands were synthesized and comprehensively characterized (including crystal structure determinations and Mössbauer spectroscopic measurements).[206]

Extensive studies on the coordination chemistry of the non-heme iron dioxygen-activating complexes led to recent discoveries of useful well-defined metal-centered oxidants. For example, iron complexes with aminopyridine ligands (BPMEN and its derivatives, TPA, and phenanthroline) were found to efficiently catalyze olefin epoxidation[207−211] and hydroxylation.[208,212−214] Interestingly, the epoxidation of olefins by H_2O_2 catalyzed by the complex $[Fe(BPMEN)(MeCN)_2]^{2+}$ was improved by the addition of acetic acid,[207] and the in situ formation of peroxoacetic acid was later inferred in this system.[209] Since peroxoacids preferentially undergo heterolytic O−O bond cleavage, high-valent iron−oxo species appear to be likely reactive intermediates in the RCO_3H-dependent epoxidations. In a related system, alkane hydroxylation products were found to depend on the spin state of iron, and different intermediates (Fe^{III}−OOH vs Fe^{V}=O) were implicated.[42] A definitive proof of the oxidizing power of high-valent iron−oxo intermediates was obtained in a recent study of the cyclohexane C−H bond oxidation with an observable, relatively stable LFe^{IV}=O species (L = N4Py and Bztpen).[193]

A dinuclear iron complex with an amidophenolate ligand promotes heterolytic bond cleavage of an alkylhydroperoxide (MPPH, 2-methyl-1-phenylprop-2-yl hydroperoxide) that was used as a mechanistic probe (homolytic and heterolytic cleavage of the O−O bond in MPPH yield distinctly different products).[215] The diiron intermediate (presumably, high-valent iron−oxo species) that results from heterolytic O−O bond cleavage is responsible for the catalytic oxidation of thioanisole and cyclohexane.[215] Similar oxygen atom transfer reactions catalyzed by a diiron−amidophenolate system were previously reported for a more potent oxygen donor (iodosobenzene).[216]

Last, but not least, the investigations of substrate oxidation with stable oxidants led to major advances in the fundamental understanding of hydrogen atom abstraction[217−219] and proton-coupled electron transfer.[220−222] Therefore, kinetic and mechanistic studies of the formation of transient iron-containing intermediates and their reactivity with substrates are timely and have high promise of yielding important mechanistic insights into dioxygen activation chemistry.

4. Kinetic and Mechanistic Studies of Mononuclear Iron Complexes

There are not too many different possibilities for a mononuclear metal dioxygen complex (Scheme 10); those are complexes that bind O_2 as an end-on superoxo or peroxo ligand, as a side-on superoxo or peroxo ligand, or as an oxo ligand (mixtures of these different types, as well as protonated forms, are known). However, the immediate reaction of dioxygen with any iron(II) complex must be the formation of a

Scheme 10

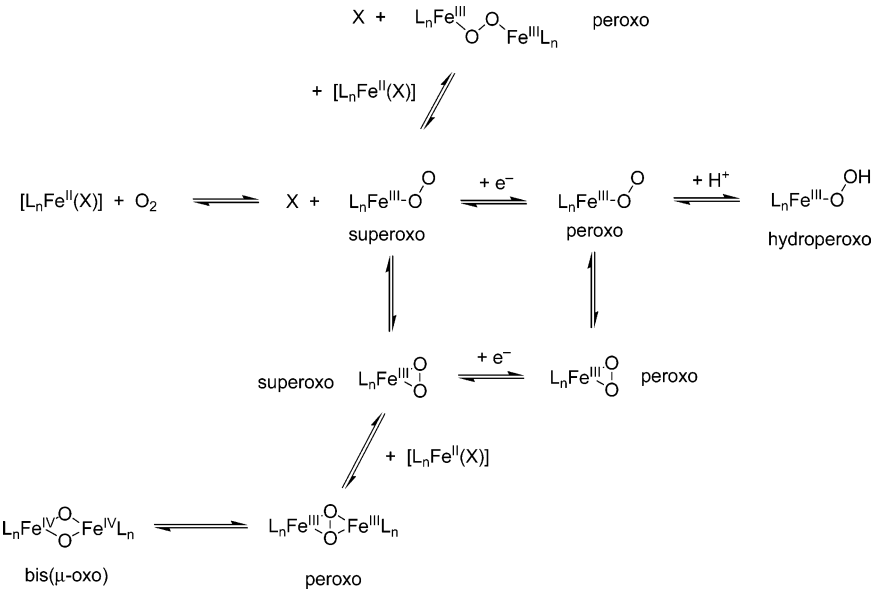

bond between one of the two oxygen atoms and the metal ion. Usually, this has the consequence that the dioxygen molecule substitutes another ligand (many times this is a solvent molecule; however, it can be an additional ligand or a ligand arm of the whole ligand) followed by an electron-transfer reaction leading to an end-on iron(III) superoxo species. An alternative pathway would be the ligand addition; e.g., a five-coordinate iron(II) complex reacts to form a six-coordinate iron(III) complex. After the formation of the first bond, quite different consecutive steps can occur (see Scheme 10 for possible pathways), leading to superoxo, peroxo, and hydroperoxo species. Further reactions with mononuclear iron complexes are possible, leading to dinuclear peroxo complexes discussed in more detail below in section 5.

Characterized mononuclear non-heme iron(III) complexes with dioxygen-derived ligands (superoxide, peroxide, and hydroperoxide) are rare. In most systems, such complexes probably form only as steady-state intermediates and do not accumulate in the reaction mixture. Kinetic studies showed that the reaction with a second equivalent of iron(II) is often a concerted or post-rate-limiting (fast) process.[21,223,224]

Iron(III) superoxo compounds were stabilized by the use of lacunar ligands that prevent the reaction with a second equivalent of Fe(II) precursor.[166] Iron(III) peroxo species have been postulated for mononuclear iron enzymes for a long time, but only recently the crystal structure of naphthalene dioxygenase has been solved that contains a side-on iron(III) peroxo unit in the active site.[3,26,67] Synthetic mononuclear iron(III) complexes with the dioxygen-derived ligands (O_2^{2-}, HO_2^-) so far eluded isolation in the crystalline state and structural characterization. Quite a few such complexes, however, were characterized by spectroscopic means.[3] Recently, a mononuclear iron(III) complex with a peroxycarbonate ligand (presumably formed from an Fe^{III}−OOH intermediate and CO_2) was isolated and crystallographically characterized.[225]

High-valent (Fe^{IV} and Fe^{V}) species have been postulated as possible products of iron(III) peroxo species decomposition by homolysis or heterolysis of the O−O bond.[3,41] While for iron−heme complexes such reactions have been characterized in significant detail,[15−19] much less is known for the analogous non-heme iron systems.[192,226] Only recently, mononuclear non-heme Fe^{IV}=O species were characterized in biological systems[30,47] and reliably identified in model compounds.[3,62] The Fe^{IV}=O complexes are strong oxidants capable of direct H atom abstraction and hydroxylation of organic substrates, as shown in recent kinetic and mechanistic studies.[65,193]

The simple aqua cation $\{Fe^{IV}O\}^{2+}_{aq}$ was generated as a short-lived intermediate in the reaction of ozone with Fe^{2+}_{aq} ($k = 8 \times 10^5$ M^{-1} s^{-1} at 25 °C) in acidic medium.[227] It should be noted that this species was characterized only by its UV−vis spectrum and the stoichiometry of its formation and reactivity.[227,228] A more detailed characterization of this interesting intermediate is clearly needed. The reactivity of $\{Fe^{IV}O\}^{2+}_{aq}$ was studied in significant detail using stopped-flow kinetic measurements.[227−231] It undergoes single-exponential self-decomposition ($\tau_{1/2} \sim 7$ s at $T = 25$ °C and pH = 1) that is decelerated in D_2O with a solvent isotope effect of 2.85, consistent with hydrogen atom abstraction from water.[228] Aqueous ferryl ion readily oxidizes Fe^{2+}, Mn^{2+}, H_2O_2, HNO_2, and even Cl^- ($k = 100 \pm 10$ M^{-1} s^{-1} at $T = 25$ °C), indicating that the redox potential of the FeO^{2+}/Fe^{3+} couple is very high ($\geq +2.0$ V).[229,230] $\{Fe^{IV}O\}^{2+}_{aq}$ hydroxylates aromatic substrates (e.g., nitrobenzene to *m*-nitrophenol ($k = (1.05 \pm 0.3) \times 10^3$ M^{-1} s^{-1} at $T = 25$ °C), but the measured reaction rates are insufficient to infer ferryl(IV) as the active species in the Fenton reaction ($Fe^{2+}_{aq} + H_2O_2$).[231] Aliphatic alcohols, aldehydes, and ethers are rapidly oxidized by $\{Fe^{IV}O\}^{2+}_{aq}$ in parallel hydrogen atom and hydride transfer reactions, the latter pathway being exemplified by the transformation of cyclobutanol into cyclobutanone.[228]

Table 2. Kinetic Parameters of Different Reaction Steps in the Oxygenation of Fe(II) Aminopolycarboxylate Complexes in Aqueous Solution (I = 0.5, [acetate buffer] = 0.1 M, pH = 6.0)[236,239]

complex	reaction step	rate constant (T = 25 °C), M^{-1} s^{-1}	$\Delta H^{\ddagger}$, kJ mol^{-1}	$\Delta S^{\ddagger}$, J mol^{-1} K^{-1}	$\Delta V^{\ddagger}$, cm^3 mol^{-1}
$[Fe^{II}(cdta)]$	1	1080(16)	44.1(2.3)	−236(8)	ND[a]
	2	103(4)	66.5(9)	18.7(24)	−20.2(23)
	3	59(5)	67.1(8)	18.0(27)	−23.0(39)
$[Fe^{II}(edta)]$[b]	2	303(40)[c]	50(2)	−30(7)	−16.1(16)
	3	147(20)[c]	45(1)	−53(4)	−16.2(25)

[a] ND = not determined. [b] First step was too fast for qualitative characterization. [c] These values are the averages of the two sets of data reported in the original paper.[236]

Several other mononuclear iron(IV) complexes (without an oxo ligand) have been well characterized, but they are not directly related to the iron oxygen chemistry.[232−234]

4.1. Complexes with Aminopolycarboxylates

4.1.1. Reactions with O_2

The kinetics of the oxidation of the iron(II) complex of EDTA, $[Fe^{II}(EDTA)(H_2O)]^{2-}$, by dioxygen leading to $[Fe^{III}(EDTA)(H_2O)]^{-}$ (autoxidation) has been investigated thoroughly by van Eldik and co-workers (earlier important work is referred to in the given references).[235,236] Three steps were distinguished in this reaction experimentally, but the first step was too fast for detailed characterization. The pH, concentration, temperature, and pressure dependence of the observed rate constants was investigated and allowed for the calculation of the activation parameters $\Delta H^{\ddagger}$, $\Delta S^{\ddagger}$, and $\Delta V^{\ddagger}$ for the second and third steps (Table 2). The mechanism in Scheme 11 was postulated.

The first reaction step was assigned as a ligand substitution of the coordinated water molecule by dioxygen followed by an intramolecular electron-transfer reaction to produce an Fe(III)−superoxo complex, which in a third step reacts with another $[Fe^{II}(EDTAH)H_2O]^{-}$ species to produce a dimeric iron peroxo complex. The rapid dissociation reaction of $[(EDTAH)Fe^{III}O_2Fe^{III}(EDTAH)]^{2-}$ leads to the formation of the monomeric $[Fe^{III}(EDTAH)H_2O]$ (the same mechanism is assigned to the less reactive unprotonated $[Fe^{II}(EDTA)H_2O]^{2-}$). Free H_2O_2 could not be detected in the reaction mixture, and no radical formation was observed in EPR experiments. The authors conclude that the produced H_2O_2 is consumed in the rapid oxidation of excess iron(II) complex. The rate constant for this process was measured to be 1.78×10^4 M^{-1} s^{-1} at pH = 6 and T = 25 °C, in close agreement with values reported previously (see section 4.1.2 below).[237,238]

According to the authors, the reaction with dioxygen is controlled by the dissociative ligand substitution of the water molecule in the seven-coordinated iron complex. The subsequent slower intramolecular electron-transfer process should then be controlled by a reorganization barrier leading from $[Fe^{II}-O_2]$ to $[Fe^{III}-O_2^{-}]$. This reaction is characterized by significantly negative $\Delta S^{\ddagger}$ and $\Delta V^{\ddagger}$ values (Table 2), which must be related to the oxidation of iron(II) and the reduction of dioxygen to superoxide. Both of these processes are expected to involve a significant decrease in partial molar volume and an increase in electrostriction. The efficiency of the ligand substitution process is controlled by the nature of the $[Fe^{II}(EDTA)(H_2O)]^{2-}$ complex, which on protonation produces a more labile $[Fe^{II}(EDTAH)(H_2O)]^{-}$ species. The latter accounts for the drastic increase in observed rate constants on decreasing the pH from 5 to 3.

Scheme 11. Proposed Mechanism for Oxygenation of the Fe(II)−EDTA Complex

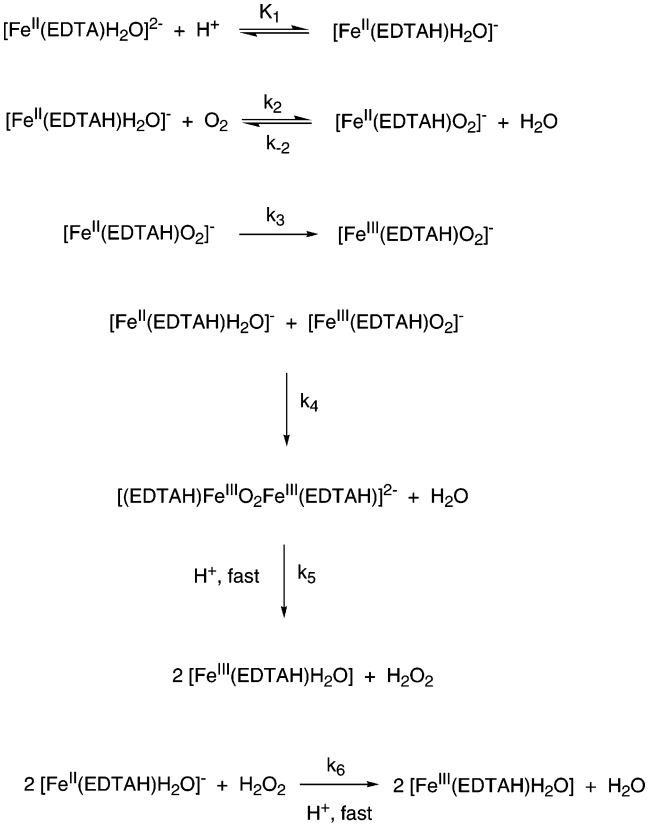

The postulated mechanism is in accord with the kinetic data; however, alternative pathways cannot be excluded. This is a consequence of the fact that in this multistep reaction only the reactant and the product can be observed spectroscopically, and intermediates could not be detected.

Some clarification for the reaction of the iron(II) EDTA system with dioxygen was obtained by using CDTA (cyclohexanediaminetetraacetate) instead of EDTA.[239] The rate constants for the three reaction steps are all smaller compared to those for the EDTA system and, therefore, allowed for the quantitative fitting of the fast initial step. Rate constants and

activation parameters are presented in Table 2. The similarity between the EDTA/iron(II) and CDTA/iron(II) systems is reflected in the same mechanism for the reaction with dioxygen as that shown in Scheme 11 (CDTA instead of EDTA).[239]

Further studies on the reaction of related iron(II) aminopolycarboxylato complexes with dioxygen were performed to investigate steric effects on these oxidations.[240] A strong decrease in reactivity was observed when the ethylene spacer in EDTA was replaced with a 1,3-propylene group in 1,3-PDTA (1,3-propylenediaminetetraacetate). However, complications encountered during the kinetic measurements did not allow for a quantitative analysis of this system.

Furthermore, in that context, it is interesting to note that a recent detailed study by van Eldik and co-workers on the reaction of NO with iron(II) aminocarboxylate complexes demonstrated a correlation between the binding ability of NO and the dioxygen sensitivity of these complexes.[241−243]

4.1.2. Reactions with O_2^- (Superoxide)

Excellent work by Bull, McClune, and Fee described quite early the reaction of the superoxide anion with $[Fe^{II}(EDTA)H_2O]^{2-}$.[237] Additionally, they investigated the potentially interfering reactions of $[Fe^{II}(EDTA)H_2O]^{2-}$ with dioxygen and hydrogen peroxide (discussed in section 4.1.1 above), as well as the reaction of $[Fe^{III}(EDTA)H_2O]^-$ with hydrogen peroxide (discussed in section 4.1.3 below). The reaction of $[Fe^{II}(EDTA)H_2O]^{2-}$ with superoxide in aqueous basic solutions leads to the formation of the iron peroxo complex $[Fe^{III}(EDTA)O_2]^{3-}$ (see section 4.1.3). The 1:1 stoichiometry was determined for this reaction, and it was observed that an excess of O_2^- did not lead to a decrease of the amount of the peroxo complex formed. The formation of $[Fe^{III}(EDTA)O_2]^{3-}$ was studied with a specially designed three-syringe stopped-flow unit and is very rapid (approaching the limits of the stopped-flow technique). Under the applied conditions, a second-order rate constant of $\sim 8 \times 10^6$ M^{-1} s^{-1} was determined (largely independent of pH), consistent with the results from other measurements using different techniques such as pulse radiolysis.[244]

The reaction of $[Fe^{III}(EDTA)H_2O]^-$ with superoxide is much more complicated and is assigned as a reduction leading to $[Fe^{II}(EDTA)H_2O]^{2-}$ and dioxygen. $[Fe^{II}(EDTA)H_2O]^{2-}$ then again reacts rapidly with O_2^- to form the peroxo complex. The calculated rate constants are in good agreement with the values derived from pulse radiolysis studies reported previously.[244,245] Formation of an iron superoxide complex as a possible intermediate has not been observed under the conditions applied.

4.1.3. Reactions with H_2O_2

An important complex that can be generated in solution is the purple $[Fe^{III}(EDTA)(\eta^2\text{-}O_2)]^{3-}$, discovered already in 1956 by mixing hydrogen peroxide with $[Fe^{III}(EDTA)(H_2O)]^-$ in basic medium (pH above 10).[246] The complex $[Fe^{III}(EDTA)(\eta^2\text{-}O_2)]^{3-}$ has been characterized in great detail by various spectroscopic techniques (as well as theoretical calculations), confirming a side-on high-spin iron(III) peroxo structure.[184,247,248]

Table 3. Summary of Activation Parameters for the Two-Step Reaction of $[Fe^{III}(EDTA)H_2O]^-$ and H_2O_2[a]

exp cond	$\Delta H^{\ddagger}$, kJ mol^{-1}	$\Delta S^{\ddagger}$, J mol^{-1} K^{-1}	$\Delta V^{\ddagger}$, cm^3 mol^{-1}
k_1, pH = 9.0	37 ± 4	−53 ± 14	6.8 ± 0.8
k_{-1}, pH = 9.0	101 ± 2	135 ± 6	18.4 ± 0.6
k_1, pH = 10.5	45 ± 2	−42 ± 5	6.9 ± 0.3
k_2, pH = 10.5	79 ± 2	−10 ± 5	−2.3 ± 0.1
k_{-2}, pH = 8.5	86 ± 2	56 ± 6	5.1 ± 0.2

[a] Experimental conditions: [complex] = 0.001 M, $[H_2O_2]$ = 0.01 − 0.04 M, I = 0.5.[249]

Very recent work by Brausam and van Eldik summarizes kinetic results for the formation of $[Fe^{III}(EDTA)O_2]^{3-}$ from hydrogen peroxide and $[Fe^{III}(EDTA)H_2O]^-$ and, additionally, provides further clarification of the mechanism.[249] As reported previously, pH plays a major role in controlling the overall reaction sequence as well as the stability of intermediate and product species; formation of $[Fe^{III}(EDTA)O_2]^{3-}$ could not be observed below pH ≈ 8. The reaction of $[Fe^{III}(EDTA)OH]^{2-}$ with hydrogen peroxide occurs in two steps (eq 6). The first reaction

$$[Fe^{III}(EDTA)OH]^{2-} + H_2O_2 \underset{k_{-1}}{\overset{k_1}{\rightleftharpoons}} [Fe^{III}(EDTA)OOH]^{2-} + H_2O \underset{k_{-2}}{\overset{k_2}{\rightleftharpoons}} \left[(EDTA)Fe^{III}\begin{smallmatrix}O\\O\end{smallmatrix}\right]^{3-} \quad (6)$$

step has been investigated previously, and results obtained in the new study are in close agreement with the published kinetic data.[237,250,251] Additionally, a small contribution of specific acid catalysis for this reaction step was found, and a temperature and pressure dependence study allowed for the calculation of activation parameters (Table 3). These measurements were performed at two different pH values: at pH = 9.0, where a back-reaction is evident (plots of k_{1obs} vs $[H_2O_2]$ exhibited a clear intercept), and at pH =10.5, where the back-reaction is insignificant.

A comparison of the activation entropies and activation volumes for k_1, at both pH values, clearly documents the importance of high-pressure measurements for the evaluation of the reaction mechanism. This has been described previously in several reviews on high-pressure kinetic measurements and will not be discussed in detail here again.[252−255] However, it is obvious that temperature dependence measurements, especially in aqueous solutions that only allow a very limited temperature window, provide $\Delta S^{\ddagger}$ values that are subject to large errors due to a linear extrapolation to $1/T = 0$, in contrast to the more reliable $\Delta V^{\ddagger}$ values (obtained from a plot of the slope of ln k vs p). Here, the negative value for the activation entropy for the first step in eq 2 would indicate a substitution reaction with an associative character; however, the activation volume clearly accounts for an interchange dissociative (I_d) mechanism. This compares well to the water exchange reaction for $[Fe^{III}(EDTA)H_2O]^-$ that also follows a dissociative interchange mechanism ($\Delta V^{\ddagger} = 3.2 \pm 0.4$

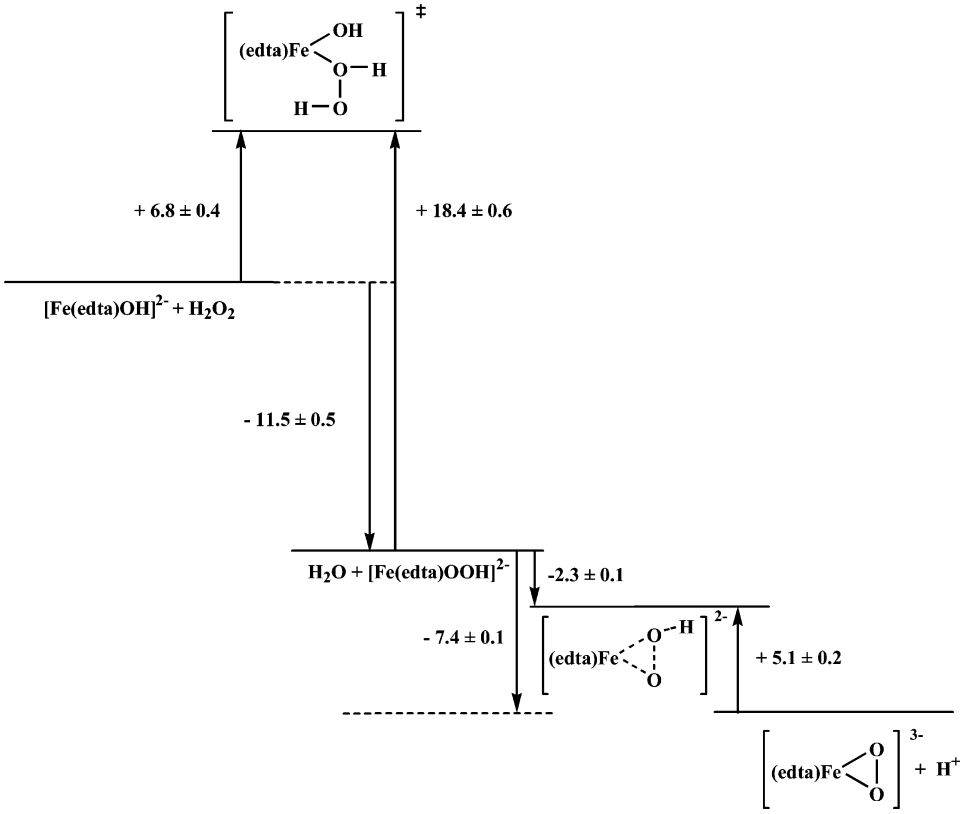

Figure 2. Volume profile for the reaction of Fe(III)-EDTA with H_2O_2.

$cm^3\ mol^{-1}$).[256] However, these measurements (by the ^{17}O NMR techniques) were performed at pH < 4. At this point, it is interesting to note that activation volumes reported for aquated iron(III) in the absence of chelating ligands are quite different: the values of −5.4 and +7.0 $cm^3\ mol^{-1}$ for water exchange on $[Fe^{III}(H_2O)_6]^{3+}$ and $[Fe^{III}(H_2O)_5OH]^{2+}$ were interpreted in terms of I_a and I_d exchange mechanism, respectively.[257,258] Furthermore, the substitution behavior of a different seven-coordinate iron(III) complex in aqueous solution has been studied recently.[259] For the back-reaction in eq 6, the dissociative character is clearly documented by the positive values for $\Delta S^{\ddagger}$ and $\Delta V^{\ddagger}$.

The second step of the reaction proved to be independent of the hydrogen peroxide concentration, indicating that this is the ring closure reaction shown in eq 6. For this reaction step, a slightly negative $\Delta V^{\ddagger}$ was found, which is in agreement with an associative interchange type of the peroxide chelation reaction. The reported volumes of activation of both steps were used to construct the volume profile shown in Figure 2 for the overall reaction.

The proposed mechanism in accord with the kinetic data is presented in Figure 3. During the peroxide chelation and dechelation reactions, the dissociation and association of one of the four carboxylates from the metal ion is proposed, such that a seven-coordinate geometry is maintained throughout the process. However, for the first step, it is not possible to conclude from the available data if a six- or seven-coordinate complex is the reactive species (i.e., if EDTA acts as a penta- or hexadentate ligand).

Another reinvestigation of the kinetics of formation of $[Fe^{III}(EDTA)(O_2)]^{3-}$ appeared recently.[260]

4.2. Complexes with Macrocyclic Ligands

4.2.1. Complexes with the Polyazamacrocycles 15aneN4, cyclam, and Pyan

The problems involved in establishing a detailed mechanism for the reaction of dioxygen with an iron(II) complex in aqueous solution have been clearly illustrated in a kinetic study on the oxidation of a macrocyclic iron system by Schrodt and van Eldik.[261] First of all, it is important to confirm that the used or postulated starting material actually exists in that form in solution. In a potentiometric titration study of the distribution of species in the $[Fe^{II}(15aneN_4)]^{2+}$ system (1,4,8,12-tetraazacyclopentadecane, one CH_2 group more than in cyclam, Scheme 9), it was demonstrated that no stable Fe(II) complex was formed at pH < 6; only the hexaaqua iron(II) species is present together with the uncoordinated protonated ligand. Without such an important preliminary investigation prior to the kinetic measurements, completely wrong results would have been obtained. Additionally, at pH values above 8.5, precipitation was observed that limited the pH range accessible for the kinetic study. Stopped-flow measurements were performed at pH = 7.5, where four different iron(II) species are present in solution: $[Fe(H_2O)_6]^{2+}$ = 1.6%, $[Fe(L)(H_2O)_2]^{2+}$ = 0.6%, $[Fe(L)(H_2O)(OH)]^{+}$ = 68.1%, and $[Fe(L)(OH)_2]$ = 29.7%. Buffers (HEPES and MOPS) that were used to maintain the pH constant were tested and showed no effect on the observed kinetics. Additionally, ionic strength was kept constant at I = 0.10 with $NaClO_4$. Pseudo-first-order measurements (excess of $Fe^{II}L$) allowed fitting of absorbance vs time data to a one-exponential function at 370 nm, where the reaction is accompa-

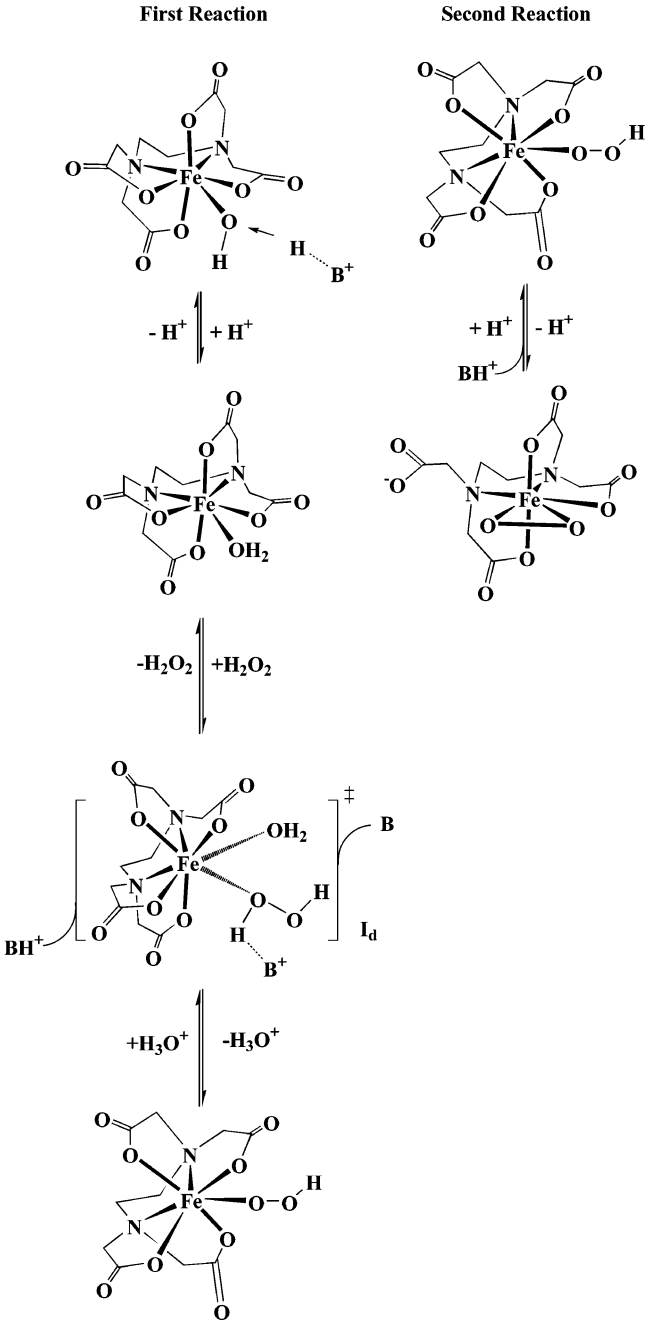

Figure 3. Proposed mechanism for the reaction of H_2O_2 with the Fe(III)−EDTA complex.

nied by a significant increase in absorbance. A nonlinear dependence of k_{obs} vs the iron(II) complex concentration was observed, and the data fit could be performed according to the following equation:

$$k_{obs} = k_1[Fe^{II}(L)] + k_2[Fe^{II}(L)]^2 \quad (7)$$

Furthermore, the oxidation of the iron(II) complex with hydrogen peroxide was investigated. The second-order rate constants for this reaction were about a factor of 2 faster compared with those for the reaction of dioxygen under similar conditions.

The proposed mechanism of the reaction of dioxygen with $[Fe^{II}(15aneN_4)]^{2+}$ is very similar to the mechanism of the iron(II)−EDTA system presented in Scheme 11. For both complexes, quite large negative values for $\Delta S^{\ddagger}$ were observed, accounting for an associative reaction step. Unfortunately, here again it was not possible to spectroscopically detect the formation of a superoxide or peroxide intermediate complex under the conditions used.

In an earlier work by Kimura and co-workers on an iron(II) macrocyclic complex with the pyridyl-containing pentaaza macrocyclic ligand Pyan (Scheme 9), it was shown that a quite stable intermediate, possibly a peroxo diiron(III) complex, was formed during the reaction with dioxygen.[262] From stopped-flow measurements in aqueous solutions (Tris buffers: 8.0 < pH < 9.5), mixed second-order rate constants were calculated (the reaction was first order in the Fe^{II} complex and in O_2).

Significant number of papers were devoted to the studies of dioxygen and hydrogen peroxide activation by the iron(II) complexes of the tetraazamacrocycle cyclam. The complex $[Fe^{II}(cyclam)(OTf)_2]$ was found to be an effective catalyst for olefin epoxidation with hydrogen peroxide in acetonitrile and methanol.[263] The same iron(II) complex catalyzed the epoxidation of olefins by dioxygen with the co-oxidation of aldehydes in acetonitrile.[264] From independent studies it is known that the $[Fe^{II}(cyclam)(MeCN)_2]^{2+}$ complex by itself reacts with dioxygen in acetonitrile at room temperature very slowly (within several days), leading to the oxidation of the ligand but not the central iron(II) ion.[265,266] Oxygenation of $Fe^{II}(cyclam)Cl_2$ in methanol proceeds faster (within several hours at room temperature) and leads to the oxidation of the central ion.[267] The reaction of $[Fe^{II}(cyclam)(MeCN)_2]^{2+}$ with H_2O_2 in acetonitrile is very fast and leads to both the oxidation of iron(II) and the degradation of the organic ligand.[268] This reaction was studied by the stopped-flow technique at 25 °C and found to proceed in three kinetically distinguishable steps with differently colored intermediates. The first and second steps were first order in both iron(II) complex and H_2O_2 with the mixed second-order rate constants $k_1 = 3.7\ M^{-1}\ s^{-1}$ and $k_1 = 0.83\ M^{-1}\ s^{-1}$, respectively. The third step was slower and had complicated kinetics. Unfortunately, the nature of the transient intermediates in the reaction of $[Fe^{II}(cyclam)(MeCN)_2]^{2+}$ with H_2O_2 was not identified due to their instability, and the authors prudently abstained from ungrounded speculations on this topic.[268] The iron−cyclam complexes are powerful activators of the dioxygen species; however, the mechanism of these remarkable reactions remains unknown.

4.2.2. Complexes with Cyclidenes

Very interesting ligands, the cyclidene macrocycles (see Scheme 12 for representative structures), were designed and extensively studied by Busch and co-workers as dioxygen carriers in which the O_2 binding site at the Fe^{II} (or Co^{II}) center is protected from autoxidation (μ-oxo dimer formation is prevented by the bridge).[166,269−271]

The 16-membered cyclidene platforms fold because of the conformational requirements of adjacent chelate rings: the low-energy chair or boat conforma-

Scheme 12. Structure of Cycledene Complexes

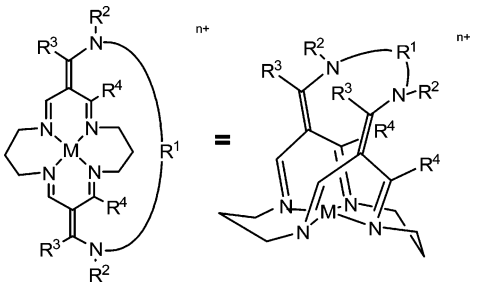

tions of the six-membered saturated rings force the adjacent unsaturated rings to tilt toward the MN_4 plane. The saddle-shaped platforms were bridged across the cavity, providing sterically protected ligand binding pockets. Dioxygen binding to cyclidenes was investigated in great detail for cobalt(II) complexes.[166] However, the limited data that are now available for the oxygenation of iron(II) cyclidenes[269−271] suggest that similar factors regulate the kinetics and equilibria of small molecule binding.

The dioxygen affinity of the Co(II) and Fe(II) cyclidene complexes is governed by both electronic and steric factors. The coordination of the fifth donor ligand, such as pyridine or imidazole, is required for efficient O_2 binding and is usually accomplished by adding the corresponding base to the macrocycle solution. The sixth coordination site of the metal should remain vacant or labile, to allow for an easy access of the O_2 ligand. The only crystal structure of the dioxygen adduct of the cobalt(II) cyclidene $[Co(MeMeC6)(O_2)(MeIm)]^{2+}$ ($R^1 = (CH_2)_6$, $R^2 = R^3 = Me$, Scheme 12) shows that O_2 binds at an angle of 121°, as expected for the coordinated superoxide, and the hexamethylene bridge flips away from the guest.[166] This flipping effectively eliminates the van der Waals repulsion between the flexible bridges and the included O_2.

The dioxygen affinity of iron(II) cyclidenes also depends on steric constraints for O_2 binding, as can be seen from comparison of the complexes with aliphatic bridges of varying length (Table 4). Dioxygen binding at a vacant site in five-coordinate C4-, C5-, and *m*-xylene-bridged cyclidenes is characterized by low activation enthalpies and large negative activation entropies, which are typical of associative processes. The six-coordinate complexes with C6- and C8-cyclidenes release the solvent molecule in the course of dioxygen binding. These ligand substitution reactions have substantially larger activation barriers but less negative activation entropies (Table 4).[271]

The electronic effects on the oxygenation rates are less pronounced, although in some cases they are still significant. The rates of dioxygen binding increase by almost an order of magnitude with an increase in the electron-withdrawing properties of R^2 and R^3 substituents in *m*-xylene-bridged cyclidenes (k_{on} = 186 M^{-1} s^{-1} for $R^2 = R^3 = Me$, and 1305 M^{-1} s^{-1} for $R^2 = Ph$, $R^3 = Bz$ at −20 °C).

Iron(II) cyclidenes also bind carbon monoxide, which is forced by the bridge into a bent configuration (the angle Fe−C−O = 170.6° in $[Fe(C5MeMe)(CO)(py)]^{2+}$) ($R^1 = (CH_2)_5$, $R^2 = R^3 = Me$).[272] As expected, this nonlinear coordination mode results in relative destabilization of the iron(II) cyclidene−carbon monoxide adducts (Table 5).[271] Remarkably, the discrimination against CO is unusually high for the C5 bridged complex $[Fe(C5PhMe)(MeIm)]^{2+}$: $K(CO)/K(O_2) = 0.03$.[271] There are very few examples of iron(II) complexes that bind O_2 more strongly than CO, including the *Ascaris* hemoglobin[273] and a synthetic sterically hindered porphyrin.[274] Molecular modeling suggests that selective recognition of O_2 by the complex $[Fe(C5PhMe)(MeIm)]^{2+}$ is caused both by the unfavorable van der Waals interactions between CO and the bridge (which are much less pronounced in the case of O_2 because of the greater bending of the latter ligand) and by favorable electrostatic interactions between the polar O_2 ligand and the walls of the cleft. The former effect destabilizes the CO adduct, while the latter one stabilizes the dioxygen complex.[271]

Table 4. Kinetic and Thermodynamic Parameters[a] for O_2 Binding to Iron(II) Cyclidene Complexes Measured in Acetonitrile/1.5 M 1-MeIm Using Stopped-Flow Spectrophotometry[271]

R^1	R^2	R^3	$\Delta H^{\ddagger}_{on}$, kJ mol^{-1}	$\Delta S^{\ddagger}_{on}$, J mol^{-1} K^{-1}	$\Delta H^{\ddagger}_{off}$, kJ mol^{-1}	$\Delta S^{\ddagger}_{off}$, J mol^{-1} K^{-1}	$\Delta H°$, kJ mol^{-1}	$\Delta S°$, J mol^{-1} K^{-1}
$(CH_2)_4$	Me	Ph	12	−276	95	76	−84	−350
$(CH_2)_5$	Me	Ph	14	−229	50	−110	−37	−120
$(CH_2)_6$	Me	Ph	41	−75	ND	ND	ND	ND
$(CH_2)_8$	Me	Ph	54	−40	ND	ND	ND	ND
m-Xy	Me	Me	11.1	−252	ND	ND	ND	ND
m-Xy	Bz	Me	11.4	−253	ND	ND	ND	ND
m-Xy	Me	Ph	15.8	−228	ND	ND	ND	ND
m-Xy	Bz	Ph	9.1	−243	ND	ND	ND	ND

[a] Dioxygen dissociation rates were determined from the nonzero intercepts of the plots of k_{obs} vs $[O_2]$, using the equation $k_{obs} = k_{on}[O_2] + k_{off}$. Equilibrium constants were estimated as $K = k_{on}/k_{off}$. ND = not determined.

Table 5. Kinetic and Thermodynamic Parameters for Carbon Monoxide and Dioxygen Binding to Iron(II) Cyclidene Complexes (R^2 = Me, R^3 = Ph) in the Acetonitrile/1.5 M 1-MeIm Mixture at 25 °C[271]

R^1	k_{on}^{CO}, $Torr^{-1}$ s^{-1}	k_{off}^{CO}, s^{-1}	K^{CO}, $Torr^{-1}$	$k_{on}^{O_2}$, $Torr^{-1}$ s^{-1}	$k_{off}^{-O_2}$, s^{-1}	K^{O_2}, Torr	$M = K^{CO}/K^{O_2}$	$k_{on}^{O_2}/k_{on}^{CO}$
$(CH_2)_4$	2.2×10^{-4}	0.06	3.6×10^{-3}	4.0×10^{-4}	1.1	4×10^{-4}	12	1.8
$(CH_2)_5$	1.1×10^{-3}	0.022	5.0×10^{-2}	4.6×10^{-2}	0.03	1.6	0.03	42
$(CH_2)_6$	0.32	0.0026	1.2×10^{2}	14.9	7	2.1	60	46
$(CH_2)_8$	1.34	0.0041	3.3×10^{2}	21.3	53	0.4	800	16

Scheme 13. Proposed Mechanism for the Activation of H_2O_2 by an Iron(II) Complex

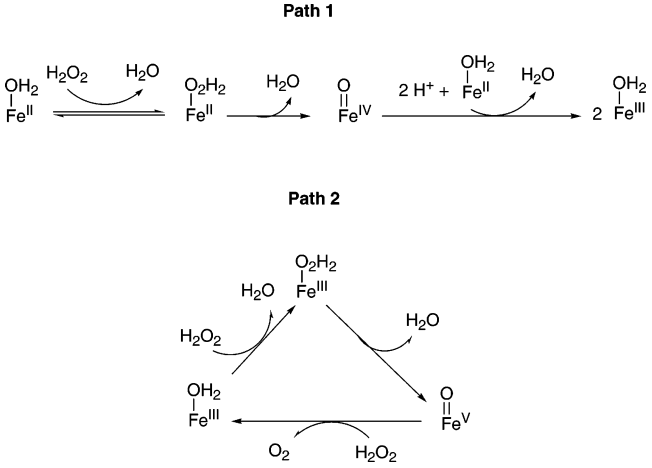

4.2.3. Complexes with Polyazamacrocycles Having Pendant Arms

Busch, van Eldik, and co-workers investigated the reactions of hydrogen peroxide with pentadentate iron(II) complexes based on tridentate macrocyclic ligands with two additional arms incorporating pyridine donor atoms ([11]aneN$_3$MePy$_2$ and [12]aneN$_3$-MePy$_2$, Scheme 9); these compounds are six-coordinate high-spin d^6 iron(II) complexes (an additional water molecule is coordinated).[275] A goal of this work was to distinguish between different reaction pathways that would lead to either hydroxyl radicals or high-valent iron-oxo species as strongly oxidative intermediates. Using substrate competition, as described previously by Rush and Koppenol (stopped-flow measurements were carried out with and without bromide anion and ABTS (2,2′-azinobis(3-ethylbenzothiazoline-6-sulfonate)) as scavengers),[276] and working with initial rate data analysis (to avoid complications with further oxidations of ABTS), a mechanism for the oxidation of LFe^{II} to LFe^{III} was proposed (Scheme 13).

The rate-limiting step was assigned as the substitution reaction of the coordinated water by hydrogen peroxide leading to an unstable complex that undergoes heterolysis to produce {LFe^{IV}=O} as a reactive intermediate. The latter is reduced by yet another molecule of LFe^{II} to yield 2 equiv of LFe^{III}. The first step of the catalytic decomposition of hydrogen peroxide by LFe^{III} is the fast substitution of the coordinated water with hydrogen peroxide followed again by heterolysis leading to LFe^{V}=O which is subsequently reduced by hydrogen peroxide to generate dioxygen. The work concludes that high-valent iron oxygen intermediates (such as LFe^{IV}=O and/or LFe^{V}=O) are responsible for the substrate oxidation in this system, instead of hydroxyl radicals. However, as the authors state, direct evidence for the nature of the suggested intermediates is lacking (a different Fe^{IV}=O complex has been structurally characterized recently;[62] see below).

Earlier work described the reaction of superoxide with two iron(II) complexes with pentadentate and hexadentate ligands (TPC and DPC; Scheme 9) derived from cyclononane.[277] Under nonaqueous conditions (stopped-flow measurement were performed in DMSO and acetonitrile solutions) for both complexes, similar pseudo-first-order rate constants were obtained (100 ± 10 and 335 ± 30 s^{-1}) for the reaction with superoxide at 25.5 °C. The results of the kinetic study and potential-step spectroelectrochemical measurements were consistent with the formation of an iron(III)−peroxo adduct as an intermediate.

The reactivity of an interesting macrocyclic system toward dioxygen and superoxide has been investigated previously by Szulbinsky and Busch using a pentadentate carboxymethylenecyclam ligand (Cyclam-acetato; Scheme 9).[278] At pH = 8.1 and T = 21 °C a second-order rate constant for the reaction of superoxide with [Fe^{III}L(Cl)]$^+$ of $(3 \pm 1) \times 10^7$ M^{-1} s^{-1} was determined; however, no activation parameters were reported. From the results of stopped-flow and electrochemical measurements, the authors conclude that an iron(III) peroxo complex was formed as an intermediate during the reaction.

4.2.4. Macrocyclic Complexes of Ferryl(IV)

The efforts of Wieghardt and co-workers to generate an (oxo)iron(V) complex using the Cyclam-acetato ligand (used previously by Szulbinsky and Busch as described above) by the reaction of ozone with the iron(III) complex resulted in the detection of an (oxo)-iron(IV) species instead.[190] It was proposed that if the (oxo)iron(V) complex were generated, it would be highly oxidizing and therefore causing hydrogen atom abstraction from a proton source leading to the (oxo)-iron(IV) product. Furthermore, the authors succeeded in the spectroscopic identification of a (nitrido)iron-(V) complex.

The most exciting report recently was the full characterization, including the determination of the crystal structure, of a nonheme (oxo)iron(IV) complex using simple tetra-*N*-methylated cyclam (TMC, Scheme 9) as ligand.[62] The complex *trans*-[Fe^{IV}(O)-(TMC)(NCCH$_3$)](OTf)$_2$ was synthesized by the oxidation of [Fe^{II}(TMC)](OTf)$_2$ with iodosobenzene (PhIO) in acetonitrile at −40 °C. Furthermore, it was possible to prepare this complex by reacting the iron(II) complex with 3 equiv of hydrogen peroxide (however, the reaction is much slower). The complex is quite stable at the low temperature and allowed for the isolation of single crystals suitable for X-ray crystallography analysis and a full spectroscopic characterization of *trans*-[Fe^{IV}(O)(TMC)(NCCH$_3$)](OTf)$_2$.[62,63] The relative stability/inertness of this complex caused by the ligand environment has the effect that the oxidative reactivity of this system is not well pronounced. In contrast, the Fe(II) complex of the parent cyclam is an effective catalyst for olefin epoxidation with hydrogen peroxide,[263] and the postulated [Fe^{IV}-(O)(Cyclam-acetato)]$^+$ decays within minutes at −40 °C (see above[190]). However, with the full spectroscopic characterization of the ferryl(IV) TMC complex, it is now possible to unambiguously detect such species as intermediates during oxidation reactions of more reactive complexes (see sections 4.4.1 and 4.4.3 below).

Recently, direct evidence for oxygen atom exchange between nonheme oxoiron(IV) complexes and $H_2{}^{18}O$

Scheme 14. Mechanism of Ligand Exchange at Non-heme Ferryl(IV) Complexes

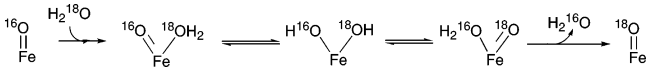

Scheme 15. Different Reactivity Pathways for the Fe(III)−Peroxo Complexes

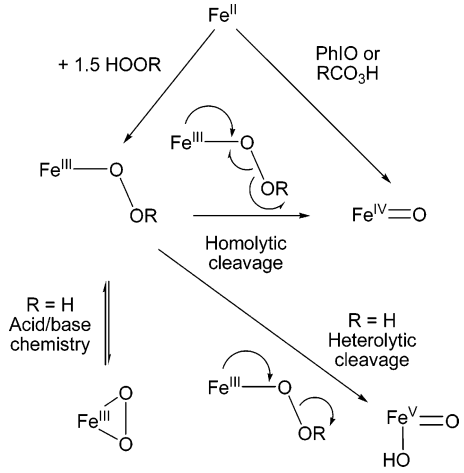

was reported using *trans*-[Fe^{IV}(O)(TMC)($NCCH_3$)]-($OTf)_2$.[279] Electrospray ionization mass spectrometry (ESI-MS) allowed for the determination of the pseudo-first-order rate constants that showed a linear dependence on the concentration of $H_2{}^{18}O$ and thus yielded the second-order rate constant for the exchange reaction of 5.4(6) M^{-1} s^{-1}. From the measurements in the temperature range from 283 to 308 K, the activation parameters of $\Delta H^{\ddagger} = 4.1(6)$ kcal mol^{-1} and $\Delta S^{\ddagger} = -57(8)$ cal mol^{-1} K^{-1} were calculated. Nearly identical rate constants and activation parameters were obtained for the oxygen exchange of the [(N4Py)Fe^{IV}=O]$^{2+}$ complex. From these findings a mechanism was proposed in which oxygen exchange occurs via a 2-fold symmetric *cis*-dihydroxo-iron(IV) transition state that is formed by coordination of a water molecule to the iron center adjacent to the oxo group (Scheme 14). This reaction pathway is an alternative to the oxo−hydroxo tautomerism mechanism suggested previously for heme models.[280]

A general scheme on the possible routes to active iron−oxygen species has been reported by Rohde et al.[26] and is presented in Scheme 15.

4.2.5. Modeling Catechol Dioxygenase Activity

Catechol dioxygenases catalyze the ring cleavage of catechols with dioxygen following two different reaction pathways for either intradiol (Fe^{III} involved) or extradiol (Fe^{II} involved) cleavage.[24,47,55] Most model systems investigated so far gave products consistent with intradiol cleavage, such as the iron−TPA system discussed below, and only a few examples are reported that show extradiol cleavage activity. Previous work by Funabiki and co-workers demonstrated that complexes derived from an in situ mixture of $FeCl_2$/$FeCl_3$ and bipyridine/pyridine could cleave 3,5-di-*tert*-butyl catechol ($dbcH_2$) to 2-pyrones, assuming an extradiol-cleavage step during the reaction.[281] Using TACN (1,4,9-triazacyclononane, Scheme 9) and dbc^{2-} as ligands, 2-pyrones were obtained upon exposure

Scheme 16. Extradiol Cleavage by Macrocyclic Iron Complex

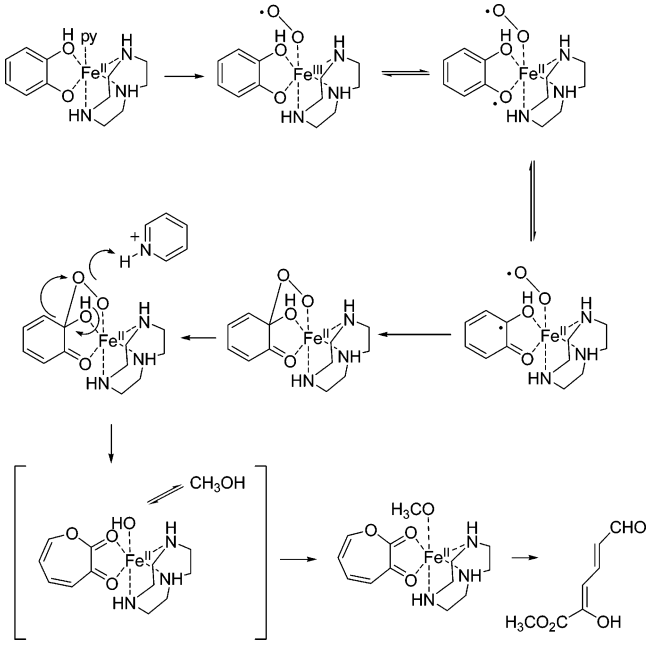

of the according iron complexes to dioxygen.[282,283] However, using $FeCl_2$/$FeCl_3$, TACN, and pyridine, the oxygenation of catechol lead to 2-hydroxymuconic semi-aldehyde methyl ester in about 50% yield.[284] A kinetic analysis of this system was performed according to the Michealis−Menten method, and two different reaction mechanisms were postulated for the extradiol and the intradiol cleavage of the iron(II) and iron(III) complexes, respectively (Schemes 16 and 17).[285]

The iron(III) complex of the tetraazamacrocycle *N,N′*-dimethyl-2,11-diaza[3,3](2,6)pyridinophane (LN_4R_2, Scheme 9) has been used as an efficient catalyst in the conversion of $dbcH_2$ to 3,5-di-*tert*-butylmuconic anhydride and, as such, in modeling the intradiol cleavage of catechol dioxygenase.[286] During the course of these investigations, it was possible to fully characterize a low-spin iron(III) semiquinonate complex and to establish that for the iron/LN_4Me_2 system most likely no initial electron-transfer step occurs to produce an iron(III) semiquinonate or a ternary semiquinonato superoxo iron(III) complex as intermediate during the intradiol cleavage reaction.[287] Furthermore, Girerd, Banse, and co-workers recently claimed that the iron(III) complex of LN_4H_2, the nonmethylated form of LN_4Me_2, showed nearly the same activity in regard to catechol cleavage as the TPA system.[288] However, no dependence of the observed rate constants on dioxygen concentration and temperature was reported. Interestingly, the authors describe that extradiol cleavage is also observed.

4.3. Complexes with Bi- and Tridentate Ligands

Several mononuclear iron(III) peroxo complexes with the chelating ligands 2,2′-bipyridyl and phenanthroline were characterized. An alkylperoxo intermediate [$Fe^{III}(bpy)_2(OO^tBu)]^{2+}$ was characterized spectroscopically from the reaction of a dinuclear precursor

Scheme 17. Intradiol Cleavage by Macrocyclic Iron Complex

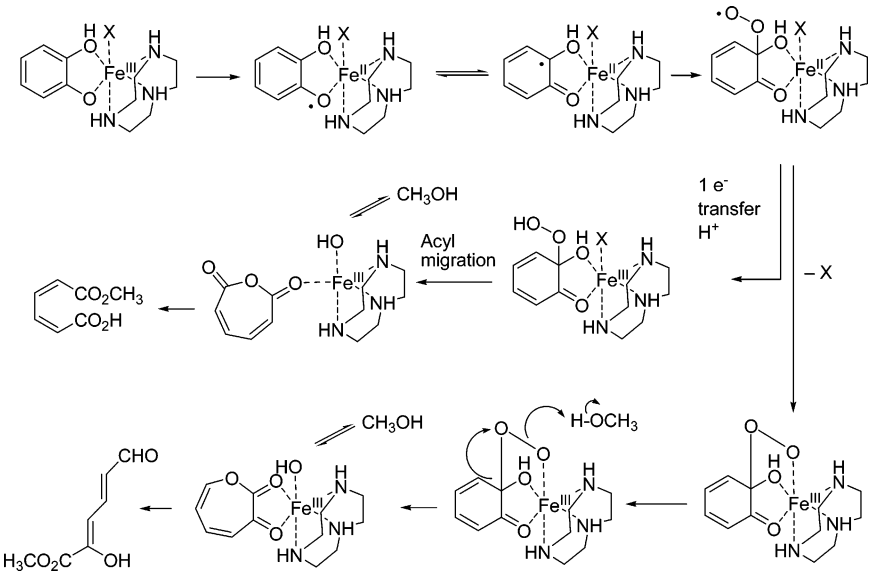

$[Fe_2O(bpy)_4(H_2O)_2]^{4+}$ with ^{t}BuOOH in acetonitrile at −10 °C.[289] Earlier, catalytic oxidation of hydrocarbons and other substrates was observed in this and related systems.[290,291] The stability and reactivity of the monoiron(III) alkylperoxo as well as of the related hydroperoxo complexes (including $[Fe^{III}(bpy)_2(OO\text{-}^tBu)]^{2+}$, $[Fe^{III}(bpy)_2(OOH)]^{2+}$, and $[Fe^{III}(phen)_2(OO\text{-}^tBu)]^{2+}$) were investigated more recently.[292] It was found that the rate of self-decomposition of the iron−peroxo intermediates did not change in the presence of organic substrates (cyclohexane, cyclohexene, or methyl phenyl sulfide), which excluded the possibility of a direct oxidation of the substrates with the identified iron peroxo intermediates.[292] It is possible that a transformation to a high-valent iron species is the rate-limiting step of the substrate oxidation in these systems.[42] The chemistry of dinuclear iron(III) peroxo complexes with 2,2′-bipyridyl, phenanthroline, and their derivatives is presented at the end of section 5.5.3.

Most recently (and based on earlier work), a highly enantioselective iron-catalyzed sulfide oxidation with hydrogen peroxide as oxidant was reported.[293] The complex used is prepared in situ from iron(III) acetylacetonate complexes and a tridentate Schiff base ligand Sbl (Scheme 9), in combination with different carboxylic acids as additives. However, so far, no kinetic investigations were performed and no mechanism was proposed.

4.3.1. Iron Complexes with Tris(pyrazolyl)borate Ligands

The usefulness of tris(pyrazolyl)borate ligands in biomimetic iron/dioxygen chemistry was demonstrated by Kitajima and co-workers, who showed that the complexes $[Fe(O_2CR)(HB(3,5\text{-}^iPr_2pz)_3)]$ can be reversibly oxygenated at low temperature in noncoordinating solvents (e.g., toluene).[294,295] Spectroscopic studies (UV−vis, resonance Raman, NMR, and EXAFS) provided evidence for the formation of dinuclear peroxo intermediate complexes during this reaction,[295] and finally the crystal structure of the complex $[Fe_2(\mu\text{-}O_2)(\mu\text{-}O_2CCH_2Ph)_2(HB(3,5\text{-}^iPr_2pz)_3)_2]$ was reported.[172]

More recently, Que and co-workers, following up on previous work, investigated the reaction of the iron(II) complex of the ligand Tp^{Ph2} (hydrotris(3,5-diphenylpyrazol-1-yl)borate) with carboxylic acids as additional ligands to gain better insight into the mechanism of α-keto acid-dependent dioxygenases.[296−299] The complex $[Fe(Tp^{Ph2})(BF)]$ turned out to be an excellent candidate for kinetic examination, as both the iron(II) precursor and the iron(III) phenolate product have been fully characterized. Using stopped-flow techniques or regular UV−vis spectroscopy, the time-resolved appearance of the iron(III) phenolate chromophore was measured at 650 nm in benzene at different temperatures. The reaction with dioxygen is second order with a rate constant of $k = 0.11\ M^{-1}\ s^{-1}$ at 30 °C and the activation parameters of $\Delta H^{\ddagger} = 25(2)$ kJ mol^{-1} and $\Delta S^{\ddagger} = -179(6)$ J mol^{-1} K^{-1} (temperature range from +10 to +70 °C). The large negative value for $\Delta S^{\ddagger}$ suggests that the rate determining step is associative; however, this value must be derived from contributions of several elementary reactions, and therefore, care must be exercised in the interpretation of these data. The effect of ring substitution in the benzoylformate ligand was investigated, and a good correlation was obtained in the Hammet plot. In contrast to the case of the BF complex, the reactions of dioxygen with the complexes with benzoate or acetate were much slower, leading to 55(5)% of the hydroxylated product. A mechanism was proposed according to Scheme 18.

4.4. Complexes with Tetra- and Pentadentate Ligands

4.4.1. Complexes with Salen Ligands

A kinetic study on the oxygenation of organic sulfides to the corresponding sulfoxides with iodosobenzene using iron(III) complexes with Salen and Salen derivatives (Scheme 9) has been published.[300] With data fitting to Michaelis−Menten kinetics, a mechanism involving iron(IV) intermediates was proposed (Scheme 19).

Scheme 18

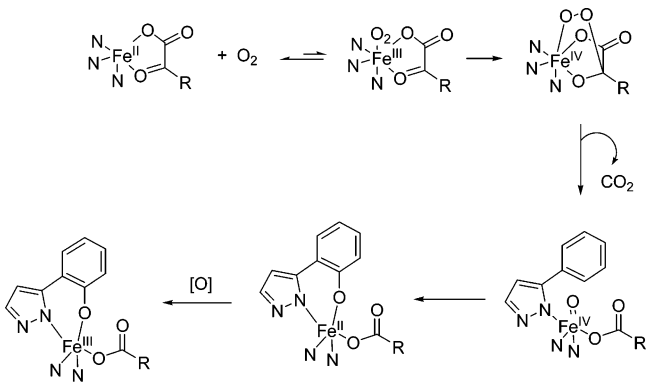

Scheme 19. Proposed Catalytic Mechanism of the Iron−Salen Complex

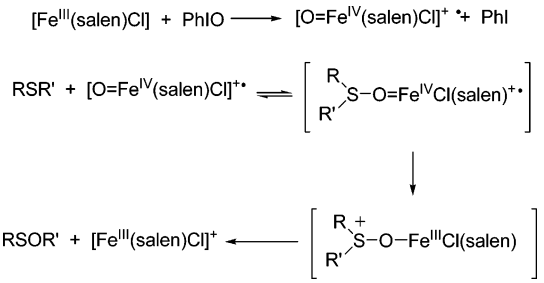

Scheme 20. Model of Iron Bleomycin

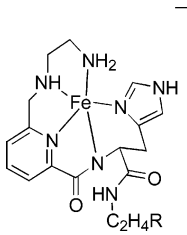

In a more recent study of iron(III) complexes with chiral Salen derivatives, it was found that only PhIO effected asymmetric sulfoxidations, while other terminal oxidants (H_2O_2, NaOCl, *m*-chlorobenzoic acid) lead to the formation of racemic products.[301] It was proposed that a ternary iodosylbenzene−salen−iron(III) complex could be directly responsible for sulfoxidation, and EPR spectroscopic evidence for such an intermediate was presented.

4.4.2. Complexes with Amide-Containing Ligands (Bleomycin Models)

Modeling the anticancer drug bleomycin, the reaction of dioxygen with iron(II) complexes with pentadentate ligands incorporating a carbamide group (Scheme 20) was investigated using stopped-flow techniques.[302] Two reaction steps were observed at 20 °C in TRIS buffer at pH 7.2 according to the fit of the absorbance vs time traces with k_{obs}(fast), showing a linear dependence on dioxygen concentration (calculated second-order rate constant for R = $CONH_2$: $k = 1.1 \times 10^4$ mol^{-1} L^{-1}), while k_{obs}(slow) was independent of dioxygen concentration ($k = 0.62$ s^{-1}). However, no activation parameters were reported. The rate constants for the complexes with other substitutents were nearly identical and very close to the data obtained for the iron(II) bleomycin under the same conditions.

4.4.3. Complexes with the Tripodal Ligand TPA and Its Derivatives

Besides the derivatives of the tridentate ligands tris(pyrazolyl)borates ($HB(3,5\text{-}R_2pz)_3$) and the macrocycle triazacyclononane (TACN), the tetradentate ligand tris(2-pyridylmethyl)amine (TPA) and its derivatives (Scheme 9) have proven to be extremely versatile ligands in bioinorganic chemistry.

Modeling successfully the intradiol cleavage of catechol dioxygenases has been accomplished using the iron(III)−TPA complex and catechol.[3,303] This system so far is the most active species in the oxidative cleavage of catechols, despite many efforts to increase the rate of this reaction using other ligands.[3,304−307] A reaction mechanism was proposed; however, the proposed intermediates could not be detected spectroscopically.[3,303] Second-order rate constants of the reaction between $[Fe^{III}(TPA)(DBC)]^+$ and O_2 in DMF (15 M^{-1} s^{-1}) and methanol (10 M^{-1} s^{-1}) were obtained at 25 °C; however, no temperature dependence measurements were performed and no activation parameters calculated.[303] In contrast, in an earlier study using tripodal NTA (nitrilotriacetate), PDA (*N*-(2-pyridylmethyl)iminodiacetate), and BPG (*N*,*N*-bis(2-pyridylmethyl)glycinate) as ligands, activation parameters were determined and demonstrated large negative activation entropies suggesting an associative reaction mechanism.[308]

Very recently, a detailed kinetic study on the TPA system was conducted, and a large negative value was obtained for the activation entropy ($\Delta H^{\ddagger} = 23 \pm 1$ kJ mol^{-1} and $\Delta S^{\ddagger} = -199 \pm 4$ J mol^{-1} K^{-1}).[309] In this study, the effect of chelate ring size (Scheme 21) in the iron complexes was investigated, similar to the cases of previous studies on the dioxygen activation with related copper complexes.[310,311] The measurements cleary demonstrated that neither increasing nor decreasing the chelate ring size of the iron TPA complex lead to higher reactivity; in contrast to the expectations, reaction rates decreased dramatically compared to that of the TPA system.

An interesting approach of using an iron(III) TPA complex for the oxidative cleavage of chloro catechols has been described by Funabiki and co-workers.[312] The reaction is about a factor of 10^3 slower compared with that of the $[Fe(TPA)(DBC)]^+$ complex.[303]

A study by Que and co-workers on modeling the extradiol-cleaving catechol dioxygenases using iron(II) complexes with 6-Me_3-TPA (a methylated analogue of TPA, R = CH_3, Scheme 9) and in comparison the related ligand 6-Me_2-bpmcn (Scheme 9) has been published recently.[313] Rate constants for the oxidation of the iron(II) catecholate complexes to the iron(III) catecholate complexes, as well as decomposition reactions of the iron(III) complexes, were reported at 22 °C in acetonitrile. Very interesting in this work is the approach to include reactions with NO with the iron(II) complexes as a "dioxygen surrogate" to obtain additional information on the mechanisms of these reactions.

Furthermore, iron complexes with TPA and substituted derivatives have been successfully used as models for α-keto acid-dependent non-heme iron enzymes, and a detailed mechanistic study was

Scheme 21. Tripodal Aminopyridine Ligands with Systematically Varied Arm Length

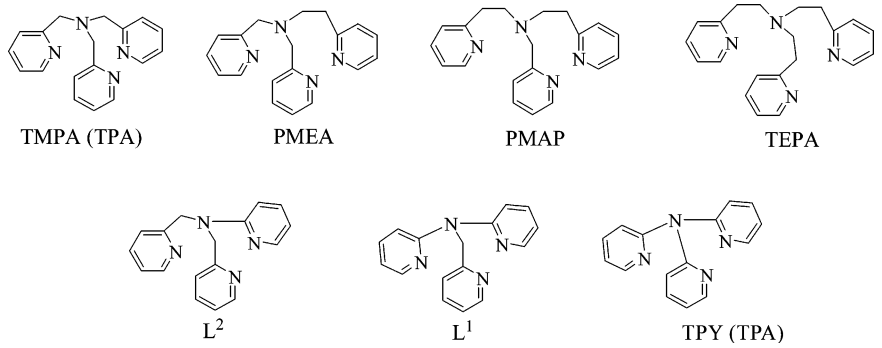

Scheme 22. Modeling α-Ketoacid-Dependent Non-heme Iron Enzymes

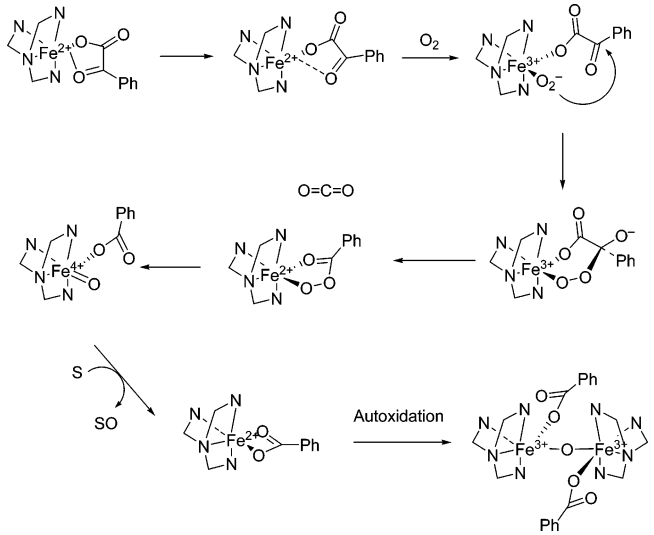

performed on these systems.[314] Using the 6-Me_3-TPA ligand, benzoylformate (BF) as the α-keto acid, and iron(II) to obtain $[Fe^{II}$(6-Me_3-TPA)(BF)]ClO_4, the kinetics of this complex with dioxygen was studied at 30 °C (unfortunately no temperature dependence study was reported, and details on the kinetic analysis are missing). The observed rate constants k_{obs} (with k_{obs} assigned as $k[O_2]$) for different $[Fe^{II}$(6-Me_3-TPA)(X-BF)]ClO_4 complexes (X = different substituents at the benzene ring of BF) allowed for a good correlation in a Hammett plot. A reaction mechanism for the oxygenation of this system was proposed (Scheme 22).

A similar iron(II) complex [Fe(II)(6-Me_3-TPA)(O_2-CPh)]$^+$ has been used as a model complex for the redox cycle of lipoxygenase with an alkyhydroperoxide as an oxidant.[315] However, kinetic measurements were only reported for the decomposition of the alkylperoxoiron(III) intermediate.

When $[Fe^{II}(TPA)(CH_3CN)_2]^{2+}$ is reacted with peracetic acid in acetonitrile at low temperatures, the formation of $[Fe^{IV}(O)(TPA)]^{2+}$ can be observed spectroscopically.[191] Indirect evidence for the formation of $[Fe^{IV}(O)(TPA)]^{2+}$ as an intermediate was obtained during the investigation of the oxidation of alkanes with the iron(II) TPA complexes and ^{t}BuOOH.[316] Very recently, Que and co-workers successfully documented the homolysis of the $Fe^{III}(OO^tBu)$ intermediate to form $[Fe^{IV}(O)(TPA)]^{2+}$ and observed a dramatic acceleration of the reaction (a "push" effect) and an improved yield of the Fe(IV) product, when a Lewis base (e. g., pyridine *N*-oxide) was added (an increase of a factor of 100 was observed for the first-order rate constant when 10 equiv of PyO was added).[192] Analysis of the temperature dependence of the reaction rates afforded activation parameters (without PyO and with 10 equiv PyO) ($\Delta H^{\ddagger}$ = 52(1) and 50(2) kJ mol^{-1}; $\Delta S^{\ddagger}$ = −74(3) and −42(10) J mol^{-1} K^{-1}) that were quite different compared to those for the iron porphyrin complexes investigated previously. The push effect in this non-heme system turned out to be much more significant than that in the heme complexes.

Complex $[Fe^{II}(TPA)(OTf)_2]$ reacts with H_2O_2 in acetone at −90 °C, yielding an unexpected complex with a solvent-derived peroxo ligand, $[Fe^{III}(TPA)(OOCMe_2OH)]^{2+}$, which is thermally unstable and decomposes in a single-exponential process (T = −75 to −45 °C; $\Delta H^{\ddagger}$ = 54(3) kJ mol^{-1}; $\Delta S^{\ddagger}$ = −42(12) J mol^{-1} K^{-1}) to form $[Fe^{IV}(O)(TPA)]^{2+}$.[226] The kinetic parameters of the O−O bond homolysis in $[Fe^{III}(TPA)(OOC(CH_3)_2OH)]^{2+}$ are very similar to those previously observed for the OO^tBu analogue (see above). The oxoiron(IV) complex $[Fe^{IV}(O)(TPA)]^{2+}$ is also thermally unstable and can oxidize substrates (e.g., PhSMe),[191,226] but the kinetics of its reactivity has not been studied.

The reaction of $[Fe^{II}(TPA)(MeCN)_2]$ with H_2O_2 in MeCN or MeCN/CH_2Cl_2 at low temperature gives a hydroperoxo complex $[Fe^{III}(TPA)(OOH)(H_2O)]^{2+}$ that was characterized spectroscopically.[226,317,318] The $[Fe^{III}(TPA)(OOH)(H_2O)]^{2+}$ intermediate decomposes with a first-order kinetics, $k = 1.2 \times 10^{-3}$ s^{-1} at −50 °C in MeCN/CH_2Cl_2 (1:1).[318] A discussion on the possible mechanism of the catalytic alkane oxidation with this and other Fe(III)−OOH intermediates outlining the importance of the spin state has been reported previously.[42] Two different mechanistic pathways were proposed for olefin cis-dihydroxylation (depending on the spin state, an electophilic or a nucleophilic mechanism is dominant).[214] Olefin cis-dihydroxylation and epoxidation reactions have been demonstrated as different facets of the reactivity of the Fe(III)−OOH intermediates, whose spin states can be modulated by the electronic and steric properties of the ligand environment (a key feature for olefin cis-dihydroxylation is the availability of two cis sites for exogenous ligand binding).[209,213] A recent study suggested that dinuclear rather than mononuclear iron(III) hydroperoxo complexes are the active intermediates in the hydrocarbon oxidations.[318]

Scheme 23

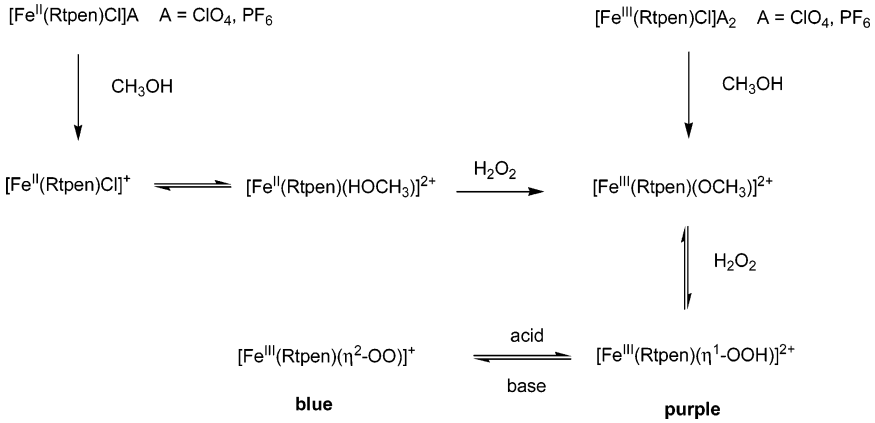

4.4.4. Tren-Based Ligands

In copper dioxygen chemistry, it has been shown that ligands derived from tren can be used very efficiently in a similar way as TPA, e.g., to stabilize an end-on superoxo complex.[319,320]

In iron chemistry, Borovik and co-workers successfully used a tren derivative (trianion of tris[(*N*′-*tert*-butylureaylato)-*N*-ethyl]amine, trenur, Scheme 9) to stabilize (by hydrogen bonding) a monomeric Fe(III)−oxo complex such that a crystal structure of this compound could be obtained.[321,322] Interestingly this oxo complex was obtained directly in a reaction of the precursor complex with dioxygen; however, no kinetic investigations were reported so far.

4.4.5. Complexes with Rtpen Ligands

If one pyridine arm in the ligand of TPA is replaced by the aliphatic amine arm $C_2H_4-NH_2$, the versatile ligand uns-penp (Scheme 9) is obtained−first introduced into copper chemistry by Mandel and coworkers[323]−that allows for a facile further ligand modification.[324−326] Substitution of the protons in unspenp by one 2-pyridylmethyl arm and a variable organic group leads to the versatile ligand system Rtpen (Scheme 9); however, synthesis of these ligands is usually performed in a different way.[327,328]

Iron(II) complexes of these ligands are not reactive toward dioxygen. However, reaction of an excess of hydrogen peroxide with either iron(II) or iron(III) complexes of Rtpen in methanol causes the formation of transient purple species characterized spectroscopically as end-on hydroperoxo complexes; furthermore, these complexes can be deprotonated to give transient blue species characterized spectroscopically as side-on mononuclear peroxo complexes.[167,327−332] A valid effort to stabilize either of these species by hydrogen bonding when using EtOHtpen as ligand (the crystal structure of $[Fe(EtOHtpen)Cl]PF_6$ indicated this possibility) unfortunately was unsuccessful and caused the opposite effect, the destabilization of the intermediate complexes. From a variety of spectroscopic techniques and some kinetic studies (see below), a general mechanism for the ligand substitution reactions was proposed (Scheme 23).

The oxidation of the iron(II) Rtpen complexes with hydrogen peroxide is a fast reaction that can be observed using stopped-flow-techniques. Unfortunately, so far, a detailed kinetic analysis of this reaction sequence could not be performed due to experimental problems. The final product of this reaction is the iron(III) complex, and the subsequent substitution reactions are the same as if the iron(III) complex is used right away from the beginning. The advantage of using the iron(II) complex as starting material is that this complex is stable in solution in contrast to the cases of the iron(III) complexes.

Scheme 24

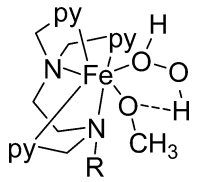

The reaction of the iron(III) complex with hydrogen peroxide has been analyzed in detail, and the following activation parameters were obtained for this reaction: $\Delta H^{\ddagger} = 53 \pm 2$ kJ mol^{-1} and $\Delta S^{\ddagger} = -72 \pm 8$ J mol^{-1} K^{-1}. The negative value for $\Delta S^{\ddagger}$ indicates a mechanism with an associative character; however, a value for $\Delta V^{\ddagger}$ to support this hypothesis is not available at present. A seven-coordinated iron(III) complex was suggested in the transition state (Scheme 24) that would give a plausible explanation for why methanol is an excellent solvent for these reactions. Once this complex is formed, loss of methanol to give the hydroperoxide product might then occur by transferring the proton on the noncoordinated peroxide oxygen atom to the methoxide group. To some extent, this transition state might suggest an explanation for the lack of formation of alkylperoxide complexes in the reactions with ^{t}BuOOH.

Furthermore, a modified ligand system of Rtpen based on a 1,3-diaminopropane unit instead of a 1,2-diaminoethane backbone has been investigated.[333] It was observed that this modification diminished considerably the stability of the Fe(III)−OOH species formed. A kinetic investigation on the formation of this species (using the methyl derivative of this ligand) revealed nearly identical activation parameters ($\Delta H^{\ddagger} = 53$ kJ mol^{-1} and $\Delta S^{\ddagger} = -66$ J mol^{-1} K^{-1}) as observed for the iron Bztpen complex described above.

Scheme 25

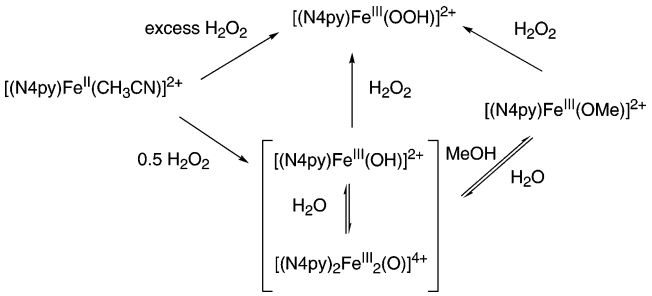

Quite interesting is the reaction of the iron(II) complex of a tren-based ligand (derived from 3-mercapto-3-methyl-2-butanone and tren and related to Rtpen) with superoxide in a methanol/THF mixture.[334] Most likely, an iron(III) hydroperoxo intermediate is formed; however, the reaction turned out to be too fast for stopped-flow measurements at ambient temperatures.

Iron(IV) complexes $[Fe^{IV}(O)(Metpen)]^{2+}$ and $[Fe^{IV}(O)(Metppn)]^{2+}$ were obtained in solution from the reaction of the respective Fe(II) complexes with ClO^- in MeOH at −60 °C and characterized by spectroscopy.[194] The ferryl(IV) complex of Metppn can epoxidize olefins; however, no kinetic parameters for these reactions have been reported.

The iron(IV) complex $[Fe^{IV}(O)(Bztpen)]^{2+}$, obtained from $[Fe^{II}(Bztpen)(OTf)](OTf)$ and PhIO in MeCN, is relatively stable at room temperature ($\tau_{1/2} = 6$ h at 25 °C) and was characterized by mass-spectrometry and Mössbauer and UV−vis spectroscopy.[193] The high-valent complex $[Fe^{IV}(O)(Bztpen)]^{2+}$ oxidizes Ph_3CH to Ph_3COH in a second-order reaction ($k = 0.083$ M^{-1} s^{-1}); Ph_3CD was hydroxylated much more slowly, indicating a very large value of the kinetic isotope effect in this reaction (KIE ∼ 50), similar to those for such reactions as methane hydroxylation by intermediate Q of MMO and taurine hydroxylation by the Fe^{IV} intermediate of the TauD enzyme.[193] Several other hydrocarbons (e.g., ethylbenzene, toluene, cyclohexane) were oxidized by $[Fe^{IV}(O)(Bztpen)]^{2+}$, and a linear correlation between the second-order reaction rates of these reactions and the C−H bond energies was obtained, pointing to the hydrogen atom abstraction as a probable mechanism.

4.4.6. Complexes with the Ligand N4Py

The pentadentate ligand N4Py (*N,N*-bis(2-pyridylmethyl)-*N*-(bis-2-pyridylmethyl)amine, Scheme 9) can be regarded as a TPA derivative in which one of the hydrogen atoms of a CH_2 group has been substituted by an additional 2-pyridinyl group. Similar to the Rtpen iron system (discussed above), the iron(II) complex of N4Py can be oxidized by hydrogen peroxide, and a quite stable hydroperoxo complex was formed during this reaction.[186] While a detailed kinetic study is still missing, crystallography together with spectroscopic measurements allowed the authors to propose a scheme describing the conversion of different species for this system (Scheme 25).

Catalytic oxidations of alkanes with this complex system using hydrogen peroxide or peracids as terminal oxidants were performed (kinetic isotope effects for the formation of cyclohexanol were investigated).[335,336] Furthermore, the reactions of the Fe(III)−OOH species with base to form the side-on peroxo derivatives of N4Py complexes were reported recently, similar to the reactions observed for Rtpen discussed above.[337]

The high-valent complex $[Fe^{IV}(O)(N4Py)]^{2+}$ was obtained and characterized by spectroscopy and mass-spectrometry very recently.[193] The properties of $[Fe^{IV}(O)(N4Py)]^{2+}$ are similar to those of $[Fe^{IV}(O)(Bztpen)]^{2+}$ (see section 4.4.5 above), but the N4Py complex is more stable and less reactive with hydrocarbons. The reactivity of the ferryl(IV) species in substrate oxidation is inversely correlated with their stability.[3] This observation lends support to the earlier claims of very short-lived (and directly unobserved), high-valent iron intermediates in different catalytic systems.

4.4.7. Complexes with Bispidine Ligands

The very interesting bispidine ligands (Scheme 9) that are used by Comba and co-workers in different areas of coordination chemistry also proved to be useful in supporting the formation of iron(III) hydroperoxo and side-on peroxo complexes.[338] While a kinetic analysis has not been reported yet, detailed spectroscopical measurements were performed and structures have been calculated for two side-on peroxo complexes, providing clear evidence for seven-coordinated species. This finding supports the formulation of seven-coordinated side-on peroxo complexes with Rtpen ligands discussed above.

5. Kinetic and Mechanistic Studies of Dinuclear Iron Complexes

As already mentioned in the Introduction, the interest in dinuclear iron complexes comes primarily from the finding of non-heme diiron active centers with an O,N-ligand environment in a number of natural proteins (mostly with dioxygen binding and activating functions).[53,57] Intense exploration of the synthetic dinuclear iron complexes with O,N-donors occurred in parallel with the remarkable progress in the study of their biological counterparts starting in the 1980s. There are a number of recent reviews describing different aspects of the chemistry of non-heme diiron proteins and their synthetic models.[4,23,27−29,160,161] Below, we concentrate on the kinetic and mechanistic studies performed with synthetic diiron species with a minimum of background information.

The non-heme diiron centers in proteins and model complexes with O,N-donors can reach a number of oxidation states spanning from $Fe^{II}Fe^{II}$ to $Fe^{IV}Fe^{IV}$. The diiron(II) state is reactive with dioxygen, yielding different products depending on the nature of ligands and the reaction conditions (Scheme 26). Outer-sphere electron transfer may occur for coordinatively saturated and sterically impeded complexes with sufficiently low redox potential.[339]

Inner-sphere oxygenation seems to be a more common reactivity pathway for diiron(II) complexes.[4,21,23] Formation of the first Fe−O bond and

Scheme 26. Established Pathways of Diiron−Oxygen Reactivity[a]

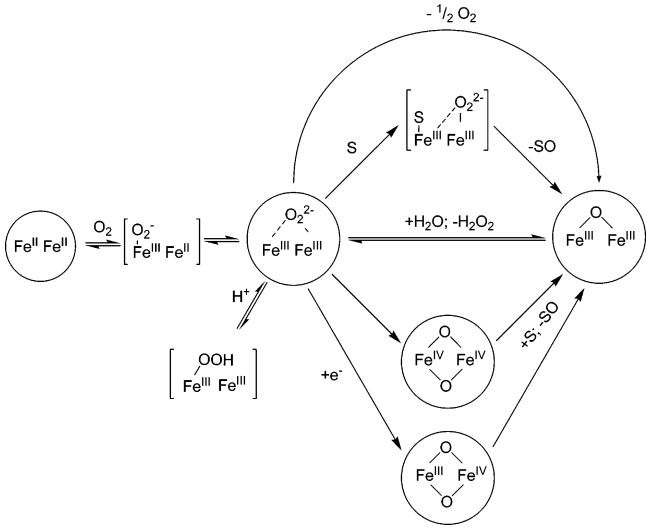

[a] Characterized species are in circles; species implied from kinetic and mechanistic studies are in square brackets.

transfer of one electron should lead to an iron(II)−iron(III)−superoxo intermediate (Scheme 26), which has not been observed for any protein or synthetic complex yet. Instead, a diiron(III)−peroxo composition is ascribed to the adducts observed in such systems, suggesting that the second electron transfer and Fe−O bonding usually are post-rate-limiting events. Several synthetic complexes with μ-1,2-peroxo-bridged diiron(III) cores were characterized structurally,[170−172,181] and such a binding mode is assumed for the peroxo−diiron(III) intermediates of several proteins (sMMO,[49,53,61] stearoyl desaturase,[48,149] ferritin,[153] and RNR mutants[50,139]) and most model compounds.[4,23,196] An unusual synthetic peroxo intermediate, probably with an $Fe^{III}-X-Fe^{III}(\eta^2\text{-}O_2)$ core, was recently characterized by spectroscopic means.[340] Protonation of the peroxide ligand gives a hydroperoxo complex; in hemerythrin, such protonation is intramolecular (a μ-OH ligand provides a proton turning into an oxo-bridge, section 2.2). Several model diiron(III)−hydroperoxo complexes were recently prepared in solution and characterized by spectroscopy.[341,342]

Peroxo−diiron(III) intermediates vary significantly in their stability and reactivity, depending on the nature of the supporting ligands and other conditions. Some of them (like oxyhemerythrin, section 2.2) form reversibly from a diiron(II) complex and dioxygen,[161] but the majority of known peroxo−diiron(III) species form irreversibly and eventually decompose into different types of products. One pathway of the peroxo−diiron(III) species decomposition is the disproportionation into oxo-bridged polyiron(III) complexes and dioxygen.[173] The peroxo intermediate of sMMO undergoes a remarkable transformation into a bis(μ-oxo)diiron(IV) species.[53] Such a reaction has not been achieved in a synthetic system yet, although (μ-oxo)diiron(IV) complexes were recently obtained from an iron(III) precursor and dioxygen, presumably via a (μ-peroxo)diiron(IV) intermediate.[206] Peroxo−diiron(III) species with exchangeable coordination sites can transfer an O atom to organic phosphines and sulfides, and there is strong evidence that the reactions occur intramolecularly upon the coordination of the substrate.[188,343−345] One-electron reduction of a peroxo−diiron(III) complex can yield an oxo-bridged $Fe^{III}Fe^{IV}$ species, a reaction that apparently occurs in the R2 RNR protein.[4,23] Similar chemistry was observed or suggested in some of the model systems leading to $Fe^{III}Fe^{IV}$ complexes.[196,201,346,347] High-valent ($Fe^{III}Fe^{IV}$ and $Fe^{IV}Fe^{IV}$) intermediates are generally much more reactive oxidants than their parent peroxo−iron complexes and can perform even such challenging reactions as alkane hydroxylation.[4,23,27] Substrate oxidation may also be caused in free radical chain processes initiated by the peroxo−iron(III) intermediates;[34,37−39,41,178] such reactions, although important and interesting, are beyond the scope of this review.

Peroxo−diiron(III) complexes can undergo not only redox but also ligand substitution reactions. Liberation of H_2O_2 was observed in the reactions with phenols and carboxylic acids, leading also to the respective phenolate or carboxylate iron(III) complexes.[178] Hydrolysis of a peroxo−diiron(III) complex results in an oxo−diiron(III) species and hydrogen peroxide. Such a reaction is responsible for the "autoxidation" of hemerythrin but is very slow for the native protein due to hydrophobic shielding of the active site (section 2.2). The hydrolysis of iron(III) peroxides is reversible, and the reverse reaction is actually much better studied for model complexes.[180,348] In biochemistry, the formation of peroxo intermediates from H_2O_2 and the (di)iron(III) resting state of redox enzymes is known as the peroxide shunt, often yielding the same reactive species as the reaction of the (di)iron(II) form with dioxygen.[15,53,168] Similar reactivity manifolds were observed with some of the model systems.[196,347,348]

Mixed-valent $Fe^{II}Fe^{III}$ intermediates were observed in several cases during the oxygenation of diiron(II) complexes, most probably due to a one-electron outer-sphere oxidation.[339,349,350] Oxo- or hydroxo-bridged diiron(III) complexes were the final products of these oxygenation reactions. The overall mechanism of these transformations is apparently complex and not well understood yet.

Oftentimes, the reactions of dioxygen with the non-heme diiron(II) complexes lead to oxo-bridged diiron(III) complexes without observable intermediates. The four-electron reduction of the O_2 molecule obviously cannot proceed in one step. It is probable that superoxo, peroxo, and high-valent iron intermediates form in such systems, but in very small steady-state concentrations, while the initial step of O_2 binding is rate-limiting (Scheme 26). Kinetic and isotope labeling studies allowed for insights into the mechanisms of several such reactions.[174,351] Compared to the formation of a peroxo- or high-valent diiron intermediate, the generation of oxo−diiron(III) complexes is less interesting from the viewpoint of dioxygen activation, because in this case all four oxidative equivalents of O_2 have been wasted on oxidizing iron, and nothing is left for the oxidation of a cosubstrate (unless the Fe^{III}/Fe^{II} potential is sufficient for such a reaction).

Very recently, two stable (μ-oxo)diiron(IV) complexes with tetraamidato ligands were obtained in a direct reaction of mononuclear iron(III) precursors and O_2.[206] This unprecedented transformation is possible due to the very strong electron-donating properties of the ligands that stabilize the high-valent state of iron and bring the Fe^{IV}/Fe^{III} redox potential down.

An important question in the chemistry of diiron complexes is whether the dinuclear composition is preserved during the O_2-activating reactions. In enzymes, the diiron center is encapsulated in a protein globule, and the ligand environment is largely preserved by the tertiary structure of the globule throughout the catalytic cycle. Synthetic complexes can change nuclearity upon a redox transformation[295] or even a change in solvent.[352] Several diiron(III) peroxides were assembled from the oxygenation of mononuclear iron(II) complexes.[172,262,295] Reactions of peroxo−diiron(III) complexes yielded not only dinuclear oxo-bridged iron(III) compounds but also tri- and tetranuclear species.[173,295,342] Careful ligand design and selection is required to provide for diiron(II) complexes that could undergo oxygenation and traverse different oxidation states, preserving their dinuclear composition.[4]

5.1. Diiron Complexes with Dinucleating Alkoxide N_6O Ligands

5.1.1. Reactions with O_2

The first detailed kinetic study of the oxygenation of diiron(II) species was done with a series of complexes of dinucleating ligands HPTP, Et-HPTB, and HPTMP (Scheme 9) by Feig et al.[168,173] The results obtained for the HPTP complex were confirmed in a later independent study by Costas et al.[345] The starting complexes $[Fe^{II}_2(\mu\text{-L})(\mu\text{-}O_2CPh)]^{2+}$ have a similar ligand environment around the two 5-coordinate iron(II) centers bridged by an alkoxide residue and a carboxylate residue and also ligated by three N-donor atoms each (Scheme 27). However, there is a significant difference in the steric accessibility of the diiron(II) centers (HPTP > Et-HPTB ≫ HPTMP), which is controlled by the structure of the dinucleating ligands. Oxygenation of the complexes in propionitrile solution at low temperatures (−70 to −20 °C) gives high yields of dioxygen adducts formulated as $[Fe^{III}_2(\mu\text{-L})(\mu\text{-1,2-peroxo})(\mu\text{-}O_2CPh)]^{2+}$. From independent studies, it is known that the formation of the HPTP and Et-HPTB peroxides is irreversible,[353] while the HPTMP dioxygen adduct forms reversibly.[354] Oxygenation of the less sterically hindered diiron(II) complexes (L = HPTP and Et-HPTB) follows mixed second-order kinetics, $v = k[Fe^{II}_2][O_2]$, with almost identical activation parameters ($\Delta H^{\ddagger}$ = 16 kJ mol^{-1} and $\Delta S^{\ddagger}$ = −120 J mol^{-1} K^{-1}).[173] The reaction of the Et-HPTB complex was also characterized by a high-pressure stopped-flow technique (the only such study for the oxygenation of a synthetic diiron(II) complex so far),[173] which gave the volume of activation $\Delta V^{\ddagger} = -13$ cm^3 mol^{-1}. The low activation barrier and negative values of $\Delta S^{\ddagger}$ and $\Delta V^{\ddagger}$ are indicative of an associative mechanism of the oxygenation reaction, which is consistent with the unsaturated coordination sphere of the starting diiron(II) complexes $[Fe^{II}_2(L)(O_2CPh)]^{2+}$ (L = HPTP or Et-HPTB) and the accessibility of the iron centers in them. Oxygenation of the more sterically constrained diiron(II)−HPTMP complex proceeds 10^2−10^3 times slower in the temperature range studied because of a much higher enthalpy of activation ($\Delta H^{\ddagger}$ = 42 kJ mol^{-1}) only partially compensated by a less unfavorable entropy of activation ($\Delta S^{\ddagger} = -63$ J mol^{-1} K^{-1}).[173] The dependence of the reaction rate on dioxygen concentration obtained under pseudo-first-order conditions (excess O_2) at −50 °C was interpreted by Feig et al. as an indication of a partial order (ca. 0.65) in O_2 or a saturation behavior in O_2.[173] However, plotting of the experimental data provided in the Supporting Information by the authors[173] allows for an alternative interpretation. The plots of k_{obs} vs $[O_2]$ at all studied temperatures can be fit satisfactorily as straight lines with significant positive intercepts (Figure 4), kinetic behavior characteristic of a reversible reaction.[103] This interpretation is supported by an independent determination of the reversibility of the reaction between the diiron(II)−HPTMP complex and O_2.[354] Therefore, all three complexes $[Fe^{II}_2(L)(O_2CPh)]^{2+}$ (L = HPTMP, HPTP, and Et-HPTB) are likely to share the same mechanism of dioxygen binding with an associative bimolecular rate-limiting step. The reactions of the less sterically hindered complexes of HPTP and Et-HPTB appear to have highly ordered transition states with dominating bond formation, as seen from the low enthalpies of activation and large negative entropy of activation (Table 6). A much higher value of $\Delta H^{\ddagger}$ and more favorable value of $\Delta S^{\ddagger}$ for the oxygenation of the diiron(II)−HPTMP complex suggests that this reaction involves a more significant degree of bond breaking between the iron(II) atoms and bridging ligands needed to give way to the incoming O_2 molecule.[173]

Scheme 27. Oxygenation of Diiron(II) Complexes with N_6O-Dinucelating Ligands

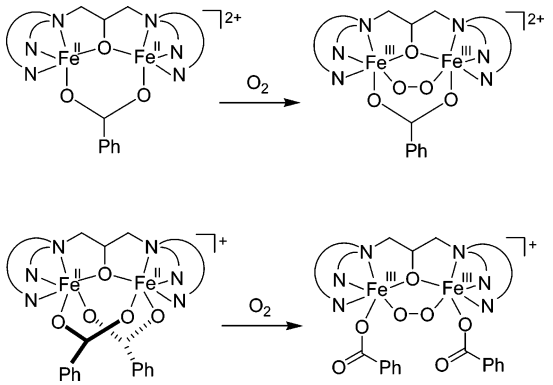

Oxygenation of the diiron(II) complexes with HPTP and two additional carboxylate ligands was studied and directly compared to the reactivity of similar complexes with one carboxylate bridge (Scheme 27).[345] The bis-carboxylate complex $[Fe^{II}_2(\mu\text{-HPTP})(\mu\text{-}O_2CPh)_2]^{+}$ has two six-coordinated iron(II) centers in the solid state. In solution (MeCN or CH_2Cl_2) at low temperature, the complex reacts with O_2 following

Table 6. Kinetic Parameters for Reactions of Diiron(II) Complexes with Dioxygen

complex	solvent	T range, °C	kinetic behavior[a]	k (−40 °C),[b] M^{-1} s^{-1}	$\Delta H^{\ddagger}$, kJ mol^{-1}	$\Delta S^{\ddagger}$, J mol^{-1} K^{-1}	ref
$[Fe_2(HPTP)(O_2CPh)]^{2+}$	EtCN	−70 to −20	P11	$9.6(3) \times 10^2$	16.5(4)	−114(2)	173
$[Fe_2(HPTP)(O_2CPh)]^{2+}$	MeCN	−40 to 0	P11	$7.3(5) \times 10^3$	15.8(4)	−101(10)	345
$[Fe_2(HPTP)(O_2CPh)]^{2+}$	MeCN/DMSO (9:1 v/v)	−40 to 0	P11	$2.8(2) \times 10^3$	8.0(3)	−143(10)	345
$[Fe_2(HPTP)(O_2CPh)_2]^{+}$	CH_2Cl_2	−80 to 0	P11	$6.7(3) \times 10^1$	16.7(2)	−132(8)	345
$[Fe_2(Et\text{-}HPTB)(O_2CPh)]^{2+}$	EtCN	−75 to −15	P11	$1.03(12) \times 10^2$	15.4(6)	−121(3)	173
$[Fe_2(HPTMP)(O_2CPh)]^{2+}$	EtCN	−45 to 20	P1p	8×10^{-1}	42.2(16)	−63(6)	173
$[Fe_2(XDK)(O_2CPh)_2(Im)_2(MeOH)]$	THF	−71 to −60	P11	$\sim 10^4$ [c]	11	−150	175
$[Fe_2(BIPhMe)_2(O_2CH)_4]$	$CHCl_3$	−35 to +40	O21	n/a	33(2)	−39(9)	174
$[Fe_2(DXL)_4(Py)_2]$	CH_2Cl_2	−80 to −30	P11	$2.15(10) \times 10^2$	4.7(5)	−178(10)	188, 340
$[Fe_2(DXL)_4(MeIm)_2]$	CH_2Cl_2	−80 to −30	P11	$3.0(2) \times 10^2$	10.1(10)	−153(10)	188, 340
$[Fe_2(DXL)_4(THF)_2]$	CH_2Cl_2	−80 to −30	P11	$3.22(15) \times 10^2$	14(1)	−135(10)	188, 340
$[Fe_2(OH)_2(6\text{-}Me_3TPA)_2]^{2+}$	CH_2Cl_2	−80 to −40	P11	$6.6(6) \times 10^{-1}$	17(2)	−175(10)	365
$[Fe_2(OH)_2(6\text{-}Me_3TPA)_2]^{2+}$	MeCN	−40 to −5	P11	1.94(11)	16(2)	−167(10)	351
$[Fe_2(OH)_2(TPA)_2]^{2+}$	CH_2Cl_2	−40 to −15	O11	$1.21(6) \times 10^1$	30(4)	−94(10)	351
$[Fe_2(OH)_2(BQPA)_2]^{2+}$	CH_2Cl_2	−70 to −40	O11	3.2(2)	36(4)	−80(10)	351
$[Fe_2(OH)_2(BQPA)_2]^{2+}$	CH_2Cl_2/NEt_3	−65 to −25	P11	2.6(3)	36(4)	−81(10)	351
$[Fe_2(OH)_2(BnBQA)_2]^{2+}$	MeCN	−45 to −20	P11	$2.67(10) \times 10^3$	16(2)	−108(10)	351
MMOH	H_2O	+3 to +35	P11	n/a	92(17)	88(42)	129
Δ9D	H_2O	+6 to +24	P10	n/a	22	−134	150
Hr	H_2O	+5 to +25	P11	n/a	17	−46	96

[a] Types of kinetic behavior: P11, formation of a peroxo−diiron(III) complex, first order in $[Fe^{II}_2]$ and first order in O_2; P10, formation of a peroxo−diiron(III) complex, first order in $[Fe^{II}_2]$ and first order in O_2; P1p, formation of a peroxo−diiron(III) complex, first order in $[Fe^{II}_2]$ and partial order in O_2; O11, formation of an oxo-bridged oligoiron(III) complex, first order in $[Fe^{II}_2]$ and first order in O_2; O21, formation of an oxo-bridged oligoiron(III) complex, second order in $[Fe^{II}_2]$ and first order in O_2. [b] Second-order rate constant. [c] Extrapolated using the activaton parameters.

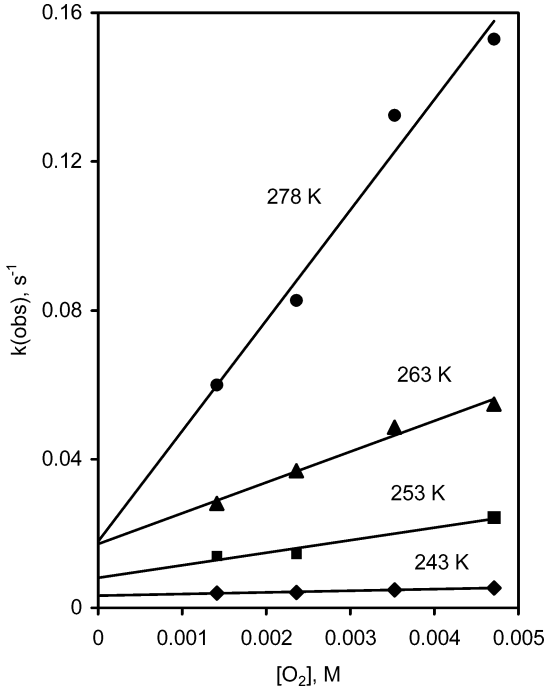

Figure 4. Kinetic plots for the oxygenation of $[Fe^{II}_2(HPTMP)(O_2CPh)]^{2+}$ in EtCN: observed pseudo-first-order rates (excess O_2) vs dioxygen concentration at different temperatures. Data are taken from the Supporting Information of ref 173.

mixed second-order kinetics to give an adduct formulated as $[Fe^{III}_2(\mu\text{-HPTP})(\mu\text{-peroxo})(\eta_1\text{-}O_2CPh)_2]^{+}$. Formation of the peroxo complex from the bis-carboxylate precursor is about an order of magnitude slower than the analogous reaction of the mono-carboxylate due to a more negative entropy of activation, while the enthalpies of activation are nearly the same (Table 6). Therefore, the additional steric bulk in the bis-carboxylate complex and the requirement for a shift from bridging to terminal mode of the carboxylate coordination give rise to a more restricted and highly organized transition state of the dioxygen-binding process.

Oxygenation of the complexes $[Fe^{II}_2(Et\text{-}HPTB)(O_2CPh)]^{2+}$, $[Fe^{II}_2(HPTP)(O_2CPh)]^{2+}$, and $[Fe^{II}_2(HPTP)(O_2CPh)_2]^{+}$ was studied in several weakly coordinating solvents (MeCN, EtCN, $CHCl_3$, CH_2Cl_2, MeCN/CH_2Cl_2 mixtures, and others) and only minor kinetic effects were observed, indicating a passive role of the solvents. There was a general tendency for somewhat higher reaction rates in solvents of higher polarity, in agreement with a polar transition state and the electron transfer during the coordination of the O_2 molecule. However, the oxygenation of $[Fe^{II}_2(HPTP)(O_2CPh)]^{2+}$ in the mixture MeCN/DMSO (9:1 v/v) was characterized by significantly different activation parameters, suggesting that a more strongly coordinating solvent (like DMSO) may change the speciation of the starting diiron(II) complex or otherwise interfere with the reaction.

Oxygenation of several other diiron(II) complexes supported by dinucleating alkoxo and aryloxo ligands was characterized thermodynamically from the determination of the O_2-binding equilibrium constants, but not kinetically.[161,171,176]

5.1.2. Reactions with Hydrogen Peroxide

Peroxo−diiron(III) complexes supported by the dinucleating ligand HPTB and its derivatives were also prepared starting from a diiron(III) precursor and H_2O_2, and the kinetics of these ligand substitution reactions was studied.[180,348,355] The reactions were carried out in strongly coordinating solvents (H_2O, MeOH, DMSO, etc.), which significantly influenced the speciation of the diiron(III) complexes and their kinetic behavior. In all of the solvents, the

Scheme 28. Proposed Two-Step Mechanism for the Reaction of Diiron(III) Complexes with H_2O_2

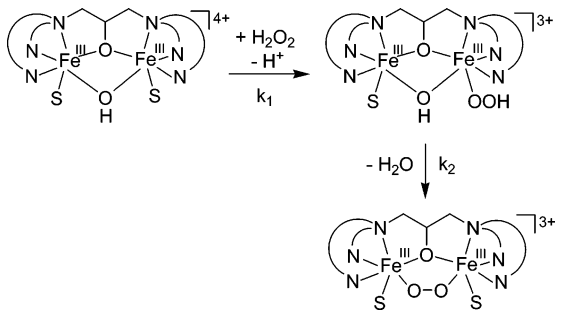

peroxo−diiron(III) complexes with the HPTB family of ligands formed quantitatively.[180,348] In methanol, the equilibrium constant of the H_2O_2 binding at 25 °C was estimated to be greater than 10^6 M^{-1}.[355]

The solid complex $[Fe^{III}_2(\mu\text{-HPTB})(\mu\text{-OH})(NO_3)_2](NO_3)_2$ dissolves in water, yielding the $[Fe^{III}_2(\mu\text{-HPTB})(\mu\text{-OH})(H_2O)_2]^{4+}$ species that reacts with H_2O_2, producing a relatively stable peroxo complex formulated as $[Fe^{III}_2(\mu\text{-HPTB})(\mu\text{-O}_2)(H_2O)_2]^{3+}$ (Scheme 28).[355] The kinetics of this reaction was studied in aqueous solution at different values of pH (pH = 3 was chosen as optimal), at ionic strength = 0.1, and in the temperature range from +5 to +35 °C by Than et al.[180] Under an excess of H_2O_2, the reaction was irreversible and followed one-phase kinetics with a mixed second-order rate law (first order in the diiron(III) complex and first order in H_2O_2) and the activation parameters $\Delta H^{\ddagger}$ = +62.5(5) kJ mol^{-1}, $\Delta S^{\ddagger}$ = +26(17) J mol^{-1} K^{-1}, and $\Delta V^{\ddagger}$ = 0(2) cm^3 mol^{-1}. Such kinetic parameters pointed to the interchange mechanism of the ligand substitution of water for hydrogen peroxide in the rate-limiting step. The authors proposed that this rate-limiting step leads to a diiron(III) complex with a terminal hydroperoxide, which is a steady-state intermediate with low concentration that rapidly gives the final product with a bridging peroxide (Scheme 28).

A similar kinetic study was done with a diiron(III)−HPTB complex containing also a cacodilate bridge.[180] The starting complex was characterized by X-ray diffraction as $[Fe^{III}_2(\mu\text{-HPTB})(\mu\text{-O}_2AsMe_2)(MeO)(MeOH)]^{3+}$ and apparently gives the $[Fe^{III}_2(\mu\text{-HPTB})(\mu\text{-O}_2AsMe_2)(H_2O)_2]^{4+}$ species upon dissolution in water at pH = 3.[180] The reaction with H_2O_2 yields a peroxo complex formulated as $[Fe^{III}_2(\mu\text{-HPTB})(\mu\text{-O}_2AsMe_2)(\mu\text{-O}_2)(H_2O)_2]^{3+}$. Kinetic traces obtained under an excess of hydrogen peroxide were fit to a two-exponential function with k_1 linearly dependent on $[H_2O_2]$ and k_2 independent of it. Activation parameters were obtained for both k_1 and k_2 (Table 7). These kinetic findings were interpreted within a mechanism similar to that for a hydroxo-bridged complex (Scheme 28), but with the second step proceeding much more slowly because of the steric interference from the μ-O_2AsMe_2 ligand.[180]

The reaction of a diiron(III) complex of the dinucleating ligand EtOH−HPTB (Scheme 9) with hydrogen peroxide was studied in several solvents (water, MeOH, MeCN, and DMSO).[348] The starting complex $[Fe^{III}_2(EtOH-HPTB)(\mu\text{-OH})(NO_3)_2](ClO_4)(NO_3)$ was structurally characterized in the solid state and found to have two six-coordinate Fe(III) centers bridged by a hydroxide group with two terminal nitrates. Solution studies indicated that the coordinated NO_3^- anions of the starting complex are almost completely substituted for solvent molecules in H_2O and DMSO but only partially substituted in MeOH and MeCN. Therefore, different species of the starting complex $[Fe^{III}_2(EtOH-HPTB)(\mu\text{-OH})(S)_2]^{n+}$ (S = NO_3^- or solvent) are present in different solvents. The rate of peroxide binding decreased by 3 orders of magnitude in the order H_2O > MeOH > MeCN > DMSO (Table 7). This strong solvent dependency was explained within the mechanism shown in Scheme 28, where the rate-limiting step is the substitution of a terminal ligand S for hydrogen peroxide. Water exchanges rapidly, and the nitrate and solvent molecules in MeOH and MeCN demonstrate intermediate rates, while the strong binding of the DMSO molecules makes the substitution process slow. The rate laws for the reaction in H_2O, MeOH, and MeCN are mixed second order: $v = k[Fe^{III}_2][H_2O_2]$. The activation parameters of the reaction measured in water and methanol (Table 7) indicated an interchange mechanism of the ligand substitution. The rate law in DMSO was more complicated: $v = k_a[Fe^{III}_2] + k_b[Fe^{III}_2][H_2O_2]$, interpreted as two reaction pathways, one of them being independent of the H_2O_2 concentration.

5.1.3. Reactions of Peroxo–diiron(III) Complexes

The stability and reactivity of the complexes $[Fe^{III}_2(\mu\text{-L})(\mu\text{-peroxo})(S)_m]^{n+}$ (L = HPTP, HPTMP, HPTB, and HPTB derivatives) depends significantly on the nature of the alkoxide-bridging ligand L, on the additional ligands S, and also on the solvent.

The decomposition of the three complexes $[Fe^{III}_2(\mu\text{-L})(\mu\text{-peroxo})(\mu\text{-O}_2CPh)]^{2+}$ (L = HPTP, HPTMP, and

Table 7. Kinetic Parameters for Reactions of Diiron(III) Complexes with Hydrogen Peroxide

complex[a]	solvent	T range, °C	k (25 °C)	$\Delta H^{\ddagger}$, kJ mol^{-1}	$\Delta S^{\ddagger}$, J mol^{-1} K^{-1}	$\Delta V^{\ddagger}$, cm^3 mol^{-1}	ref
$[Fe_2(HPTB)(OH)]^{4+}$	H_2O, pH = 3, I = 0.1	+5 to +35	$1.60(4) \times 10^{3}$ [b]	62.5(5)	+26(17)	0(2)	180
$[Fe_2(HPTB)(O_2AsMe_2)]^{4+}$	H_2O, pH = 3, I = 0.1	+5 to +35	$1.60(4) \times 10^{3}$ [c]	57(2)[b]	+2(9)[b]	0.2(30)[b]	180
			$1.9(1) \times 10^{-1}$ [d]	79(4)[c]	+8(13)[c]	−0.3(9)[c]	
$[Fe_2(EtOH-HPTB)(OH)]^{4+}$	H_2O, pH = 3	around RT	$1.46(7) \times 10^{3}$ [b]	55(1)	0(3)	n/a	348
$[Fe_2(EtOH-HPTB)(OH)]^{4+}$	MeOH	0 to +30	$4.90(15) \times 10^{2}$ [b]	53(3)	−17(1)	n/a	348
$[Fe_2(EtOH-HPTB)(OH)]^{4+}$	MeCN	25	$1.15(10) \times 10^{2}$ [b]	n/a	n/a	n/a	348
$[Fe_2(EtOH-HPTB)(OH)]^{4+}$	DMSO	25	3.0(3)[e]	n/a	n/a	n/a	348
			$3.6(5) \times 10^{-3}$ [f]				

[a] Solvent molecules omitted from the formulas. [b] Second-order reaction (k, M^{-1} s^{-1}). [c] Second-order reaction phase (k_1, M^{-1} s^{-1}). [d] First-order reaction phase (k_2, s^{-1}). [e] Second-order reaction pathway (k_b, M^{-1} s^{-1}). [f] First-order reaction pathway (k_a, s^{-1}).

Scheme 29. Pathways of Reactivity and Decomposition of the Diiron(III)−Peroxo Complexes with Alkoxide-Bridging Dinucleating Ligands

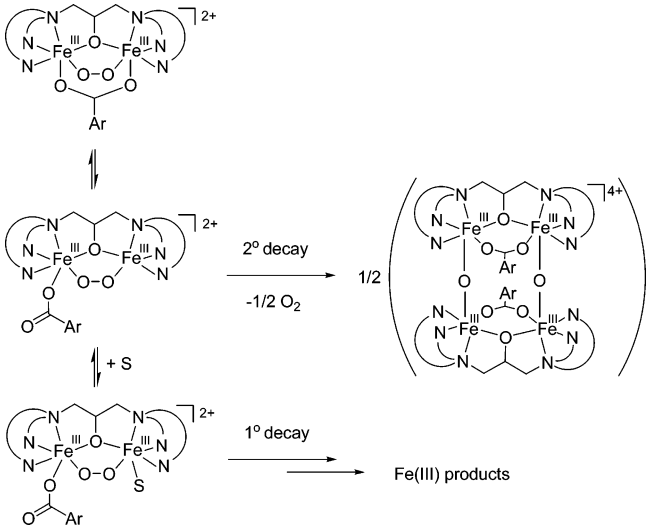

HPTB) was studied in detail and kinetically quantified in thoroughly purified EtCN.[173] These complexes undergo a disproportionation reaction to form dioxygen and oxo-bridged tetrairon(III) complexes (Scheme 29). Isotope-labeling studies using $^{16}O_2$ and $^{18}O_2$ showed that no mixed-labeled $^{16}O-^{18}O$ formed in the reaction. The decomposition reaction is second order in the peroxo−diiron(III) complex and is not influenced significantly by the presence of excess O_2. The reactions demonstrate high activation enthalpies (52 to 113 kJ mol^{-1}) and positive activation entropies (+22 to +187 J mol^{-1} K^{-1}). A proposed mechanism includes a nucleophilic attack of a peroxide from one molecule of the peroxo−diiron(III) complex onto an Fe(III) center of the second molecule leading to a peroxo-bridged tetrairon transition state.[173] One of the peroxo ligands is released as an O_2 molecule, so that no new O−O bond is formed; the O−O bond of the second peroxo ligand is broken to give two oxo bridges in the final tetrairon(III) complex. The close contact of the two $Fe^{III}_2(O_2)$ units required for the reaction becomes more difficult with the deepening of the pocket created by the dinucleating ligand L. This steric factor clearly governed the relative stability of the peroxo complexes that increased in the order HPTP < HPTMP ∼ HPTB.[173]

Electronic effects can also influence the relative stability of these peroxo complexes. The rate of decomposition of $[Fe^{III}_2(\mu\text{-L})(\mu\text{-O}_2)(\mu\text{-O}_2\text{CPh})]^{2+}$ (L = HPTP or Et-HPTB) increased upon introduction of the electron-donating substituents (Me, OMe) in the para-position of the benzoate ligand, and it decreased with the electron-withdrawing groups (Cl, NO_2).[170,345] However, the decay rates for the bis-carboxylate adducts $[Fe^{III}_2(\mu\text{-HPTP})(\mu\text{-O}_2)(\eta_1\text{-O}_2\text{CAr})_2]^{2+}$ (Ar = p-C_6H_4X) were not significantly influenced by the different substituents on the benzoate ligands.[345]

The complexes $[Fe^{III}_2(L)(O_2)(\mu\text{-O}_2\text{CPh})]^{2+}$ (L = HPTP, HPTB, and Et-HPTB) become much more stable in the presence of DMSO or Ph_3PO.[355] It was shown that these ligands (S) add to an iron(III) center to form $[Fe^{III}_2(\text{Et-HPTB})(O_2)(\eta^1\text{-O}_2\text{CPh})(\eta^1\text{-S})_2]^{2+}$; the rate of decomposition of $[Fe^{III}_2(\text{HPTP})(O_2)(\mu\text{-O}_2\text{CPh})]^{2+}$ was inversely proportional to the added Ph_3PO concentration, indicating a reversible binding.[345] Under a large excess of S, complete substitution of the carboxylate occurs to form $[Fe^{III}_2(L)(O_2)(\eta_1\text{-S})_2]^{3+}$; a relatively stable complex $[Fe^{III}_2(\mu\text{-Et-HPTB})(\mu\text{-O}_2)(\eta_1\text{-OPPh}_3)_2](BF_4)_3$ was isolated and structurally characterized.[170] Similarly, the introduction of a second benzoate ligand greatly stabilizes the dioxygen adducts: the bis-carboxylate complex $[Fe^{III}_2(\text{HPTP})(O_2)(\eta_1\text{-O}_2\text{CPh})_2]^{+}$ decays much more slowly than its mono-carboxylate counterpart $[Fe^{III}_2(\text{HPTP})(O_2)(\mu\text{-O}_2\text{CPh})]^{2+}$.[345] The rate law of the decomposition reaction also changes: the mono-carboxylate complex decays via a second-order pathway, while decomposition of the bis-carboxylate is a first-order process (Scheme 29).

The increased stability of the bis-adducts $[Fe^{III}_2(L)(O_2)(\eta_1\text{-S})_2]^{n+}$ (S = $ArCO_2^-$, DMSO, Ph_3PO) compared to the mono-carboxylates $[Fe^{III}_2(\text{HPTP})(O_2)(\mu\text{-O}_2\text{CPh})]^{2+}$ appears to be due to two reasons. First, there is a larger steric bulk created by the additional ligand S around the peroxo−diiron(III) core. Second, the bis-adducts are less labile toward ligand addition and substitution compared to the complexes with a bridging carboxylate that may undergo a dynamic shift (Scheme 29).[345] Both reasons would account for the suppression of the fast bimolecular pathway of decomposition requiring the association of two peroxo−diiron(III) cores.

The diiron(III)−peroxo complex with one carboxylate $[Fe^{III}_2(\text{HPTP})(O_2)(O_2\text{CPh})]^{2+}$ was found to oxidize such substrates as triphenylphosphine, methyl phenyl sulfide, alcohols, phenols, and thiophenols, but not hydrocarbons (even 9,10-dihydroanthracene with weak C−H bonds) at −40 °C in dichloromethane.[345] The bis-carboxylate $[Fe^{III}_2(\text{HPTP})(O_2)(O_2\text{CPh})_2]^{+}$ does not oxidize any of the above substrates under the same conditions. Kinetic studies showed that the O atom transfer from $[Fe^{III}_2(\text{HPTP})(O_2)(O_2\text{CPh})]^{2+}$ to PPh_3 is a fast reaction accelerating linearly at low [PPh_3] but reaching a plateau at higher [PPh_3]. Such behavior indicates a preequilibrium binding of the substrates to the diiron center prior to the oxidation. Noncoordinating substrates do not react, and neither do the diiron(III)−peroxo complexes without an open or easily exchangeable coordination site.[345]

5.2. Complexes with Dinucleating Dicarboxylates

Rigid dinucleating dicarboxylate ligands XDK^{2-}, $PXDK^{2-}$, and $BXDK^{2-}$ (Scheme 9) were used for the prepartion of complexes closely mimicing the coordination environment of the diiron(II) active sites in methane monoxygenase.[175,177] A large series of such model complexes were synthesized and shown by X-ray crystallographic analysis to have the structure $[Fe^{II}_2(\mu\text{-L})(\mu\text{-O}_2\text{CR})(\eta^1\text{-O}_2\text{CR})(\eta^1\text{-L}_N)_2(S)_n]$ with three carboxylate bridges, one terminal carboxylate, two terminal nitrogenous bases L_N, and occasional solvent molecules S (Scheme 30). The diiron(II) complexes are asymmetric, with one Fe^{II} center six-coordinate and the other four- or five-coordinate. The complexes react with dioxygen, and their dinuclear composition is believed to be preserved during the reaction due to the structurally constrained nature of the dicarboxylate ligands.[175,177,356]

Scheme 30. Proposed Mechanism for Oxygenation of Diiron(II) Complexes with Dinucleating Dicarboxylate Ligands

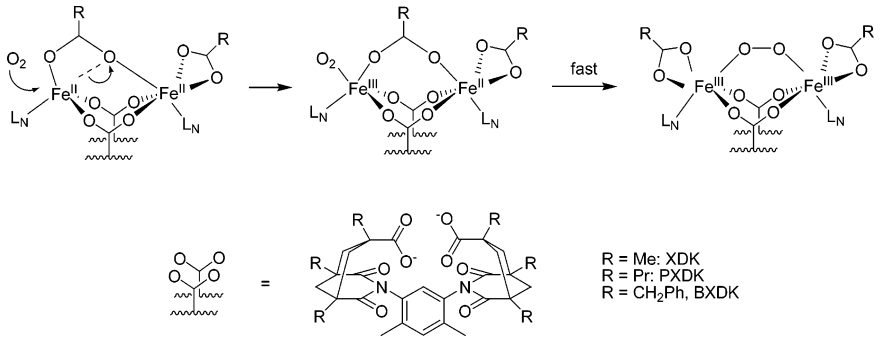

The complexes $[Fe^{II}_2(XDK)(O_2CPh)_2(Im)_2(MeOH)]$ and $[Fe^{II}_2(\mu\text{-}PXDK)(\mu\text{-}O_2C^tBu)_2(MeIm)_2]$, prepared first, reacted with dioxygen very rapidly, with pseudo-first-order rate constants on the order of 10^2 s^{-1} under excess $[O_2] \approx 5$ mM and at the temperature ca. −70 °C in THF.[175] The activation parameters estimated for the oxygenation of the XDK−Im complex, $\Delta H^{\ddagger} \approx 16$ kJ mol^{-1} and $\Delta S^{\ddagger} \approx -120$ J mol^{-1} K^{-1}, are in accord with the values obtained for other diiron(II) complexes (Table 6). The reaction gave small yields of transient intermediates with visible spectral properties reminiscent of (μ-peroxo)diiron(III) species. The intermediates were short-lived and decomposed within minutes or less at temperatures as low as −76 °C. Such instability precluded any detailed characterization of the oxygenated species.[175]

In the second generation of the $[Fe^{II}_2(L)(O_2CR)_2(L_N)_2]$ complexes, more sterically hindered ligands were employed: L = BXDK (containing three benzyl substituents) and $O_2CR = O_2CAr^iPr3$ and O_2CPhCy (bulky monocarboxylates, Scheme 9).[177] The resulting diiron(II) complexes gave high yields of dioxygen adducts that were stable enough at temperatures below −70 °C for detailed characterization. On the basis of the results of Mössbauer, Raman, UV−vis, and other spectroscopies, the intermediates were assigned as (μ-1,2-peroxo)diiron(III) complexes. The rates of their formation depended primarily on the nature of the nitrogenous base L_N. For L_N = Im and *N*-alkylimidazoles, the reaction was very fast (complete within seconds at ca. −70 °C) and required stopped-flow instrumentation, while for L_N = Py it was about 5 orders of magnitude slower and could be followed by conventional UV−vis spectrophotometry. This effect was explained by the higher electron-donating ability of imidazole compared to pyridine that increases the reducing power of the Fe^{II} centers. The influence of carboxylate ligands on the rate of oxygenation was small and rather unexpected: bulkier carboxylates lead to somewhat faster rates. For example, the complex $[Fe^{II}_2(BXDK)(O_2CPhCy)_2(Py)_2]$ with a benzyl-substituted dinucleating ligand reacted with O_2 about four times faster than its methyl-substituted analogue $[Fe^{II}_2(XDK)(O_2CPhCy)_2(Py)_2]$. This effect (relatively minor) was explained by the weaker $Fe^{II}-O_{carboxylate}$ bond in the more strained complexes with bulkier carboxylates that may alleviate the O_2 coordination (Scheme 30).[177] For four pyridine-containing complexes, the kinetics of oxygenation was studied in THF at −77 °C and found to follow the mixed second-order rate law, $v = k[Fe^{II}_2][O_2]$. A mechanism proposed for the oxygenation reaction includes the attack of the O_2 molecule on the unsaturated (five-coordinate) iron(II) center concomitant with the carboxylate shift at this center followed by the coordination to the second, six-coordinate iron(II) center and additional ligand rearrangement (Scheme 30).[177]

The oxygenation of the complexes $[Fe^{II}_2(BXDK)(O_2C^tBu)_2(py)_2]$ and $[Fe^{II}_2(PXDK)(O_2CPhCy)_2(MeIm)_2]$ was irreversible at the studied temperature (ca. −70 °C), as concluded from the persistence of the peroxide species upon vacuum/Ar purge cycles and from the lack of exchange of bound $^{18}O_2$ for free $^{16}O_2$ observed by resonance Raman spectroscopy.[177]

The reactivity of two peroxo complexes, $[Fe^{III}_2(O_2)(PXDK)(O_2CPhCy)_2(1\text{-}Bu\text{-}Im)_2]$ and $[Fe^{III}_2(O_2)(BXDK)(O_2CPhCy)_2(Py)_2]$, was studied in some detail.[178] They did not react with such substrates as PPh_3, $PhCH_2NMe_2$, cyclohexene-3-one, ferrocene, or pentamethylferrocene, indicating weak oxidizing properties of the peroxo−diiron(III) complexes. The PXDK complex decayed in the presence of cobaltocene, thus tentatively placing its redox potential between −1.33 and −0.59 V vs Fc^+/Fc. The complex $[Fe^{III}_2(O_2)(PXDK)(O_2CPhCy)_2(1\text{-}Bu\text{-}Im)_2]$ reacted with 2,4-di-*tert*-butylphenol at −77 °C in THF to form ligand substitution products, an iron(III) phenoxide, and hydrogen peroxide; H_2O_2 was also liberated upon treatment with HO_2CPhCy or CO_2 (kinetics of these reactions was not studied). A general conclusion was made that these peroxo complexes lack electrophilic reactivity and are instead nucleophilic.[178]

All the above-mentioned diiron(III)−peroxo complexes $[Fe^{III}_2(O_2)(L)(O_2CR)_2(L_N)_2]$ (L = PXDK and BXDK) were unstable and slowly decomposed even at −77 °C.[177,178] The decay strongly accelerated at higher temperatures, indicating a rather high activation energy for the process, but no quantitative kinetic data were reported. The decomposition products were tentatively identified as oxo-bridged iron(III) complexes, but their exact composition was not established. The peroxide decay was not accompanied by the evolution of O_2; instead the consumption of additional dioxygen was observed in some cases. There was no ligand oxidation in the process (the dicarboxylates were recovered), but substantial oxidation of solvent was detected.[178] For example, THF produced γ-butyrolactone, and cyclopentane gave cyclopentanol and cyclopentatnone. The kinetic iso-

tope effect $k_H/k_D = 6.2$ was measured for the oxidation of THF. It was also found that the decomposition products of the diiron(III)−peroxo complexes catalyzed the autoxidation of the solvents in air at room temperature, which was quenched by an addition of a noncoordinating radical trap (2,4,6-tri-*tert*-butylphenol). It was concluded that the iron complexes initiate free-radical oxidation of the ethers and hydrocarbons.[178]

5.3. Complexes with Sterically Hindered Monocarboxylates

Another class of carboxylate ligands that were very useful in modeling the active centers of non-heme diiron enzymes are 2,6- or 2,4,6-substituted benzoates, e.g., O_2CAr^{Tol}, O_2CAr^{Mes2}, and DXL (Scheme 9). Diiron(II) complexes of these sterically hindered ligands were recently introduced by Lee and Lippard[357] and independently by Hagadorn, Que, and Tolman[28,179] and showed three structural types: tetracarboxylate-bridged paddle-wheel, dicarboxylate-bridged windmill, and nonsymmetric tricarboxylate-bridged complexes (Scheme 31).[4,23,28] The preferential

Scheme 31. Different Structures of Diiron(II) Complexes with Bulky 2,6-Disubstituted Benzoates

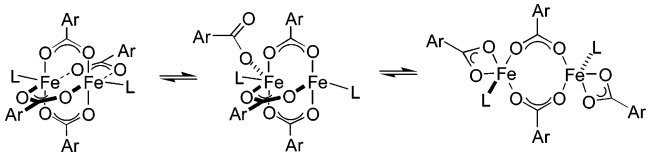

structure of a given complex depends on the steric requirements of specific carboxylate ligands and additional capping ligands (usually, nitrogen donors or THF). Carboxylate shifts are rather rapid in these complexes, so that different forms can interconvert in solutions (Scheme 31).[358] The self-assembled diiron(II) complexes with sterically hindered carboxylates displayed rich biomimetic chemistry, which was recently reviewed,[4,23,28] although new publications continue to appear.[188,189,359] This section will focus on the kinetics and mechanisms of formation and reactivity of dioxygen-derived intermediates in these systems.

5.3.1. Reactions with O_2

All diiron(II) complexes with sterically hindered carboxylates were dioxygen sensitive. The products of their reactions with O_2 depend dramatically on the exact structure of the ligand and on reaction conditions.[4,23,28]

The complex $[Fe_2(O_2CAr^{Tol})_4(Py)_2]$, when exposed to dioxygen in the methylene chloride solution, rapidly produced an emerald-green intermediate, which was stable at low temperature for 6 h but converted into a yellow diiron(III) product upon warming. Similar behavior was observed for the analogous complex with 4-^{t}Bu-pyridine as a capping ligand; the lifetime of 12 h was reported for this species.[123,201] No intermediate was observed, however, for the complex with capping THF in place of capping pyridine.[357] Despite the similarities in the visible spectrum of the green intermediate ($\lambda_{max} \approx 660-670$ nm, $\epsilon = 1600-1700$ M^{-1} cm^{-1})[123,201] compared to the spectra of iron(III) peroxo complexes, resonance Raman spectroscopy revealed no isotope-sensitive Fe−O or O−O vibrations, thus ruling out the formulation of the intermediate as a peroxo species.[201] Mössbauer and EPR spectroscopy established the presence of an equimolar mixture of $Fe^{II}Fe^{III}$ (valence-delocalized) and $Fe^{III}Fe^{IV}$ (valence-trapped) intermediates, along with small amounts (up to 30%) of the $Fe^{III}Fe^{III}$ product.[123,201] Importantly, the rates of formation of both mixed-valence complexes are essentially the same, as determined by freeze-quench EPR ($k_{obs} = 0.18$ min^{-1} in CH_2Cl_2 saturated with O_2 at −78 °C; 1.12 mM $[(4\text{-}^t\text{Bupy})_2Fe_2(\mu\text{-}O_2CAr^{Tol})_4]$).[201] These experimental observations are in agreement with the mechanism of oxygenation shown in Scheme 32. It was proposed that the reaction of a diiron(II) complex with O_2 initially generates an unobservable intermediate (either diiron(III)−peroxo or diiron(IV) species), which reacts with the remaining diiron(II) complex via a one-electron-transfer process yielding equal amounts of $Fe^{II}Fe^{III}$ and $Fe^{IV}Fe^{III}$ species.[123,201] The $Fe^{III}Fe^{III}$ impurity may originate from an independent reaction between the $Fe^{II}Fe^{II}$ starting material and O_2 at low temperature, but a diiron(III) complex is also obtained from the comproportionation of the $Fe^{II}Fe^{III}$ and $Fe^{IV}Fe^{III}$ species upon warming.[201,357] The total consumption of dioxygen, determined in manometric experiments (0.75 mol of O_2 per each mole of diiron(II) complex), exceeds the stoichiometric amount (0.5 mol) necessary for the formation of either the $Fe^{II}Fe^{III}$ and $Fe^{III}Fe^{IV}$ mixture or the $Fe^{III}Fe^{III}$ product.[201] Interestingly, no high-valent $Fe^{III}Fe^{IV}$ intermediate accumulates in the presence

Scheme 32. Dioxygen Activation by the Diiron(II) Complexes of the Ligand O_2CAr^{Tol} (e.g., $[Fe_2(O_2CAr^{Tol})_4(4\text{-}^t\text{BuPy})_2]$)

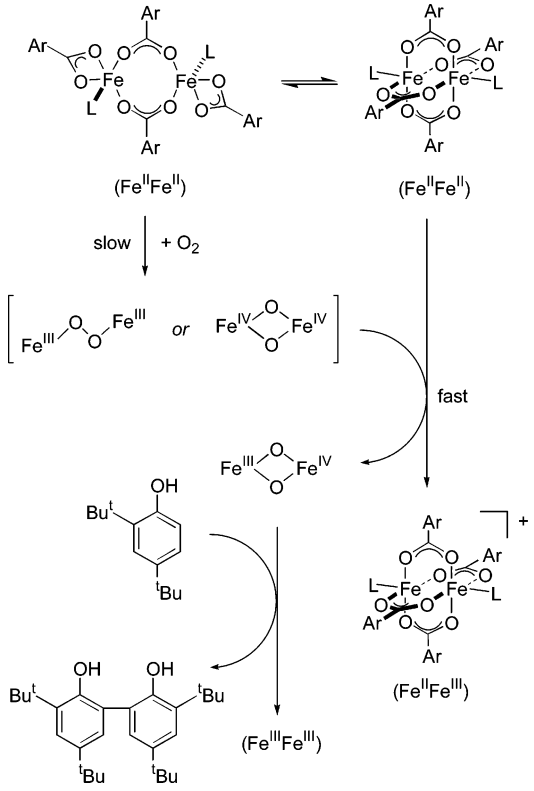

Scheme 33. Dioxygen Activation by the Diiron(II) Complexes of the Ligand DXL

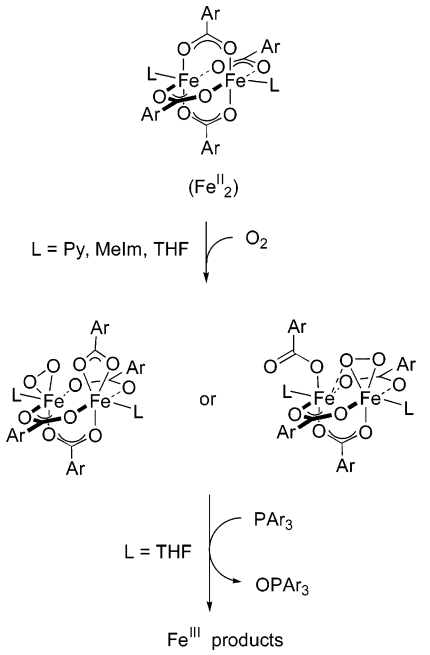

of acid, although formation of the $Fe^{II}Fe^{III}$ species is not affected by acid.[201] Unfortunately, the kinetics of these exciting reactions was not studied in detail.

Diiron(II) complexes with the carboxylate ligand DXL (Scheme 9) showed different reactivity with dioxygen. Oxygenation of the paddle-wheel complexes $[Fe^{II}_2(DXL)_4(L)_2]$ (L = Py, MeIm, THF) at low temperature in scrupulously dry noncoordinating solvents (e.g., CH_2Cl_2 or toluene) cleanly produced an intermediate containing coordinated O_2 (Scheme 33).[188,340] This conclusion was based on resonance Raman data: oxygenation of $[Fe^{II}_2(DXL)_4(Py)_2]$ by $^{16}O_2$ lead to a ν(O−O) band at 822 cm^{-1}, which shifted to 779 cm^{-1} for the $^{18}O_2$-derived intermediate.[340] The ^{16}O-vibrational frequency is somewhat lower than the ^{16}O-^{16}O stretch in typical μ-1,2-peroxo complexes (848−910 cm^{-1}) and resembles the O−O stretch of a side-on, η^2-bound peroxide (with typical values of 816−827 cm^{-1}). The EPR-silent intermediate has two nonequivalent irons, which are present in a 1:1 ratio ($\delta(1) = 1.14$, $\Delta E_Q(1) = 1.27$; and $\delta(2) = 0.52$, $\Delta E_Q(2) = 0.71$ mm/s). The first signal may correspond to a peroxo−iron(III) center, and the second signal is typical for high-spin iron(III) complexes with N,O ligands. Furthermore, a relatively low coupling constant ($J = 30$ cm^{-1}) was determined from the low-temperature Mössbauer measurements in the applied magnetic field. Usually, higher J values (66−200 cm^{-1}) were reported for peroxo-bridged complexes. All spectroscopic data, taken together, allow for two possible structures of the intermediate, which are shown in Scheme 33. Regardless of the exact structure of the intermediate, which remains to be unambiguously established, it is clear that this species contains an O−O fragment coordinated to at least one metal center in a diiron(III) complex.[340]

The UV−vis spectra of the red-brown dioxygen adducts obtained from the diiron(II) precursors with different capping ligands (Py, MeIm, THF) are similar ($\lambda_{max} \approx 500-550$ nm, $\epsilon \approx 1000-1200$ cm^{-1}) but not identical, indicating that the capping ligand is not lost upon oxygenation.[188,340] No evidence for the formation of mixed-valent $Fe^{II}Fe^{III}$ or $Fe^{III}Fe^{IV}$ complexes was reported in the case of the ligand DXL. If traces of water or other impurities were present in the solvent, no intermediates were observed, and the reaction yielded directly Fe(III) oxidation products that were not characterized.[188,340]

The kinetics of dioxygen binding to the diiron(II) complexes $[Fe^{II}_2(DXL)_4(L)_2]$ (L = Py, MeIm, THF) was studied in detail by a cryogenic stopped-flow technique.[188,340] Oxygenation of these coordinatively unsaturated complexes (both iron(II) centers are five-coordinate) occurs rapidly and is complete within seconds even at $T = -80$ °C. The dioxygen binding was found to be an irreversible second-order process (first order in diiron complex and first order in dioxygen). The second-order rate law suggests that rapid dioxygen binding to five-coordinate iron(II) center(s) occurs in a bimolecular associative process. Additionally, low activation enthalpies and large negative activation entropies (Table 6) were determined, typical of associative reactions. Capping ligands L (Py, MeIm, THF) exerted little effect on the kinetic parameters of the oxygenation step, indicating that the electron-donating properties of the monodentate ligands do not alter significantly dioxygen binding rates. Furthermore, oxygenation of the three complexes with different capping ligands proceeded in an isokinetic regime, suggesting a similar rate-determining step for the series of complexes. An isokinetic temperature T_{iso} for the series is seen as a common intersection point of the linear Eyring plot ($T_{iso} = 216 \pm 4$ K), as well as from the linear correlation between activation enthalpy and activation entropy (the slope of the linear fit gave $T_{iso} = 215 \pm 4$ K).[188]

Notably, dioxygen binding to $[Fe^{II}_2(DXL)_4(L)_2]$ (L = Py, MeIm, THF) ($t_{1/2} \approx 10$ s at −80 °C)[188] is significantly faster than the oxygenation of the more sterically constrained complex $[Fe^{II}_2(O_2CAr^{Tol})_4(4\text{-}^tBupy)_2]$ ($t_{1/2} \approx 10$ min at −78 °C).[201] These observations support the importance of steric control in the oxygenation rates of dinuclear iron(II) complexes.

5.3.2. Iron-Based Oxidation of External Substrates

One of the first reports on dioxygen reactivity of diiron complexes with sterically hindered carboxylates uncovered the ability of these systems to oxidize added substrates.[357] Specifically, an intermediate that was generated from a windmill complex $[Fe_2(\mu\text{-}O_2CAr^{Tol})_2(O_2CAr^{Tol})_2(Py)_2]$ and O_2 at −78 °C oxidized 2,4,6-tri-*tert* butylphenol into the phenoxyl radical.[357] Since the oxygenation of this complex produced a 1:1 mixture of $Fe^{II}Fe^{III}$ and $Fe^{III}Fe^{IV}$ species,[123,201] it was important to identify which mixed-valent intermediate brings about the phenol oxidation. The pure Fe(II)Fe(III) complex, prepared independently by a one-electron oxidation of a diiron(II) precursor with Cp_2Fe^+ or AgOTf,[360] did not react with phenols.[201] It was therefore concluded that the high-valent Fe^{III}-Fe^{IV} complex was responsible for the phenoxyl radical production. The oxidation of 2,4-di-*tert*-butylphenol

Table 8. Kinetic Parameters for Decomposition of Peroxo−Diiron(III) Complexes

complex	solvent	order	k_{decomp} (0 °C)	half-life[a] (0 °C), s	$\Delta H^{\ddagger}$, kJ mol^{-1}	$\Delta S^{\ddagger}$, J mol^{-1} K^{-1}	ref
$[Fe_2(HPTP)(O_2)(O_2CPh)]^{2+}$	EtCN	2	9.4×10^3 M^{-1} s^{-1}	0.07	51.9(27)	22(6)	173
$[Fe_2(HPTP)(O_2)(O_2CPh)]^{2+}$	MeCN	2	1.7×10^3 M^{-1} s^{-1}	0.4	44(5)	−21(16)	345
$[Fe_2(HPTP)(O_2)(O_2CPh)]^{2+}$	MeCN, 20 equiv Ph_3PO	2	1.1×10^{-1} M^{-1} s^{-1}	600	40(4)	−97(16)	345
$[Fe_2(HPTP)(O_2)(O_2CPh)]^{2+}$	CH_2Cl_2/DMSO (9:1 v/v)	1	1.45×10^{-1} s^{-1}	4.8	49(4)	−79(12)	345
$[Fe_2(HPTP)(O_2)(O_2CC_6F_5)]^{2+}$	CH_2Cl_2/DMSO (9:1 v/v)	1	4.6×10^{-2} s^{-1}	15	60(4)	−50(8)	345
$[Fe_2(HPTP)(O_2)(O_2CPh)_2]^{+}$	MeCN	1	1.43×10^{-4} s^{-1}	50000	103(4)	59(15)	345
$[Fe_2(HPTMP)(O_2)(O_2CPh)]^{2+}$	EtCN	2	7.3(15) M^{-1} s^{-1}	90	113.3(77)	187(27)	173
$[Fe_2(Et\text{-}HPTB)(O_2)(O_2CPh)]^{2+}$	EtCN	2	1.6×10^1 M^{-1} s^{-1}	44	80.6(39)	74(14)	173
$[Fe_2(Et\text{-}HPTB)(O_2)(O_2CPh)]^{2+}$	MeCN	1	8.8×10^{-3} M^{-1} s^{-1}	80	65(3)	−46(21)	170
$[Fe_2(O_2)(DXL)_4(Py)_2]$	CH_2Cl_2	1	1.2×10^{-1} s^{-1}	6	60(4)	−44(10)	188
$[Fe_2(O_2)(DXL)_4(MeIm)_2]$	CH_2Cl_2	1	2.4×10^{-1} s^{-1}	3	50(4)	−73(10)	188
$[Fe_2(O_2)(DXL)_4(THF)_2]$	CH_2Cl_2	1	5×10^{-1} s^{-1}	1.5	49(4)	−72(10)	188
MMOH	H_2O	1	1.7×10^{-1} s^{-1}	4	122(4)	188(13)	129
Δ9D	H_2O	1	7×10^{-5} s^{-1}	1×10^{5} [b]	80	−41	150

[a] At $c = 10^{-3}$ M starting concentration [first-order $t_{1/2} = (\ln 2)/k$; second-order $t_{1/2} = (\ln 2)/kc$]. [b] At 6 °C.

yielded ~40% of the phenoxyl radical coupling product (3,3′,5,5′-tetra-*tert*-butyl-1,1′-di-2,2′-phenol), which agrees well with the amount of the $Fe^{III}Fe^{IV}$ species determined by the EPR quantitation.[201] The reaction of one-electron phenol oxidation with an Fe(III)Fe(IV) species resembles the chemistry of RNR.[23,50] Therefore, the complex $[Fe_2(\mu\text{-}O_2CAr^{Tol})_2(O_2CAr^{Tol})_2(Py)_2]$ can be considered as a functional model of the R2 RNR protein. Another functional model of R2 RNR, which is based on the diiron complexes of the aminopyridine ligand 6-Me$_3$-TPA,[347] is described in section 5.4 below.

Another carboxylate-bridged complex, $[Fe_2(\mu\text{-}O_2CAr^{Tol})_4(4\text{-}^tBu\text{-}Py)_2]$, promoted oxidative dealkylation of dibenzylpropylamine with dioxygen, yielding low to moderate yields (13−29%, based on Fe_2) of benzaldehyde.[361] The performance of this system improves significantly by tethering the reactive fragment ($PhCH_2N$) to a coordinating group (section 5.3.3 below).

The reactivity of the dioxygen adducts with the diiron−DXL complexes was investigated in detail (Scheme 33).[188] These diiron complexes were different in the nature of the monodentate capping ligand L (L = pyridine, 1-methylimidazole, or THF). These capping ligands exerted little effect on the kinetic parameters of the oxygenation step,[188,340] as discussed above. In contrast, the three dioxygen adducts, tentatively formulated as $[Fe^{III}_2(O_2)(DXL)_4(L)_2]$, displayed different reactivity with the substrates: only the peroxo complex with L = THF oxidized triphenyl phosphine into Ph_3PO at −80 °C in the absence of free dioxygen. The yield of the product (Ph_3PO) was rather high (80% based on the starting diiron(II) complex). The ^{18}O label from $^{18}O_2$ was almost quantitatively incorporated into the phosphine oxide product. Detailed kinetic investigations (single- and double-mixing stopped flow experiments over the temperature range from −80 to −40 °C) were used to study the mechanism of this O-transfer reaction.[188]

The self-decay of all three dioxygen adducts $[Fe^{III}_2(O_2)(DXL)_4(L)_2]$ follows first-order kinetics (for L = MeIm and THF, only in the absence of excess O_2) with relatively low activation enthalpies (49−60 kJ mol^{-1}) and negative activation entropies (−73 to −44 J mol^{-1} K^{-1}) (Table 8). The adduct stability decreases in the following order ($t_{1/2}$ values extrapolated to 193 K are listed in parentheses): L = Py (5 days) > L = 1-MeIm (10 h) > L = THF (4 h). In the presence of excess Ph_3P, the THF-containing intermediate decays at 193 K with $t_{1/2} = 4$ s (ca. 10^4-fold acceleration), while the decomposition of the Py and 1-MeIm complexes did not change.[188] Coordination of the substrate to one of the iron centers is necessary for productive oxidation, as can be judged from the saturation kinetics of phosphine oxidation. These and other kinetic results agree with the mechanism of substrate oxidation shown in Scheme 34. The following kinetic parameters were reported (at $T = -80$ °C): $k_1 = 0.17 \pm 0.03$ s^{-1} (corresponding to the rate of THF dissociation) and $k_2/k_{-1} = 1.7 \pm 0.2$ (corresponding to the relative rates of the reaction with PPh_3 and THF rebound).[188] In contrast to recently reported phosphine oxidation with O_2 catalyzed by a diiron(III) complex, which turned out to be mediated by THF-derived radicals,[362] the reaction in Scheme 34 is retarded by excess THF. The observed first-order rate constants of intermediate decay, measured under saturating phosphine concentration, were almost identical for a series of phosphine derivatives with varying substituents in the *para*-positions of the phenyl rings (OMe, Me, Cl, and F). Furthermore, reaction of the THF-derived peroxo intermediate with pyridine or 1-methylimidazole displayed the same kinetics as the reactions with triarylphosphines. The activation parameters for the substitution of THF for

Scheme 34. Proposed Mechanism of the Oxygen Atom Transfer from a Diiron−Dioxygen Adduct to Triarylphosphines

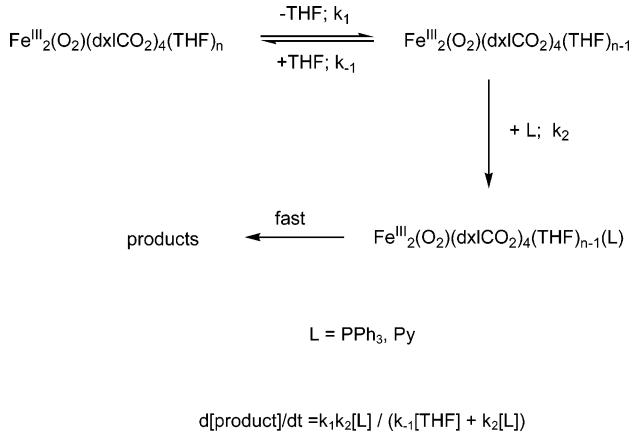

pyridine at the dioxygen adduct were also nearly identical to the activation parameters of the PPh_3 oxidation. Thus, a single-turnover oxygen atom transfer from dioxygen to PPh_3 was kinetically controlled by the dissociation of a monodentate THF ligand from the diiron(III)−peroxo intermediate. It can be concluded that diiron(III)−peroxo complexes with exchangeable ligands can transfer an oxygen atom to coordinating substrates that are good oxygen acceptors (like phosphines). Coordination of the substrate (Ph_3P) to one of the iron centers precedes an oxygen atom transfer.[188]

It is important to note that iron(III)-coordinated peroxides are usually considered to be nucleophilic and unreactive in substrate oxidations.[178] In contrast, protonated peroxides can be responsible for substrate oxidations; activated bleomycin, $(Blm)Fe^{III}(OOH)$, is the best-known example of a coordinated hydroperoxide as an active oxidant (section 2.1). The discovery of phosphine oxidation with a dioxygen adduct of $[Fe_2(DXL)_4(THF)_2]$ clearly shows that an oxygen atom can be transferred from peroxide to good oxygen acceptors (such as phosphines) within the same coordination sphere. It is highly unlikely that any protons could have been present in the reaction media (carefully dried and purified CH_2Cl_2), because an intermediate is extremely moisture-sensitive and does not form in the presence of any traces of moisture or other impurities. Therefore, coordinated peroxides themselves can oxidize reactive substrates via inner-sphere pathways. Substrate coordination is essential for this oxygen atom transfer.[188] These results of the kinetic investigations with model diiron complexes parallel an ongoing work on the reactivity of enzyme peroxo intermediates (e.g., intermediate P from methane monooxygenase) with organic substrates (e.g., olefins).[125,129]

5.3.3. Iron-Based Oxidation of Tethered Substrates

Several diiron(II) complexes with oxidizable groups appended to a capping ligand were reported by Lippard and co-workers (Scheme 35).[189,349,361] The major finding of these studies is a significant increase in the efficiency of oxidation of functional groups positioned close to the diiron center. Although no detailed kinetic data on these reactions were published, the yields of oxidation products for a series of substrates were mechanistically informative.[189] When PPh_2 groups were introduced into the molecules of pyridine ligands, the complex $[Fe_2(\mu\text{-}O_2CAr^{Tol})_3(O_2CAr^{Tol})(2\text{-}Ph_2Ppy)]$ yielded 95% 2-Ph_2P(O)py upon exposure to O_2 in the CH_2Cl_2 solution for 25 min. Moreover, catalytic formation of 2-pyridylphosphine oxide (up to 13 turnovers) was also observed in the presence of excess 2-Ph_2Ppy. Under similar conditions, complexes with 3-Ph_2Ppy or 4-Ph_2Ppy produced 43% or 53% of a phosphine oxide, respectively. It is clear that close proximity to the reactive diiron center facilitates phosphine oxidation, giving advantage to the 2-Ph_2Ppy derivative.[189] The authors cautioned, however, that the exact geometry of the starting complexes was also somewhat different (triply carboxylate-bridged for 2-PhPpy; doubly carboxylate-bridged, windmill for 3-PhPpy; and quadruply bridged, paddle wheel for 4-PhPpy). Sulfoxidation of a 2-PhSpy ligand occurred under analogous conditions (29% sulfoxide was recovered after 90 min of treating the complex $[Fe_2(\mu\text{-}O_2CAr^{Tol})_3(O_2CAr^{Tol})(2\text{-PhSpy})]$ with O_2), and oxidation of 2-benzylpyridine resulted in the formation of α-phenyl-2-pyridylmethanol. No intermediates were observed in these reactions, indicating that dioxygen coordination at the diiron(II) center may be the rate-limiting step.[189]

Scheme 35. Oxidation of Substrates Tethered to Diiron(II) Carboxylate Complexes

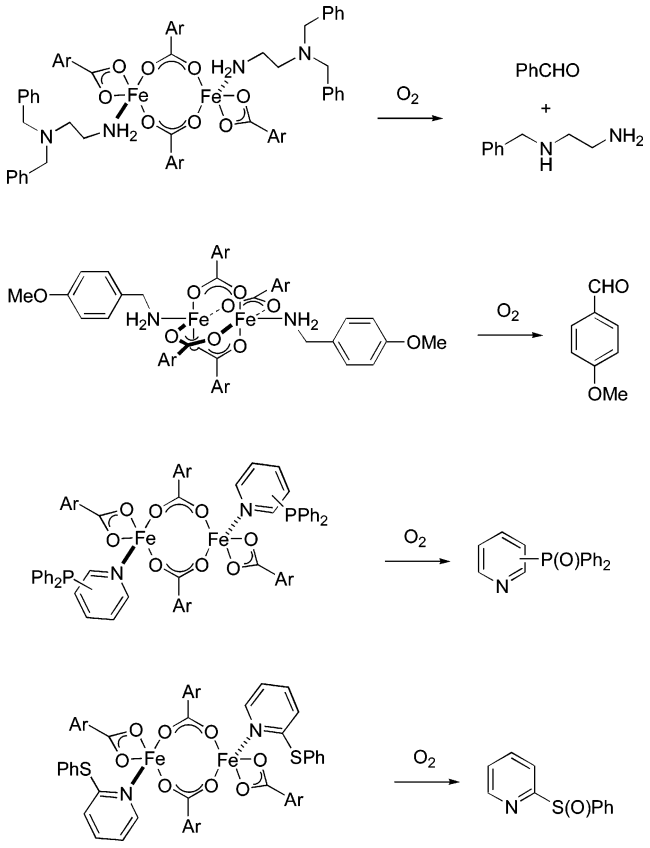

A somewhat different reaction, oxidative dealkylation of amines (as opposed to benzylic hydroxylation described above), was also reported for the complexes with $H_2N(CH_2)_2N(CH_2Ph)_2$ or $H_2N{-}CH_2Ar'$ (Ar′ = *p*-OMePh).[349,361] Oxidation of the tethered $H_2N(CH_2)_2N(CH_2Ph)_2$ gave much higher yields than oxidation of a control noncoordinating $H_3C(CH_2)_2N(CH_2Ph)_2$ (60% vs 13−29%).[361] The oxygen atom in the product (PhCHO) originates from O_2, as follows from the isotope labeling studies. Although no intermediates were observed in these reactions, it was proposed that a high-valent species is responsible for the substrate oxidation, and possible mechanisms were hypothesized (Scheme 36).[361] The proposal of a high-valent complex acting as an active oxidant was confirmed in a recent study of benzylamine oxidation.[349] The paddle-wheel complex $[Fe_2(\mu\text{-}O_2CAr^{Tol})_4(H_2NCH_2Ph^{p\text{-}OMe})_2]$ reacted with O_2 at −78 °C in CH_2Cl_2, giving a mixture of the Fe(II)Fe(III) and Fe(III)Fe(IV) mixed-valent species. The time scale for the oxygenation (∼200 s), obtained in a stopped-flow experiment, agrees reasonably well with the time scale for the oxygenation of a similar complex, [(4-

Scheme 36. Proposed Mechanism of Tethered Substrate Oxidation

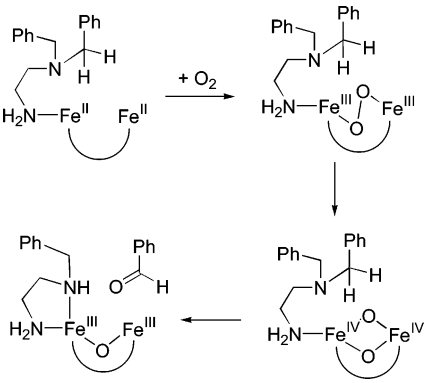

^{t}Bupy)$_2$Fe$_2$(μ-O$_2$CAr^{Tol})$_4$], estimated under similar conditions by EPR as ~10−20 min.[201] The intermediate decays at −78 °C over ~6 h; the products of the low-temperature decomposition were not reported. Oxygenation at room temperature yielded 26(7)% anisaldehyde. Using tethered H$_2$N(CHD)Ph$^{p\text{-OMe}}$ in place of a tethered (*p*-methoxy)benzylamine afforded a 1:3 mixture of *p*-OMePhC(O)H and *p*-OMePhC(O)D. This kinetic isotope effect, $k_H/k_D \approx 3$, is consistent with benzylic C−H bond cleavage being involved in a rate-limiting step. Successful oxidation of simple benzylamines rules out the possible involvement of a lone pair on a second nitrogen in the oxidation of a substituted ethylenediamine, H$_2$N(CH$_2$)$_2$N(CH$_2$Ph)$_2$, which was discussed above.[349,361] Unambiguous assignment of the benzylamine oxidation mechanism might become possible after further kinetic and mechanistic studies.

5.3.4. Iron-Promoted Free Radical Oxidation

A substrate oxidation reaction seemingly similar to those described above occurred upon bubbling O$_2$ through a THF solution of [Fe$_2$(Me$_3$TACN)$_2$(μ-O$_2$CAr^{Tol})$_2$]$^{2+}$ containing Ph$_3$P.[363] Importantly, this reaction, which yielded Ph$_3$PO, was catalytic with very high turnover numbers (>2000). Similar diiron complexes with nonhindered carboxylate bridges did not catalyze the phosphine oxidation; the terphenyl-derived carboxylates were necessary.[362,363] At low temperature, stoichiometric oxidation of phosphine was observed. A blue-green ($\lambda_{max} = 640$ nm, $\epsilon = 2000$ M^{-1} s^{-1}) EPR-silent intermediate was formed at −78 °C. The structure of this species was not determined, but its spectroscopic properties (notably, the lack of EPR signals characteristic of mixed-valent intermediates) may correspond to a peroxo complex.[362] It was noted, however, that this intermediate is not responsible for the catalytic phosphine oxidation, because phosphine oxide formation was also observed in the presence of a diiron(III) complex that was isolated from the reaction of diiron(II) precursor and O$_2$ at room temperature. Further detailed investigations established the critical role of solvent, particularly THF, in catalytic oxidation: no phosphine oxide was detected in toluene, CH$_2$Cl$_2$, CHCl$_3$, acetone, or acetonitrile.[362] Even though phenol radical inhibitors did not suppress the phosphine oxide formation, the radical character of the reaction was suggested by its solvent specificity. Detailed and careful analysis of the THF-derived products uncovered the radical species responsible for the phosphine oxidation (Scheme 37). The diiron complex is only involved in the initiation of free radicals required for the co-oxidation of PPh$_3$ and THF with O$_2$. Interestingly, light is required for the initiation reaction, suggesting that a photochemical step is involved. This study highlights the difficulties often faced by researches in distinguishing between metal-based and radical-based oxidation.[362]

Scheme 37. Free Radical Mechanism of Coupled Oxidation of Ar$_3$P and THF Initiated by a Diiron(III) Carboxylate Complex

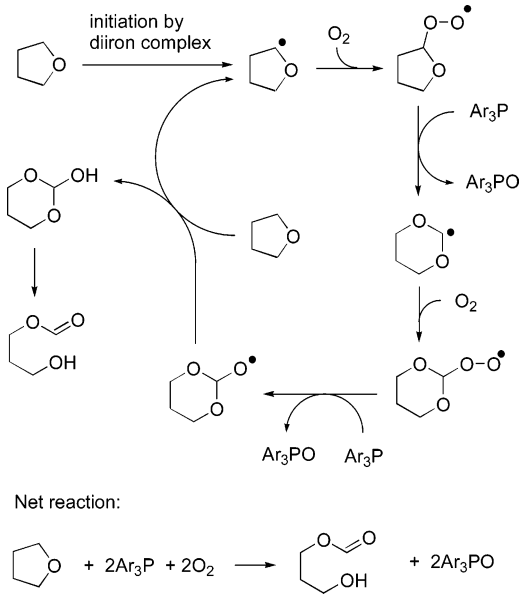

5.4. Complexes with Polyamine Ligands Supported by Carboxylato Bridges

Relatively simple polydenate amine ligands (TACN, TPA, and their derivatives) can yield dinucelar iron(II) complexes bridged by carboxylato and/or hydroxo groups. Such a self-assembly synthetic strategy is attractive due to its relative simplicity compared to the use of dinucleating ligands (sections 5.1 and 5.2). A more recent self-assembly synthetic approach (the use of interlocking, bulky 2,6-disubstituted benzoates) was described in section 5.3. It should be noted, however, that the complexes with polyamines usually have a much higher ratio of N vs O donor atoms in the coordination sphere of iron than the carboxylate-rich enzymes such as MMO, RNR, or Δ9D. Nevertheless, important mechanistic information was obtained from the studies of dioxygen activation with the synthetic diiron complexes based on polyamines, as discussed below.

An outstanding kinetic and mechanistic work was reported by Lippard and co-workers on the oxygenation of two diiron(II) complexes, [Fe$_2$(BIPhMe)$_2$(HCO$_2$)$_4$] and [Fe$_2$(OH)(Me$_3$TACN)$_2$(CH$_3$CO$_2$)$_2$]$^+$, in which simple formate or acetate groups were utilized as bridges between two metal centers capped by polyamine ligands.[174] Both complexes reacted with O$_2$ in chloroform, ultimately yielding oxo-bridged diiron(III) oxidation products (Scheme 38). No inter-

Scheme 38. Oxygenation of the Diiron(II) Complexes $[Fe^{II}_2(BIPhMe)_2(O_2CH)_4]$ and $[Fe^{II}_2(OH)(Me_3TACN)_2(O_2CMe)_2]^+$

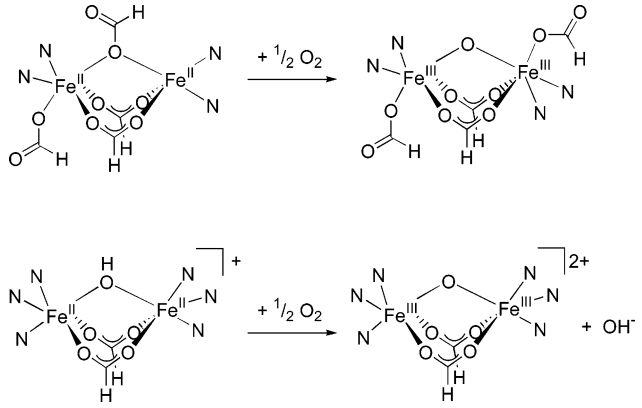

Scheme 39. Proposed Mechanism for the Oxygenation of $[Fe^{II}_2(BIPhMe)_2(O_2CH)_4]$ and $[Fe^{II}_2(OH)(Me_3TACN)_2(O_2CMe)_2]^+$

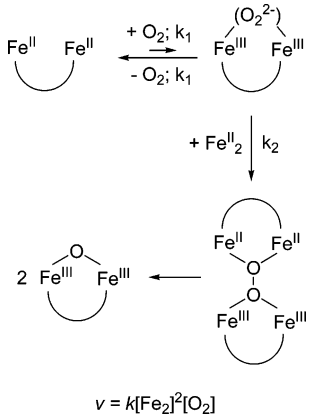

$v = k[Fe_2]^2[O_2]$

mediates were observed spectrophotometrically for the BIPhMe complex, while a transient green species ($\lambda_{max} \approx 700$ nm) was detected for the Me_3TACN complex. Due to small absorbance changes and similar rates of the formation and decay of this intermediate, the kinetics of these processes was not studied in detail. The intermediate was initially proposed to be a peroxo−diiron(III) species,[174] but a more recent study by Payne and Hagen identified dark green mixed-valent $Fe^{II}Fe^{III}$ complexes in similar systems.[339] It appears that the transient species observed during the oxygenation of $[Fe_2(OH)(Me_3TACN)_2(CH_3CO_2)_2]^+$ was also an $Fe^{II}Fe^{III}$ complex, but in a low yield.

Even though dioxygen adducts do not accumulate during the oxygenation of the diiron(II) complexes with BIPhM and Me_3TACN ligands, the formation of such intermediates is strongly implicated by detailed kinetic studies.[174] The oxygenation reactions were found to follow a third-order rate law (first order in dioxygen and second order in a diiron complex), and the mechanism shown in Scheme 39 was proposed to account for this unique observation. The first order with respect to dioxygen rules out intramolecular carboxylate rearrangements as a possible rate-limiting step. NMR experiments confirmed that carboxylate shifts are rapid for the investigated complexes. Triphenylphosphine was not oxidized during the reaction of the diiron(II) complexes with O_2, which indicated that high-valent iron intermediates did not form in the reactions.

A small value of the activation enthalpy (33 kJ mol^{-1}) and a significant negative value of the activation entropy (−39 J mol^{-1} K^{-1}) obtained for the oxygenation of $[Fe_2(BIPhMe)_2(HCO_2)_4]$ (Table 6) agree with the rate-limiting association of two molecules of the diiron(II) complex and a molecule of O_2. The transition state for the oxidation of diiron(II) complexes was proposed to contain a side-on peroxo bridge that is connected to both diiron units (Scheme 39). Molecular mechanics calculations indicated that such tetranuclear intermediates (or transition states) are not highly strained.

Another piece of evidence in favor of the inner-sphere interaction of $[Fe^{II}_2(OH)(Me_3TACN)_2(CH_3CO_2)_2]^+$ with O_2 in $CHCl_3$ was obtained by the Lippard group from the ^{18}O isotope label incorporation from $^{18}O_2$ into the (oxo)diiron(III) product as observed by resonance Raman spectroscopy.[174] However, no incorporation of an isotopic label was observed by the Hagen group by mass spectrometry upon the reaction of a similar complex $[Fe^{II}_2(^{18}OH)(Me_3TACN)_2(Ph_3CCO_2)_2]^+$ with $^{16}O_2$ in MeCN that yielded exclusively $[Fe^{II}Fe^{III}(^{18}O)(Me_3TACN)_2(Ph_3CCO_2)_2]^{2+}$, and it was concluded that the formation of the mixed-valent $Fe^{II}Fe^{III}$ complex proceeded by an outer-sphere mechanism.[339] It remains unclear if the formation of the mixed-valent intermediate was on the path of formation of the (oxo)diiron(III) complex from the acetate complex $[Fe^{II}_2(OH)(Me_3TACN)_2(CH_3CO_2)_2]^+$. The existence of several reaction pathways is possible in these systems, with an outer-sphere oxygenation dominant for the complex with the bulky Ph_3CCO_2 carboxylates and an inner-sphere mechanism prevailing for the analogous acetate complex.

5.5. Complexes with Polyamine Ligands Supported by Hydroxo and Oxo Bridges

The rich chemistry of iron complexes with the aminopyridine tripodal ligand TPA and its derivatives was already introduced in section 4.4.2. This ligand family yielded iron peroxo and high-valent intermediates in both mononuclear and dinuclear systems, thus allowing (at least in principle) for direct comparisons of the reactivities of the mononuclear and dinuclear active species.[27,164,165] Perhaps the most interesting aspect of the Fe−TPA system is the formation of well-characterized high-valent $[Fe^{III}Fe^{IV}(\mu\text{-}O)_2(L)_2]^{3+}$ (L = TPA, 5-Me_3-TPA, 6-Me_3-TPA) species upon interaction of a (μ-oxo)diiron(III) precursor with H_2O_2.[27,164,197,364] Establishing the structure and spectroscopic features of the synthetic $Fe_2(\mu\text{-}O)_2$ diamond-core complexes helped enormously in assigning the structure to the methane monooxygenase intermediate Q, which is currently believed to contain an $Fe^{IV}_2(\mu\text{-}O)_2$ core.[23,64,164] However, the $Fe^{III}Fe^{IV}$ complexes with TPA and its derivatives do not reach the +4 oxidation state of both irons in MMO Q, and instead they resemble in this respect intermediate X of RNR.[23,29,50]

A diiron(II) diamond-core, bis-hydroxo-bridged complex $[Fe^{II}_2(\mu\text{-}OH)_2(6\text{-}Me_3\text{-}TPA)_2]^{2+}$ was synthesized

Scheme 40. Proposed Mechanism of Oxygenation of Bis(μ-hydroxo)diiron(II) Complexes

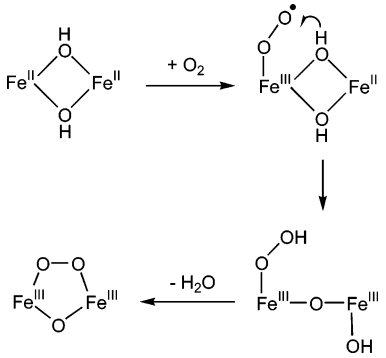

and structurally characterized recently.[347] This complex reacted with O_2 at low temperature to generate a metastable peroxo intermediate, which could undergo an acid-promoted conversion to an $Fe^{III}Fe^{IV}$ species capable of oxidizing phenols.[347] This system thus mimics all essential steps in the formation of the diiron(III)−tyrosyl radical cofactor of RNR (Scheme 7). Subsequently, several new diiron(II) complexes with TPA-like ligands were also shown to react with O_2. The kinetic and mechanistic aspects of the diiron−TPA reactivity with O_2 and with H_2O_2 are summarized below.

5.5.1. Reactions with O_2

Dinuclear complexes of the general type $[Fe^{II}_2(\mu\text{-}OH)_2(L)_2]^{2+}$ (L = 6-Me_3-TPA, TPA, BQPA, and Bn-BQA) react with O_2.[347,351,365] Under carefully selected conditions, the oxygenation of complexes with 6-Me_3-TPA, BQPA, and BnBQA (but not TPA itself) gives diiron(III) peroxo species in high yield. Low temperature and the presence of organic bases favor the formation of the peroxo intermediates. Under other conditions, the reaction products were oxo-bridged iron(III) oligomers $[Fe^{III}_n(O)_n(L)_n]^{n+}$ (n = 2 or 3), and no intermediates accumulated during the oxygenation reaction.[351] The dioxygen adduct with 6-Me_3-TPA was comprehensively characterized by spectroscopic techniques (including an EXAFS structural determination) and formulated as a 1,2-bridged peroxo complex $[Fe^{III}_2(\mu\text{-}O)(\mu\text{-}O_2)(6\text{-}Me_3\text{-}TPA)_2]^{2+}$.[347]

The kinetics of the reactions between dioxygen and $[Fe^{II}_2(\mu\text{-}OH)_2(L)_2]^{2+}$ (L = 6-Me_3TPA, TPA, BQPA, and BnBQA) in solution (CH_2Cl_2 or MeCN) was studied by stopped-flow techniques at low temperatures.[351,365] In all cases, the reaction was first order in the diiron(II) complex and first order in O_2 (second order overall) and characterized by a low enthalpy of activation ($\Delta H^{\ddagger}$ from 16 to 36 kJ mol^{-1}) and a strongly negative entropy of activation ($\Delta S^{\ddagger}$ from −177 to −80 J mol^{-1} K^{-1}). The values of oxygenation rate constants and activation parameters are compared in Table 6. For any particular diiron(II) complex, the kinetic parameters do not depend substantially on the solvent (dichloromethane or acetonitrile) and the observable reaction product (peroxo- or oxo-bridged diiron(III) complexes). These data suggest that the first and rate-limiting step of the reactions is the association of a diiron(II) complex and O_2 (Scheme 40) even though the starting complex has both six-coordinate Fe^{II} centers.[351,365] An outer-sphere one-electron transfer would appear quite unlikely, because the potential for the O_2/O_2^- redox pair in the organic solvents (∼ −1.25 V vs Fc^+/Fc in MeCN or CH_2Cl_2)[366,367] is about 1 V more negative than those determined for the $Fe^{II}Fe^{III}/Fe^{II}Fe^{II}$ redox pairs.[351]

The loss of a water molecule, required for the conversion of an $Fe_2(OH)_2$ core into an $Fe_2(O)(O_2)$ core, occurs after the rate-limiting oxygenation step, as suggested by the small effect of water addition on the reaction rate (a decrease in the overall reaction rates would have been expected for the rate-limiting extrusion of water leading to a vacant coordination site at the diiron(II) core).[365] Similarly to the oxygenation of hemerythrin (section 2.2), the O_2 binding to $[Fe_2(OH)_2(6\text{-}Me_3TPA)_2]^{2+}$ did not display an H/D kinetic isotope effect (the oxygenation rates were essentially identical in the presence of H_2O or D_2O). This observation rules out a rate-limiting O−H bond breaking (hydrogen atom transfer or proton-coupled electron transfer). Furthermore, the complex $[Fe_2(OH)_2(6\text{-}Me_3TPA)_2]^{2+}$ reacts with NO at a rate about 100-fold faster than that with O_2 ($\Delta H^{\ddagger} = 29 \pm 2$ kJ/mol, $\Delta S^{\ddagger} = -77 \pm 15$ J/K mol for NO binding).[365] These activation parameters, close to the corresponding values for dioxygen binding (Table 6), suggest that both nitrosylation and oxygenation of the complex $[Fe_2(OH)_2(6\text{-}Me_3TPA)_2]^{2+}$ share a similar associative mechanism. Both reactions are entropically controlled, low-barrier processes.[365]

It is likely that the two one-electron-transfer events during the formation of the diiron(III)−peroxo complex from the diiron(II) precursor and O_2 occur sequentially, rather than simultaneously. Such an assumption implies the formation of a diiron−superoxo intermediate (Scheme 40).

Binding of the O_2 molecule to the six-coordinate iron(II) center in the bis-hydroxo bridged complexes may require the formation of a seven-coordinate intermediate. Although seven-coordinate peroxo species are not unprecedented (for example, seven-coordinate structures are well documented for the Fe−EDTA complexes[368]), an alternative pathway would include breaking one of the Fe−ligand bonds on binding O_2. Examination of the crystal structure of the 6-Me_3TPA complex identified two plausible candidates for the dissociating ligand: a long Fe−O(H) bond in the asymmetric $Fe_2(OH)_2$ core (which has one short, ∼1.99 Å, and one long, ∼2.18 Å, Fe−OH bond) or an in-plane pyridine pendant arm (the in-plane Fe−N(py) distance is quite long, ∼2.30 Å).[365]

Extreme steric hindrance about iron coordination sites in complexes with 6-Me_3TPA protects the peroxo intermediate from oxidative decomposition (a desired effect) but simultaneously makes iron(II) centers hardly accessible even to a small incoming O_2 molecule. The oxygenation of this complex was slow ($t_{1/2}$ ≈ 30 min at −40 °C).[365] Some decrease in the steric bulk about Fe(II) coordination sites was expected to allow for the facile oxygenation of dinuclear Fe(II) model complexes. This hypothesis was tested with less sterically hindered complexes supported by BQPA or TPA ligands and an analogous tridentate

ligand BnBQA.[351] For both tetradentate ligands (BQPA or TPA), however, no significant gains in oxygenation rates were achieved. The less negative activation entropy for these complexes was compensated by higher activation enthalpies (Table 6). A decrease in the steric bulk about the diiron(II) center resulted in the formation of a more "compact" and symmetric $Fe_2(OH)_2$ core, which lacked long, weak Fe−OH bonds. The in-plane Fe−N(py) bonds also became shorter than those in the complex with 6-Me_3-TPA.[351] The least sterically hindered complex, $[Fe^{II}_2(OH)_2(TPA)_2]^{2+}$, did not form any peroxide intermediates upon oxygenation.

A remarkable 1000-fold acceleration of dioxygen binding to the $Fe^{II}_2(OH)_2$ core was accomplished by replacing one pyridine arm in the polydentate ligand BQPA with a noncoordinating benzyl group.[351] The resulting complex, $[Fe^{II}_2(\mu\text{-}OH)_2(BnBQA)_2(CH_3CN)_2]^{2+}$, differs from the other bis(μ-hydroxo)diiron(II) complexes in having a tridentate meridional ligand (BnBQA) and a molecule of coordinated MeCN instead of a tripodal tetradentate ligand. The use of tridentate BnBQA introduces MeCN as the sixth ligand on each iron in place of the third arm of the tetradentate ligands, and its kinetic lability lowers the activation enthalpy for oxygenation. At the same time, the reduced steric crowding around the diiron core of $[Fe_2(OH)_2(BnBQA)_2]^{2+}$ also makes the activation entropy less unfavorable. There is no correlation between the half-wave redox potentials for the Fe^{III}-Fe^{II}/$Fe^{II}Fe^{II}$ redox couples and the oxygenation rates of diiron(II) complexes. In particular, complexes with BQPA and BnBQA exhibit nearly identical redox potentials, but the oxygenation rate for the latter is about 10^3 times faster. Therefore, the dramatic increase in the oxygenation rate is not caused by electronic factors. This study reveals the critical role of a vacant or labile site at diiron(II) centers for facile oxygenation.

The addition of a base (NEt_3 or other noncoordinating amine) does not influence the oxygenation rate, but in some cases (especially for the ligand BQPA), it increases substantially the yield of peroxo intermediates. Added amines interfere in the reaction after the rate-limiting step, because there are no changes in the UV−vis spectrum of the starting diiron(II) complex and the kinetics of its reaction with O_2. The remarkable effect of added base in promoting the peroxo intermediate formation revealed the involvement of a proton-sensitive step that controls the reactivity of the initial O_2 adduct (Scheme 40). It was proposed that, in the absence of base, the intermediate O_2 adduct can oxidize residual diiron(II) complex, yielding diiron(III) oxidation products.[351] Alternatively, base can deprotonate the hydroxo bridge in the diiron−O_2 adduct, promoting formation of a diiron(III)−peroxo species.[365]

5.5.2. Reactions with H_2O_2

Even though hydrogen peroxide is a very useful reagent for generating peroxo or high-valent intermediates from diiron(III) complexes, kinetic and mechanistic investigations of this "peroxide shunt" pathway are limited. To the extent of our knowledge, the only detailed study[346] was performed for the oxo-bridged diiron(III) complex with TPA ligand, $[Fe^{III}_2(\mu\text{-}O)(TPA)_2(OH)(H_2O)]^{3+}$.

Scheme 41. Mechanistic Scheme for the Reaction of the Diiron(III)−TPA Complex with Hydrogen Peroxide in Acetonitrile at −40 °C

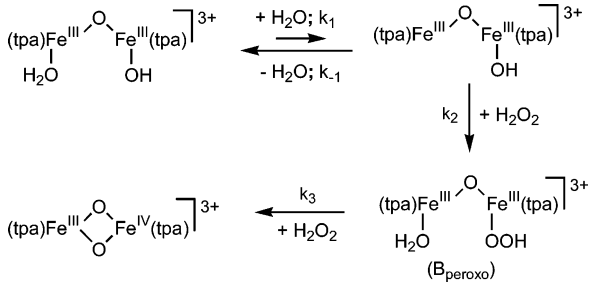

Que and co-workers discovered that the diamond-core $Fe^{III}Fe^{IV}(\mu\text{-}O)_2$ complexes with TPA and its derivatives are formed from the corresponding Fe^{III}_2 complexes and H_2O_2 at low temperature.[27,164,195] The mechanism of this reaction was later studied by stopped-flow spectrophotometry, revealing other, previously unknown intermediates in this system (Scheme 41).[346] A transient diferric peroxo complex gradually converting into a high-valent species was directly observed. Stopped-flow experiments in acetonitrile at −40 °C produced kinetic traces typical of a two-step process with sequential rate constants k'_{obs} and k''_{obs}. The initial and final spectra agree well with those reported for $[Fe^{III}_2(\mu\text{-}O)(TPA)_2(OH)(H_2O)]^{3+}$ and $[Fe^{III}Fe^{IV}(\mu\text{-}O)_2(TPA)_2]^{3+}$, correspondingly.[195] The spectrum of the novel intermediate $B_{(peroxo)}$ has a broad maximum at about 700 nm (ϵ = 1800 dm^3 mol^{-1} cm^{-1}), which is very similar to the cases of the H_{peroxo} intermediate of methane monooxygenase (λ_{max} = 700 nm, ϵ = 1800),[129] the peroxo intermediate of a mutant ribonucleotide reductase (λ_{max} = 700 nm, ϵ = 1500),[139] and the peroxo diferric intermediate of ferritin.[153] Such a LMCT band is a common feature in the spectra of diferric peroxo complexes.[369] Thus, the species B_{peroxo} is most probably $[Fe^{III}_2(\mu\text{-}OH)(\mu\text{-}O_2)(TPA)_2]^{3+}$ or $[Fe^{III}_2(\mu\text{-}O)(TPA)_2(OOH)(H_2O)]^{3+}$. Additional spectroscopic and kinetic experiments are needed to clarify the structure of the short-lived intermediate B_{peroxo}. The data on ligand substitution rates (see below) support the end-on hydroperoxo formulation.

The formation of the intermediate B_{peroxo} in acetonitrile (characterized by the observed rate constant k'_{obs}) is decelerated by water and accelerated by hydrogen peroxide with the following rate law:

$$k'_{obs} = k_1(k_2/k_{-1})[H_2O_2]/\{(k_2/k_{-1})[H_2O_2] + [H_2O]\} \quad (8)$$

Such kinetic dependency implies the existence of a steady-state intermediate between the diiron(III) precursor and B_{peroxo} (Scheme 41). This steady-state intermediate forms upon the loss of a water molecule from $[Fe^{III}_2(\mu\text{-}O)(TPA)_2(OH)(H_2O)]^{3+}$ and can therefore be formulated as $[Fe^{III}_2(\mu\text{-}O)(TPA)_2(OH)]^{3+}$ or $[Fe^{III}_2(\mu\text{-}O)(TPA)_2(OH)(MeCN)]^{3+}$.

Scheme 42. Mechanistic Scheme for the Reaction of the Diiron(III)−TPA Complex with Urea

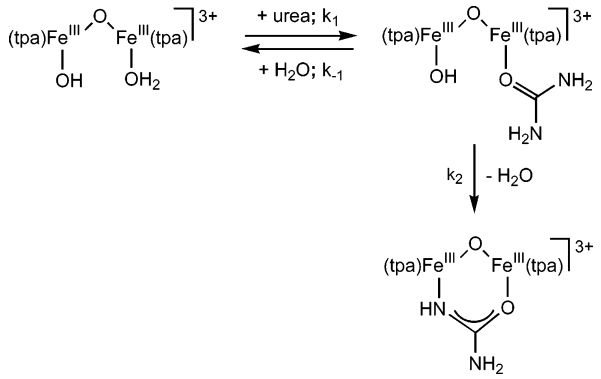

The rate of the following transformation, $B_{peroxo} \rightarrow [Fe^{III}Fe^{IV}(\mu\text{-}O)_2(TPA)_2]^{3+}$, does not depend on $[H_2O]$ but is proportional to $[H_2O_2]$ (eq 9):

$$k''_{obs} = k[H_2O_2] \quad (9)$$

Hydrogen peroxide apparently acts as a reducing agent in this reaction (Scheme 41). The presence of a reductant is essential for the action of native ribonucleotide reducatase, presumably in order to reduce the $Fe^{III}{}_2$−peroxo intermediate to the high-valent $Fe^{III}Fe^{IV}$ intermediate X (although it may be not obvious at a glance, the transformation of an $Fe^{III}{}_2$−peroxo species into a into an $Fe^{III}Fe^{IV}$ species indeed involves a one-electron reduction).[53]

The formation of a peroxo intermediate B_{peroxo} (Scheme 41) is essentially a ligand substitution reaction, in which a coordinated water molecule is replaced with coordinated peroxide. The mechanism of ligand binding to $[Fe_2(\mu\text{-}O)(TPA)_2(OH)(H_2O)]^{3+}$ was probed in an independent study that used urea as a potentially bidentate redox-inactive incoming ligand.[370] To establish the urea binding mode in its complex with $Fe_2(\mu\text{-}O)(TPA)_2$, the ureate adduct was synthesized and fully characterized. X-ray diffraction revealed an unusual bridging coordination mode of deprotonated urea that replaced both H_2O and HO^- ligands in the iron(III) coordination sphere.[370] Detailed equilibrium and kinetic studies supported a stepwise mechanism of the ureate formation (Scheme 42).[370] The first step in urea substitution is very rapid (it was too fast at 25 °C even for the stopped-flow technique). This step corresponds to a monodentate coordination of the incoming urea molecule accompanied by the elimination of one water molecule initially bound to the iron(III) center. This reaction is similar in rate to the process of formation of B_{peroxo} from the diiron(III) precursor and H_2O_2.[346,370] The second step in ureate formation, substitution of the OH^- coordinated to the second iron(III) center, proceeds slowly (much more slowly than the reaction between B_{peroxo} and H_2O_2). It appears that the substitution of the second monodentate ligand (hydroxide) in $[Fe_2(\mu\text{-}O)(OH)(OH_2)(TPA)_2]$ is unlikely to be involved in formation of B_{peroxo}. Mechanistic and kinetic data on ligand substitution suggest an end-on structure for B_{peroxo} (as opposed to the structure with the bridging peroxo ligand). Further spectroscopic studies are needed in order to unambiguously assign the structure of the peroxo intermediate in the diiron−TPA system.

Scheme 43. Reactivity Manifold in the System $[Fe_2(\mu\text{-}O)(TPA)_2(OH)(H_2O)]^{3+}$−$H_2O_2$−Substrates with Rate Constants Measured in Acetonitrile at −40 °C

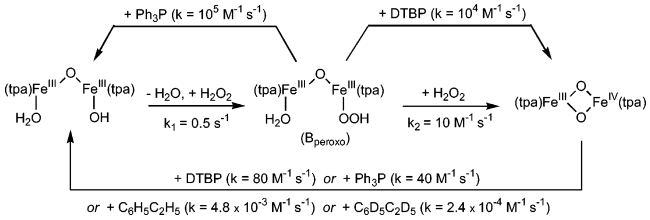

5.5.3. Activation of O_2 and H_2O_2

The diiron peroxo and high-valent intermediates with TPA and related ligands are capable of oxidizing substrates. Kinetic and mechanistic studies on the reactivity of the diiron intermediates derived from H_2O_2 are summarized in this section. In one study,[347] the reactivity of the intermediates generated from a diiron(II) precursor and dioxygen is also described.

The oxidative properties of the diiron−peroxo intermediate $[Fe^{III}{}_2(\mu\text{-}O)(TPA)_2(OOH)(H_2O)]^{3+}$ and the high-valent complex $[Fe^{III}Fe^{IV}(\mu\text{-}O)_2(TPA)_2]^{3+}$ were studied using triphenylphosphine (Ph_3P) and 2,4-di-*tert*-butylphenol (DTBP) as substrates. Earlier it was found that $[Fe^{III}Fe^{IV}(\mu\text{-}O)_2(TPA)_2]^{3+}$ oxidizes both substrates within seconds, producing Ph_3PO and 3,3′,5,5′-tetra-*tert*-butyl-1,1′-di-2,2′-phenol, respectively.[371,372] The kinetics of this reaction was studied by cryogenic stopped-flow experiments.[373] The reactivities of the two Fe−TPA intermediates (B_{peroxo} and $Fe^{III}Fe^{IV}$) were found to be very different (Scheme 43). The decay of the peroxo intermediate B_{peroxo} greatly accelerated in the presence of the reducing substrates. Most interestingly, the use of the one-electron-reducing substrate (DTBP) transformed B_{peroxo} into the high-valent species. The reaction of B_{peroxo} with Ph_3P showed an extremely high rate ($\sim 10^5$ M^{-1} s^{-1} at −40 °C). Thus, the peroxo−diiron(III) intermediate B_{peroxo} appears to be a far more reactive species than the high valent $Fe^{III}Fe^{IV}$ intermediate. Even though the $Fe^{III}Fe^{IV}$ species reacts with both DTBP and Ph_3P, catalytic oxidation of these substrates in the H_2O_2−**1** system probably involves B_{peroxo}, which reacts with the substrates several orders of magnitude faster (Scheme 43).[373] Detailed mechanistic studies of substrate oxidations with individual peroxo and high-valent oxo−diiron intermediates are in progress.

The complex $[Fe^{III}Fe^{IV}(\mu\text{-}O)_2(TPA)_2]^{3+}$ generated from the diiron(III) precursor and H_2O_2 was shown to react not only with phosphines and phenols but also with hydrocarbons containing benzylic hydrogens (cumene and ethylbenzene).[371] Interestingly, in addition to the hydroxylation products (1-phenylethanol or cumyl alcohol) and trace amounts of ketones, dehydrogenation products (α-methylstyrene or styrene) were also formed. Oxidation of ethylbenzene with $[Fe^{III}Fe^{IV}(\mu\text{-}O)_2(TPA)_2]^{3+}$ in CH_3CN at −40 °C is a clean second-order reaction (first order in diiron complex and first order in substrate) with a very

Scheme 44. Dioxygen Activation by the Complex $[Fe^{II}_2(\mu\text{-}OH)_2(6\text{-}Me_3\text{-}TPA)_2]^{2+}$ Modeling the Dioxygen Activating Cycle of RNR R2

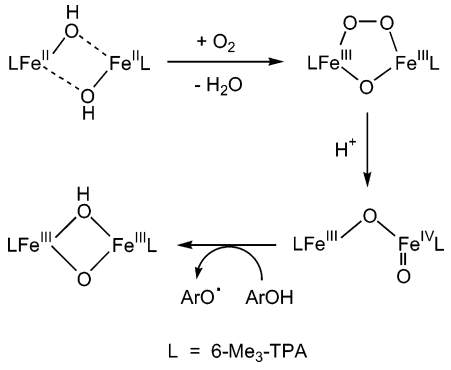

large kinetic isotope effect ($k_H/k_D = 20$, Scheme 43). These results indicate that the C−H bond breaking occurs at the rate-limiting step. It was proposed that the first, slow step in the substrate oxidation is a hydrogen atom abstraction from the benzylic CH groups by the Fe(III)Fe(IV) species. The resulting radical then rapidly reacts with a second molecule of the Fe(III)Fe(IV) complex, which either abstracts a β-hydrogen atom, giving an olefin, or transfers an oxygen atom, giving an alcohol.[371]

An analogous high-valent iron−oxo complex with 5-Me_3-TPA also quantitatively and rapidly oxidizes triphenylphosphine and 2,4-di-*tert*-butylphenol, although the kinetics and mechanism of these reactions were not studied.[371]

The TPA derivative bearing three methyl substituents in the 6-positions of the pyridine rings, 6-Me_3-TPA, provides significant steric hindrance about the diiron site. This results in slower reactions at the diiron center, as was discussed in section 5.5.1 for the dioxygen binding to $[Fe^{II}_2(\mu\text{-}OH)_2(6\text{-}Me_3\text{-}TPA)_2]^{2+}$. The transformations of the diiron peroxo and high-valent oxo species in this case are also relatively slow, which allowed Que and co-workers to follow the individual reaction steps shown in Scheme 44. The decay of $[Fe^{III}_2(\mu\text{-}O)(\mu\text{-}O_2)(6\text{-}Me_3\text{-}TPA)_2]^{2+}$ at −30 °C in the presence of 1 equiv of $HClO_4$ is a clean first-order process that yields an Fe(III)Fe(IV) species.[347] For the peroxo intermediate generated from a diiron(II) precursor and O_2, the rate of decay (measured by the change in optical absorbance) is identical to the rate of formation of the Fe(III)Fe(IV) complex (determined by EPR) and has the value of 1.2×10^{-3} s^{-1} ($T = -30$ °C, MeCN).[347] An essentially identical value of the rate constant was obtained for the self-decay of the peroxo species generated via a different pathway from the diiron(III) precursor and H_2O_2 ($k = 1.6 \times 10^{-3}$ s^{-1}, $T = -30$ °C, MeCN).[196] The source of an electron that is required for the formation of an $Fe^{III}Fe^{IV}$ species from the peroxo complex was not established in the 6-Me_3-TPA system, but it was proposed that H_2O_2 formed from hydrolysis is a possible candidate.[347] The analogous conversion of complexes with an unsubstituted TPA ligand was shown to depend on the concentration of H_2O_2 (section 5.5.2).

An interesting example of a diiron complex with a dinucleating pyridine-containing ligand bis-py_3 was

Scheme 45

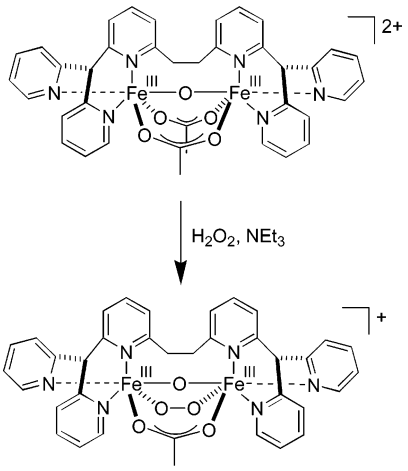

reported by Kodera.[374] The positions of three pyridine groups in each compartment of this ligand resemble those in TPA, but the additional tertiary amine donor is absent in bis-py_3. A μ-1,2-peroxo complex $[Fe^{III}_2(O_2)(O)(OAc)(\text{bis-}py_3)](OTf)$ was isolated as a solid from the reaction of a (μ-oxo)(μ-carboxylato)diiron(III) precursor and H_2O_2 in the presence of a base (NEt_3) at low temperature (243 K, CH_3CN) (Scheme 45). Even though the material did not yield single crystals of X-ray quality, successful purification of the peroxo complex provided an unusual opportunity to study its reactivity in the absence of other compounds present during the much more common in situ preparation of transient peroxo species (the absence of excess H_2O_2 is particularly important). Self-decomposition of the peroxo complex followed a first-order rate law ($k = 2.5 \times 10^{-5}$ s^{-1} at 300 K in CH_3CN). Similarly to the case of the 6-Me_3-TPA complex, decomposition of the peroxo complex supported by bis-py_3 is catalyzed by mineral acids (e.g., $HClO_4$) and by organic acid chlorides ($k = 8.0 \times 10^{-2}$ at 273 K in CH_3CN/CH_2Cl_2 containing 3.0×10^{-2} M *m*-chlorobenzoyl chloride). The self-decomposition rate of the peroxo complex can be further increased by a factor of 20 in the presence of dimethylformamide (11 vol %). Remarkably, the peroxo complex becomes a potent oxidant in the presence of acyl chloride and DMF: cyclohexane and cyclohexene were oxidized into cyclohexanol and cyclohexenol, respectively (small quantities of cyclohexenone were also formed in the latter case). The peroxo complex itself was inactive in the substrate oxidations. Furthermore, the presence of $HClO_4$ or *m*-$ClC_6H_4C(O)Cl$ did not activate the peroxo species toward alkane hydroxylation. The presence of both acyl chloride and DMF were critical for peroxide activation.[374] The mechanisms of substrate oxidation in this novel system deserve further investigation.

Another family of dinuclear oxo-bridged iron complexes that activate hydrogen peroxide contain derivatives of 2,2′-bipyridine or *o*-phenanthroline as ligands. Mononuclear peroxo iron complexes with bpy and phen were considered in section 4.3. Iron(II) tends to form with these ligands very stable mononuclear low-spin tris-chelates, which are unreactive with dioxygen. However, iron(III) readily forms oxo-bridged dimers with the $Fe^{III}_2(\mu\text{-}O)(L)_4$ core and two

vacant sites that can be occupied by labile monodentate ligands (solvent molecules, anions, etc.) and are accessible to small molecules. The complex $[Fe^{III}_2(\mu\text{-}O)(phen)_4(H_2O)_2]^{2+}$ was recently shown to activate peroxoacetic acid for the epoxidation of terminal alkenes.[210] Analogous (μ-oxo)diiron(III) complexes with bpy, phen, and their derivatives catalyze oxidation of alkanes and other substrates with alkyl hydroperoxides.[290,291] The mechanism of catalysis in most of these systems remains unknown, but mono- and dinuclear iron(III) peroxo complexes were identified in several of them.[289,292,375]

The studies of the kinetics and mechanisms of peroxide formation and reactivity in bpy-type complexes are limited to the systems containing chiral ligand (−)-4,5-pinenebipyridine, pb.[343,344,375] These studies were initiated by an exciting finding by Fontecave, Ménage, Que, and co-workers of catalytic activity of the complex $[(pb)_2(H_2O)Fe^{III}_2(\mu\text{-}O)Fe^{III}(OH_2)(pb)_2]^{4+}$ in the enantioselective oxidation of aryl sulfides with H_2O_2.[343] The reactions were performed in acetonitrile under argon at 0 °C with the ratio complex/sulfide/H_2O_2 = 1/600/10. Using the oxidant as a limiting reagent minimized the formation of other products (such as sulfones). The yields of sulfoxides determined after 10 min of reaction were in the range from 45 to 90% (based on H_2O_2). Moderate enantioselectivity of catalytic sulfoxidations (from 4 to 40%) was reported. Using a more potent oxygen donor, PhIO, increased the yields of sulfoxides, but very little enantioselectivity was found in this case. No enantioselectivity was reported with ^{t}BuOOH as an oxygen source, in accord with the tendency of alkyl peroxides to undergo hemolytic O−O bond cleavage and promote nonselective, radical oxidations. The importance of H_2O_2 as an oxygen source was also confirmed by ^{18}O-labeling experiments, which unambiguously confirmed that the oxygen atom in the product (sulfoxide) originated from the oxidant ($H_2{}^{18}O_2$). It was proposed that an iron−peroxo species is responsible for enantioselective sulfoxidation with H_2O_2.[343]

Spectroscopic studies (UV−vis, resonance Raman, HF-EPR, Mössbauer) and mass spectrometry showed the presence of two diiron(III) peroxo complexes in solution formed upon mixing of $[(pb)_2(H_2O)Fe(\mu\text{-}O)Fe(OH_2)(pb)_2]^{4+}$ with H_2O_2 (Scheme 46).[343,375] One of these complexes contains a μ-1,2-peroxide bound to both iron centers, and the other complex contains an end-on hydroperoxide ligand coordinated to one iron atom.[375] It is reasonable to assume that the two peroxo complexes rapidly interconvert under the conditions of catalytic sulfoxidation, because the broad optical absorbance band with $\lambda_{max} \approx 650$ nm (which originates from an overlap of the individual spectra of each of the peroxo species) decreased in intensity but did not change shape in the course of sulfide oxidation.

The kinetics of methyl phenyl sulfide oxidation was followed spectrophotometrically by an increase in the product concentration, as well as by a decrease in the diiron(III) peroxide concentration, and consistent results were obtained. The reaction rate displayed saturation behavior as a function of both H_2O_2 and substrate (sulfide) concentrations; the initial rates followed Michaelis−Menten kinetics. These results indicate intramolecular oxidation of the coordinated substrate by a coordinated peroxide (Scheme 46). Furthermore, the sulfide oxidation showed product inhibition, suggesting that sulfoxide occupies iron(III) coordination sites and thus competes with the substrate and/or H_2O_2. The proposed mechanism (Scheme 46)[343] is similar to the mechanism of phophine oxidation by diiron complexes with TPA (Scheme 43).

Scheme 46. Proposed Mechanism of Sulfoxidation with H_2O_2 Catalyzed by a (μ-Oxo)diiron(III) Complex with 4,5-Pinenedipyridine

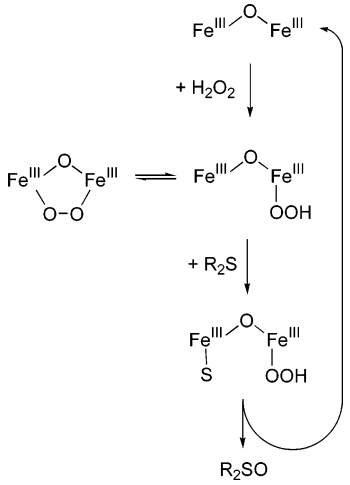

Comparing the rates of oxidation of several different phenyl methyl sulfides showed that electron-donating substituents on the phenyl ring facilitate the oxygen-transfer process. In particular, $\log(V_{max})$ gave a linear Hammett correlation with a negative slope ($\rho = -0.55$), in agreement with a nucleophilic character of the sulfide and an electrophilic character of an oxygen donor (coordinated peroxide or, more likely, hydroperoxide).[343]

The monomeric iron(II) complex with pb ligand, $[Fe(pb)_2(CH_3CN)_2]^{2+}$, also acted as a catalyst in sulfide oxidation with hydrogen peroxide.[344] The sulfoxidation rates, however, were much lower than those reported for the dinuclear catalyst $[(pb)_2(H_2O)Fe(\mu\text{-}O)Fe(OH_2)(pb)_2]^{4+}$.[343] In addition to low yields, mononuclear catalyst resulted in negligible enantiomeric excess (not exceeding 5%) in sulfoxide products. Even though the monomeric complex also demonstrated saturation kinetics in sulfide oxidations, consistent with an inner-sphere oxygen transfer, it was concluded that "two metal centers are better than one"[344] for the productive and selective sulfide oxidation. Presumably, the intermediate containing both the substrate and the (hydro)peroxide bound at the same iron(III) site is less effective than its dinuclear counterpart, which would contain (hydro)peroxide at one iron(III) center and the substrate coordinated at another iron(III) center.

6. Practical Aspects of Kinetic Studies

To obtain useful mechanistic insights, kinetic data need to be properly acquired, properly treated, and

properly interpreted.[376] This is often a nontrivial task, especially for rapid multistep reactions between air-sensitive compounds and gaseous reagent(s), with transient intermediates unstable at room temperature. General aspects of reaction kinetics are described in several excellent books.[103,377,378] The applications of kinetic techniques to determining the mechanisms of inorganic reactions were treated in monographs and review articles.[378−387] Finally, a recent review on the kinetic methodology of small molecule binding to transition metal complexes is available.[388]

The majority of reactions between iron(II) complexes and O_2 or other oxygen donors are accompanied by changes in the UV−vis spectra. Not surprisingly, spectrophotometric registration is commonly used in kinetic measurements. Relatively slow reactions ($t_{1/2}$ > 1 min) can be followed by conventional spectrophotometry; rapid reactions are studied by the stopped-flow, flash photolysis, or temperature jump techniques. The stopped-flow methodology is somewhat more general, as it is applicable to any process that occurs on the millisecond and above time scale (the mixing time of commercially available instruments is on the order of 1 ms). Flash photolysis and temperature jump methodologies allow chemists to follow more rapid reactions (down to microsecond time scale), although they are only applicable to photosensitive systems (flash photolysis) or reversible reactions with a temperature-sensitive equilibrium (T-jump), which are relatively rare in iron−oxygen chemistry. Spectrophotometric registration has an advantage of being an experimentally simple method that allows for the very rapid and accurate determination of concentrations of reactants/products. Modern rapid-scanning or diode-array spectrophotometers dramatically changed the information content of kinetic data: instead of single-wavelength data acquisition, time-resolved full spectra can be collected and analyzed. Global fitting of time-resolved spectra provides reliable values of individual rate constants, as well as full individual optical spectra of intermediates and products of the studied reaction. This methodology, which was described elsewhere,[324] is particularly useful for characterizing multistep processes. However, it should be remembered that diode-array spectrometry requires several orders of magnitude brighter light intensity, and chances of photochemical interference increase in proportion.[129] Although UV−vis spectroscopy remains the most convenient tool in detecting transient reaction intermediates, it does not provide sufficient information regarding their chemical structures. Ideally, each intermediate has to be characterized by additional spectroscopic methods (e.g., resonance Raman, Mössbauer, EXAFS, EPR).[190,191,201,340,375] Kinetic data can be helpful in identifying experimental conditions where each of the intermediates is preferentially formed. Variations of the rapid freeze-quench technique are often used for such spectroscopic studies.[65,66,201] In addition, electrospray mass spectroscopy can be adapted to the in situ determination of unstable reaction intermediates.[389] In some cases, lowering of temperature allowed for the crystallization of an intermediate and the determination of its structure by diffractometry.[62,170−172,197,202,225]

The choice of solvent and other experimental conditions (temperature, pressure, additives, etc.) is very important for successful kinetic studies in iron−oxygen systems. In biomimetic studies, it is desirable to use water as a solvent. In aqueous solutions the speciation of the iron complex(es) has to be independently established, because it significantly influences the rates, mechanisms, and products of the oxygenation reactions. Obviously, pH and ionic strength have to be controlled in kinetic measurements. The analysis of these issues for the iron−15aneN4 system is available in section 4.2.1.

The choice of buffers for oxidation reactions with iron complexes should be made carefully. Simple buffering anions (like phosphate, borate, carbonate, acetate, or citrate) can coordinate to iron (especially to Fe^{III}), while noncoordinating organic buffers (like HEPES, MOPS, etc.) may act as reducing substrates for the iron−oxygen intermediates. Another complication, which is often overlooked, is the possibility of formation of active oxidants from buffers, e.g., peroxocarbonate from carbonate, peroxoacids from carboxylates, etc.[209,390] Even if these reactions do not occur in the absence of the metal complex, they can be catalyzed by iron compounds, as was recently shown for iron-catalyzed olefin epoxidation with hydrogen peroxide in the presence of acetic acid (peracetic acid was found and proposed to act as the active oxidant).[209] Moreover, buffers that do not undergo direct chemical reactions with the components of the investigated system may participate in general acid/base catalysis.[249]

Some additional problems of investigating the iron−oxygen reactivity in aqueous media include hydrolytic decomposition of iron complexes (particularly significant for iron(III) reaction products), relatively low solubility of O_2 in water (1.234 mM at room temperature, Table 9), and relatively high freezing point of water that does not allow performance of kinetic measurements in liquid solution at low temperatures.

Many reactions in the iron−oxygen systems were studied in organic solvents, where iron(II) and iron(III) complexes are usually stable. Transient intermediates were stabilized at low temperatures (down to ∼ −90 °C in appropriate solvents), and the mechanisms of their formation and reactivity were studied in detail using low-temperature stopped-flow methodology.[324] Of course, an organic solvent should not undergo catalytic oxidation with dioxygen or other oxygen donors under experimental conditions. Another potential problem was identified in recent studies on catalytic oxidations: solvents that easily form peroxides (such as THF or diethyl ether) can promote substrate oxidation.[362] Solvents stabilized against autoxidation contain compounds that potentially can react with iron−oxygen intermediates (alkenes, phenols, etc.). If stabilized solvent has to be used in kinetic studies, the control experiments in the absence of stabilizers have to be performed. Solvent purity is critically important for obtaining reliable and reproducible kinetic results;[345] in some

Table 9. Solubility of Dioxygen in Common Solvents at 25 °C

solvent	*L* (Ostwald coefficient)	vapor pressure at 25 °C,[395] kPa	solubility of dioxygen at 25 °C and 760 Torr (total pressure), mM	ref
water	0.03116	3.17	1.234	391
isooctane	0.38	6.5	14.6	391
toluene	0.22(2)	3.79	8.7(8)	391
dichloromethane	0.25; 0.257 (20 °C)	58.2; 46.4 (20 °C)	4.3 (3.8 at 720 Torr total pressure); 5.8 (20 °C)	391, 396, 397
chloroform	0.278 (20 °C)	21.3 (20 °C)	9.1 (20 °C)	391, 397
methanol	0.25	16.9	8.5	391
ethanol	0.244	7.87	9.2	391
tetrahydrofuran	0.245	21.6	7.9	391
acetone	0.28; 0.28(3) (20 °C)	30.8; 24.6 (20 °C)	8.0; 9(1) (20 °C)	391, 398
acetonitrile	0.224	11.8	8.1	399, 400
propionitrile	0.23	6.14	8.8	401
DMF	0.12	0.44	4.8	399
DMSO	0.051	0.08	2.1	399, 400

cases, traces of moisture are detrimental, and solvents need to be rigorously dried.[188]

There are some experimental difficulties related to the use of gaseous dioxygen as a reagent. For kinetic experiments in solution, the gas should be dissolved before the chemical reaction. However, preparing gas solutions with known concentration is not a trivial task.

The values of dioxygen solubility are commonly given in reference literature as Ostwald coefficients (L), defined as the ratio of the absorbed gas volume to the absorbing liquid volume (Table 9).[391,392] Because dioxygen behaves very much like an ideal gas at ambient conditions and its solubility in common liquids is small, L may be considered nearly independent of pressure. The values L can be converted to the molar solubility S (mol L^{-1}) using a simple formula: $S = LP/(TR)$, where P is the dioxygen partial pressure, R is the gas constant, and T is temperature.[391,392] The partial pressure of dioxygen should be calculated taking into account the saturation vapor pressure of the solvent (P_S), which is especially important for volatile solvents. For example, if tetrahydrofuran (P_S = 21.6 kPa) is saturated with O_2 at a total pressure of 101.3 kPa, the partial pressure of O_2 is 79.7 kPa.

The values of dioxygen solubility have to be determined experimentally for each given temperature.[391,392] Unfortunately, there are no published data for the O_2 solubility in liquids at the cryogenic temperatures (−80 to −40 °C) commonly used to observe intermediates during the oxygenation of iron(II) complexes. Analysis of the existing data for the O_2 solubility in several solvents (acetone, isooctane, methanol) in a relatively wide temperature range (−25 to +25 °C)[393] shows that the solubility of dioxygen expressed as the equilibrium concentration at 1 atm total pressure moderately increases with the drop in temperature, in part due to the decrease in the solvent vapor pressure (Table 10). It is probable that the O_2 solubility in common organic solvents does not change more than 2−3 times upon cooling from room temperature to as low as −80 °C. Although such an estimate may be useful for some purposes, it is insufficient to conduct precise thermodynamic and kinetic measurements. There is a clear need for direct experimental measurement of dioxygen solubility in organic solvents at cryogenic temperatures.

Table 10. Solubility of Dioxygen at 1 atm Total Pressure[393]

solvent	*T*, °C	P_S, Torr	*L*	*S*, mM
methanol	−25	5.4	0.2427	11.8
	0	30.1	0.2446	10.5
	+25	127.2	0.2476	8.4
acetone	−25	16.0	0.2390	11.5
	0	69.3	0.2570	10.4
	+25	229.3	0.2794	8.0
isooctane	−25	2.5	0.3874	19.0
	0	12.8	0.3701	16.2
	+25	49	0.3725	14.2

There are at least two successful approaches to get solid thermodynamic and kinetic data from the low-temperature oxygenation experiments in the absence of the solubility values. In one approach, the standard state of dioxygen is assumed as the gas at 1 atm, in which case the activity of O_2 is equal to its partial pressure for a solution saturated with the gas at any given temperature. In a typical experimental setup, a stream of dioxygen gas (pure or diluted with inert gas) is bubbled through the solution of a metal complex until saturation is reached. Then the yield of a dioxygen adduct is determined by spectrometry, and if the oxygenation reaction is slow enough, kinetic parameters can be measured too. Such an approach has been successfully used for the comparison of the affinities[176,354] and reactivities[177] of different compounds toward dioxygen at the same temperature. However, it is impossible to compare the parameters of an oxygenation reaction obtained at different temperatures with this approach.

Alternatively, a solution of O_2 can be prepared at room temperature (20 or 25 °C), where the solubility is known, and then cooled without contact with a gas phase before mixing with a solution of the metal complex.[324] Because the solubility of dioxygen in liquids typically rises with the fall in temperature, there is no loss of the gas from solution. The only change in the O_2 concentration with cooling comes from a (relatively small) thermal contraction of the solvent, which can be accounted for using the following formula: $C_T = C_0(d_T/d_0)$, where C_T and d_T are, respectively, the concentration and density of the solution at temperature T, and C_0 and d_0 are the known values at room temperature. Because of the small solubility of O_2 in liquids, the density of the solution can be assumed equal to that of pure solvent. For several common solvents, densities were experi-

Table 11. Temperature Dependence of Solvent Density[a]

solvent	d(298 K), g cm^{-3}	a	b	ref
dichloromethane	1.325	1.862	1.800×10^{-3}	365
chloroform	1.475	2.012	1.800×10^{-3}	174
acetone	0.7864	1.1218	1.1248×10^{-3}	402
propionitrile	0.7766	1.0688	9.801×10^{-4}	401

[a] Data for other solvents are available in ref 395.

mentally determined in a wide range of temperatures and fit satisfactorily with the following equation: $d_T = a - bT$ (T in K; the parameters a and b are tabulated in Table 11).

Using this procedure, it is possible to define the standard state of dioxygen as the hypothetical 1 M solution and compare directly results obtained at different temperatures, including the extraction of thermal activation parameters from kinetic data. Because the dioxygen solution is prepared in advance, it was possible to use this procedure for the stopped-flow experiments and determine the rate constants of fast oxygenation reactions over a wide temperature range.[173,174,188,324,345]

Before a kinetic study, the reaction should be understood in terms of its stoichiometry and yield (clean reactions are preferable). Reactants, products, and byproducts should be characterized, and suitable experimental conditions chosen (solvent, additives, temperature range). Basic kinetic characterization of a reaction includes the determination of a rate law (concentration dependency) and thermal activation parameters (entropy and enthalpy of activation). These data alone can provide substantial mechanistic information.[103,377,378] The measurement of the volume of activation is also very useful, but it requires highly specialized equipment and so far has not been applied to the reactions at low temperature.[252−255] Additional mechanistic insights can be obtained from the systematic variation of the reaction medium and of the electronic and steric properties of the reactants (the Hammett correlation is the best known example of such an approach).[103,377,378] "Dioxygen surrogates" (NO and CO) were successfully used to better understand oxygenation reactions.[269,270,365] Kinetic isotope effects (like H/D and $^{16}O/^{18}O$), which can be determined from product distribution, are especially useful if direct kinetic measurements are impossible or difficult.[41,394] Taken together, kinetic data can provide a wealth of mechanistic information.

7. Summary and Perspective

The chemistry of dioxygen activation with non-heme iron complexes has been rapidly developing in recent years. Dramatic progress was accomplished in designing structural and functional models of iron-containing dioxygen carriers and redox enzymes. Many new examples of iron−peroxo species were reported, most of which were characterized spectroscopically. Importantly, novel high-valent complexes ($Fe^{III}Fe^{IV}$ and $Fe^{IV}Fe^{IV}$ species in dinuclear systems, and Fe^{IV}=O species in mononuclear systems) were obtained. Although crystallographic characterization of transient intermediates is still difficult (only several examples of X-ray structures of such species are known), their chemical structures can often be unambiguously determined from detailed spectroscopic studies. These recent successes in ligand design and in intermediate identification and characterization provide enormous opportunities for the deeper understanding of dioxygen activation that will ultimately lead to the rational preparation of selective reagents and catalysts. Detailed mechanistic studies are necessary in order to fully describe a sequence of events in the course of dioxygen activation processes.

Until recently, there were relatively few kinetic studies on dioxygen and peroxide activation with non-heme iron complexes. While the importance of kinetic and mechanistic studies has been well recognized, they were experimentally very challenging. Fortunately, this situation is changing, in part due to advances in kinetic methodology. Cryogenic stopped-flow methodology is no longer unheard of in the bioinorganic community, and some instrumentation is commercially available, thus making possible observation of rapid reactions with transient, thermally unstable intermediates. Modern data acquisition and analysis techniques (time-resolved acquisition of full spectra and global fitting analysis), supported by readily available software packages, facilitate interpretation of kinetic results, especially for multistep reactions. The proposed mechanistic schemes can now be subjected to rigorous testing.

Even though kinetic data are still often collected under ambient conditions, the value of activation parameters (obtained over a wide temperature range) in assigning intimate reaction mechanisms is somewhat greater appreciated in the current literature. The message advocated by Zuberbühler, Karlin, and co-workers several years ago still needs to be repeated, however: "It is important to note that in our experience comparisons of kinetic or equilibrium constants at a given temperature can sometimes be very misleading, and we caution that discussion of activation or thermodynamic parameters should be preferred wherever possible."[9] Knowledge of activation volumes is also very helpful but unfortunately unavailable for the reactions at cryogenic temperatures because of technical limitations.

Due to recent synthetic, spectroscopic, kinetic, and mechanistic studies, dioxygen binding to non-heme iron(II) centers is now much better understood. In most cases, this is an associative, low-barrier, entropically controlled process. Importantly, systematic mechanistic studies began playing an important role in guiding the design of facile dioxygen-binding complexes. Reactions with hydrogen peroxide, although synthetically very useful, have been rarely understood mechanistically. Even less knowledge was acquired regarding further steps in dioxygen activation (such as generating high-valent species from iron peroxo complexes, and their reactivity with substrates). There is no doubt that these areas will rapidly develop in the nearest future, providing critical information on the mechanisms of individual reaction steps in formation and the reactivity of iron−

oxygen intermediates. The factors that govern the stability and reactivity of these intermediates need to be identified in future mechanistic investigations, including a combination of kinetic, spectroscopic, structural, and computational approaches.

8. Acknowledgments

The authors are grateful to all their group members and collaborators, past and present, who contributed to the research described and referenced in this work. We would also like to thank the following individuals: Prof. M. Abu-Omar, Dr. A. Bakac, Prof. D. H. Busch, Prof. S. J. Lippard, and Prof. R. van Eldik for sharing preprints of their manuscripts; and an anonymous reviewer for the careful work with the manuscript and many valuable suggestions. Financial support from the NSF (CHE 0111202 to E.R.-A.) and the DFG (SPP 1118 and SCHI 377/6-2 to S.S.) is gratefully acknowledged.

9. References

(1) Lippard, S. J.; Berg, J. M. *Principles of Bioinorganic Chemistry*; University Science Books: Mill Valley, CA, 1994.
(2) *Bio-Coordination Chemistry*; Que, L., Jr., Tolman, W. B., Eds.; In *Comprehensive Coordination Chemistry II*; McCleverty, J. A., Meyer, T. J., Eds.; Elsevier: Oxford, U.K., 2004; Vol. 8.
(3) Costas, M.; Mehn, M. P.; Jensen, M. P.; Que, L., Jr. *Chem. Rev.* **2004**, *104*, 939−986.
(4) Tshuva, E. Y.; Lippard, S. J. *Chem. Rev.* **2004**, *104*, 987−1012.
(5) Lewis, E. A.; Tolman, W. B. *Chem. Rev.* **2004**, *104*, 1047−1076.
(6) Mirica, L. M.; Ottenwaelder, X.; Stack, T. D. P. *Chem. Rev.* **2004**, *104*, 1013−1045.
(7) Kim, E.; Chufán, E. E.; Kamaraj, K.; Karlin, K. D. *Chem. Rev.* **2004**, *104*, 1077−1134.
(8) *Bioinorganic chemistry of copper*; Karlin, K. D., Tyeklar, Z., Eds.; Chapman & Hall: New York, 1993.
(9) Karlin, K. D.; Kaderli, S.; Zuberbühler, A. D. *Acc. Chem. Res.* **1997**, *30*, 139−147.
(10) Solomon, E. I.; Chen, P.; Metz, M.; Lee, S. K.; Palmer, A. E. *Angew. Chem., Int. Ed.* **2001**, *40*, 4570−4590.
(11) Stack, D. T. P. *Dalton Trans.* **2003**, 1881−1889.
(12) Tolman, W. B. *Acc. Chem. Res.* **1997**, *30*, 227−237.
(13) Holland, P. L.; Tolman, W. B. *Coord. Chem. Rev.* **1999**, *190*−*192*, 855−869.
(14) Schindler, S. *Eur. J. Inorg. Chem.* **2000**, 2311−2326.
(15) Sono, M.; Roach, M. P.; Coulter, E. D.; Dawson, J. H. *Chem. Rev.* **1996**, *96*, 2841−2187.
(16) Valentine, J. S. Dioxygen Reactions. In *Bioinorganic Chemistry*; Bertini, E., Gray, H. B., Lippard, S. J., Valentine, J. S., Eds.; University Science Books: Sausalito, CA, 1994; pp 253−313.
(17) Collman, J. P.; Zhang, X. Functional analogues of the oxygen binding and activating heme proteins. In *Comprehensive Supramolecular Chemistry*; Lehn, J.-M., Ed.; Pergamon/Elsevier: Oxford, 1996; Vol. 5; pp 1−32.
(18) Momenteau, M.; Reed, C. A. *Chem. Rev.* **1994**, *94*, 659−698.
(19) Meunier, B.; de Visser, S. P.; Shaik, S. *Chem. Rev.* **2004**, *104*, 3947−3980.
(20) Bakac, A. *Prog. Inorg. Chem.* **1995**, *43*, 267−351.
(21) Feig, A. L.; Lippard, S. J. *Chem. Rev.* **1994**, *94*, 759−805.
(22) Warburton, P. R.; Busch, D. H. Dynamics of iron(II) and cobalt(II) dioxygen carriers. *Perspectives on Bioinorganic Chemistry*; JAI Press: London, 1993; Vol. 2, pp 1−79.
(23) Lee, D.; Lippard, S. J. Nonheme Di-iron Enzymes. In *Comprehensive Coordination Chemistry II*; McCleverty, J. A., Meyer, T. J., Eds.; Elsevier: Oxford, U.K., 2004; Vol. 8, pp 309−342.
(24) Foster, T. L.; Caradonna, J. P. Non-heme Mono-iron Enzymes. In *Comprehensive Coordination Chemistry*; McCleverty, J. A., Meyer, T. J., Eds.; Elsevier: Oxford, U.K., 2004; Vol. 8. pp 343−368.
(25) He, C.; Mishina, Y. *Curr. Opin. Chem. Biol.* **2004**, *8*, 201−208.
(26) Rohde, J.-U.; Bukowski, M. R.; Que, L., Jr. *Curr. Opin. Chem. Biol.* **2003**, *7*, 674−682.
(27) Que, L., Jr.; Tolman, W. B. *Angew. Chem., Int. Ed.* **2002**, *41*, 1114−1137.
(28) Tolman, W. B.; Que, L., Jr. *J. Chem. Soc., Dalton Trans.* **2002**, 653−660.
(29) Solomon, E. I.; Brunold, T. C.; Davis, M. I.; Kemsley, J. N.; Lee, S.-K.; Lehnert, N.; Neese, F.; Skulan, A. J.; Yang, Y.-S.; Zhou, J. *Chem. Rev.* **2000**, *100*, 235−349.
(30) Krebs, C.; Price, J. C.; Baldwin, J.; Saleh, L.; Green, M. T.; Bollinger, J. M., Jr. *Inorg. Chem.* **2005**, *44*, 742−757.
(31) Niederhoffer, E. C.; Timmons, J. H.; Martell, A. E. *Chem. Rev.* **1984**, *84*, 137−203.
(32) Vaska, L. *Acc. Chem. Res.* **1976**, *9*, 175−183.
(33) Cramer, C. J.; Tolman, W. B.; Theopold, K. H.; Rheingold, A. L. *Proc. Natl. Acad. Sci. U.S.A.* **2003**, *100*, 3635−3640.
(34) Sawyer, D. T. *Oxygen Chemistry*; Oxford University Press: New York, 1991.
(35) Goldstein, S.; Meyerstein, D.; Czapski, G. *Free Radical Biol. Med.* **1993**, *15*, 435−445.
(36) Sawyer, D. T.; Sobkowiak, A.; Matsushita, T. *Acc. Chem. Res.* **1996**, *29*, 409−416.
(37) Walling, C. *Acc. Chem. Res.* **1998**, *31*, 155−157.
(38) MacFaul, P. A.; Wayner, D. D. M.; Ingold, K. U. *Acc. Chem. Res.* **1998**, *31*, 159−162.
(39) Goldstein, S.; Meyerstein, D. *Acc. Chem. Res.* **1999**, *32*, 547−550.
(40) Stavropoulos, P.; Celenligil-Cetin, R.; Tapper, A. E. *Acc. Chem. Res.* **2001**, *34*, 745−752.
(41) Costas, M.; Chen, K.; Que, L., Jr. *Coord. Chem. Rev.* **2000**, *200*−*202*, 517−544.
(42) Chen, K.; Costas, M.; Que, L., Jr. *J. Chem. Soc., Dalton Trans.* **2002**, 672−679.
(43) Fabian, I.; Csordas, V. *Adv. Inorg. Chem.* **2003**, *54*, 395−461.
(44) Shilov, A. E.; Shul'pin, G. B. *Chem. Rev.* **1997**, *97*, 2879−2932.
(45) Shilov, A. E.; Shteinman, A. A. *Acc. Chem. Res.* **1999**, *32*, 763−771.
(46) Shul'pin, G. B. *C. R. Chimie* **2003**, *6*, 163−178.
(47) Abu-Omar, M. M.; Loaiza, A.; Hontzeas, N. *Chem. Rev.* **2005**, *105*, 2227−2252.
(48) Fox, B. G.; Lyle, K. S.; Rogge, C. E. *Acc. Chem. Res.* **2004**, *37*, 421−429.
(49) Baik, M.-H.; Newcomb, M.; Friesner, R. A.; Lippard, S. J. *Chem. Rev.* **2003**, *103*, 2385−2419.
(50) Stubbe, J. *Curr. Opin. Chem. Biol.* **2003**, *7*, 183−188.
(51) Ryle, M. J.; Hausinger, R. P. *Curr. Opin. Chem. Biol.* **2002**, *6*, 193−201.
(52) Solomon, E. I. *Inorg. Chem.* **2001**, *40*, 3656−3669.
(53) Wallar, B. J.; Lipscomb, J. D. *Chem. Rev.* **1996**, *96*, 2625−2657.
(54) Lange, S. J.; Que, L., Jr. *Curr. Opin. Chem. Biol.* **1998**, *2*, 159−172.
(55) Que, L., Jr.; Ho, R. Y. N. *Chem. Rev.* **1996**, *96*, 2607−2624.
(56) Nivorozhkin, A. L.; Girerd, J.-J. *Angew. Chem., Int. Ed. Engl.* **1996**, *35*, 609−611.
(57) Nordlund, P.; Eklund, H. *Curr. Opin. Sruct. Biol.* **1995**, *5*, 758−766.
(58) Edmondson, D. E.; Huynh, B. H. *Inorg. Chim. Acta* **1996**, *252*, 399−404.
(59) Kurtz, D. M., Jr. *J. Biol. Inorg. Chem.* **1997**, *2*, 159−167.
(60) Kurtz, D. M., Jr. Dioxygen-binding Proteins. In *Comprehensive Coordination Chemistry II*; McCleverty, J. A., Meyer, T. J., Eds.; Elsevier: Oxford, U.K., 2004; Vol. 8; pp 229−260.
(61) Merkx, M.; Kopp, D. A.; Sazinsky, M. H.; Blazyk, J. L.; Müller, J.; Lippard, S. J. *Angew. Chem., Int. Ed.* **2001**, *40*, 2782−2807.
(62) Rohde, J.-U.; In, J.-H.; Lim, M. H.; Brennessel, W. W.; Bukowski, M. R.; Stubna, A.; Münck, E.; Nam, W.; Que, L., Jr. *Science* **2003**, *299*, 1037−1039.
(63) Decker, A.; Rohde, J.-U.; Que, L., Jr.; Solomon, E. I. *J. Am. Chem. Soc.* **2004**, *126*, 5378−5379.
(64) Lipscomb, J. D.; Que, L., Jr. *J. Biol. Inorg. Chem.* **1998**, *3*, 331−336.
(65) Price, J. C.; Barr, E. W.; Glass, T. E.; Krebs, C.; Bollinger, J. M., Jr. *J. Am. Chem. Soc.* **2003**, *125*, 13008−13009.
(66) Proshlyakov, D. A.; Henshaw, T. F.; Monterosso, G. R.; Ryle, M. J.; Hausinger, R. P. *J. Am. Chem. Soc.* **2004**, *126*, 1022−1023.
(67) Karlsson, A.; Parales, J. V.; Parales, R. E.; Gibson, D. T.; Eklund, H.; Ramaswamy, S. *Science* **2003**, *299*, 1039−1042.
(68) Hecht, S. M. *Acc. Chem. Res.* **1986**, *19*, 383−391.
(69) Stubbe, J.; Kozarich, J. W.; Wu, W.; Vanderwall, D. E. *Acc. Chem. Res.* **1996**, *29*, 322−330.
(70) Stubbe, J.; Kozarich, J. W. *Chem. Rev.* **1987**, *87*, 1107−1136.
(71) Petering, D. H.; Mao, Q.; Li, W.; DeRose, E.; Antholine, W. Metallobleomycin−DNA interactions: structures and reactions related to bleomycin-induced DNA damage. In *Metal Ions in Biological Systems*; Siegel, A., Siegel, H., Eds.; Marcel Dekker: New York, 1996; Vol. 33, pp 619−648.
(72) Burger, R. M. *Chem. Rev.* **1998**, *98*, 1153−1169.
(73) Boger, D. L.; Cai, H. *Angew. Chem., Int. Ed. Engl.* **1999**, *38*, 448−476.
(74) Abasalon, M. J.; Wu, W.; Kozarich, J. W.; Stubbe, J. *Biochemistry* **1995**, *34*, 2076−2086.
(75) Burger, R. M.; Peisach, J.; Horwitz, S. B. *J. Biol. Chem.* **1981**, *256*, 11636−11644.
(76) Burger, R. M.; Kent, T. A.; Horwitz, S. B.; Münck, E.; Peisach, J. *J. Biol. Chem.* **1983**, *258*, 1559−1564.
(77) Westre, T. A.; Loeb, K. E.; Zaleski, J. M.; Hedman, B.; Hodgson, K. O.; Solomon, E. I. *J. Am. Chem. Soc.* **1995**, *117*, 1309−1313.

(78) Sam, J. W.; Tang, X.-J.; Peisach, J. *J. Am. Chem. Soc.* **1994**, *116*, 5250−5256.
(79) Burger, R. M.; Tian, G.; Drlica, K. *J. Am. Chem. Soc.* **1995**, *117*, 1167−1168.
(80) Neese, F.; Zaleski, J. M.; Zaleski, K. L.; Solomon, E. I. *J. Am. Chem. Soc.* **2000**, *122*, 11703−11724.
(81) Sugiura, Y.; Takita, T.; Umezawa, H. Bleomycin antibiotics: metal complexes and their biological action. In *Metal Ions in Biological Systems*; Siegel, H., Ed.; Marcel Dekker: New York, 1985; Vol. 19, pp 81−108.
(82) Loeb, K. E.; Zaleski, J. M.; Westre, T. E.; Guajardo, R. J.; Mascharak, P. K.; Hedman, B.; Hodgson, K. O.; Solomon, E. I. *J. Am. Chem. Soc.* **1995**, *117*, 4545−4561.
(83) Chen, J.; Stubbe, J. *Curr. Opin. Chem. Biol.* **2004**, *8*, 175−181.
(84) Wilkins, R. G.; Harrington, P. C. *Adv. Inorg. Chem.* **1983**, *5*, 51−85.
(85) Wilkins, P. C.; Wilkins, R. G. *Coord. Chem. Rev.* **1987**, *79*, 195−214.
(86) Stenkamp, R. E. *Chem. Rev.* **1994**, *94*, 715−726.
(87) Wilkins, R. G. Kinetics of Formation of Biological Oxygen Carriers. In *Oxygen Complexes and Oxygen Activation by Transition Metals*; Martell, A. E., Sawyer, D. T., Eds.; Plenum Press: New York, 1987; pp 49−60.
(88) Brunold, T. C.; Solomon, E. I. *J. Am. Chem. Soc.* **1999**, *121*, 8277−8287.
(89) Holmes, M. A.; Trong, I. L.; Turley, S.; Sieker, L. C.; Stenkamp, R. E. *J. Mol. Biol.* **1991**, *218*, 583−593.
(90) Armstrong, F. A.; Harrington, P. C.; Wilkins, R. G. *J. Inorg. Biochem.* **1983**, *18*, 83−91.
(91) Brunold, T. C.; Solomon, E. I. *J. Am. Chem. Soc.* **1999**, *121*, 8288−8295.
(92) Wirstam, M.; Lippard, S. J.; Friesner, R. A. *J. Am. Chem. Soc.* **2003**, *125*, 3980−3987.
(93) Friesner, R. A.; Baik, M.-H.; Gherman, B. F.; Guallar, V.; Wirstam, M.; Murphy, R. B.; Lippard, S. J. *Coord. Chem. Rev.* **2003**, *238*−*239*, 267−290.
(94) Alberding, N.; Lavalette, D.; Austin, R. H. *Proc. Natl. Acad. Sci. U.S.A.* **1981**, *78*, 2307−2309.
(95) Bates, G.; Brunori, M.; Amiconi, G.; Antonini, E.; Wyman, J. *Biochemistry* **1968**, *7*, 3016−3020.
(96) Petrou, A. L.; Armstrong, F. A.; Sykes, A. G.; Harrington, P. C.; Wilkins, R. G. *Biochim. Biophys. Acta* **1981**, *670*, 377−384.
(97) Projahn, H.-D.; Schindler, S.; van Eldik, R.; Fortier, D. G.; Andrew, C. R.; Sykes, A. G. *Inorg. Chem.* **1995**, *34*, 5935−5941.
(98) de Waal, D. J. A.; Wilkins, R. G. *J. Biol. Chem.* **1976**, *251*, 2339−2342.
(99) Armstrong, G. D.; Sykes, A. G. *Inorg. Chem.* **1986**, *25*, 3155−3139.
(100) Farmer, C. S.; Kurtz, D. M.; Phillips, R. S.; Ai, J. Y.; Sanders-Loehr, J. *J. Biol. Chem.* **2000**, *275*, 17043−17050.
(101) Lloyd, C. R.; Eyring, E. M.; Ellis, W. R., Jr. *J. Am. Chem. Soc.* **1995**, *117*, 11993−11994.
(102) Xiong, J.; Phillips, R. S.; Kurtz, D. M., Jr.; Jin, S.; Ai, J.; Sanders-Loehr, J. *Biochemistry* **2000**, *39*, 8526−8536.
(103) Espenson, J. H. *Chemical Kinetics and Mechanisms*; McGraw-Hill: New York, 1981.
(104) Lloyd, C. R.; Raner, G. M.; Moser, A.; Eyring, E. M.; Ellis, W. R., Jr. *J. Inorg. Biochem.* **2000**, *81*, 293−300.
(105) Yedgar, S.; Tetreau, C.; Gavish, B.; Lavalette, D. *Biophys. J.* **1995**, *68*, 665−670.
(106) Zimmer, J. R.; Tachi-iri, Y.; Takizawa, H.; Handa, T.; Yamamura, T.; Kihara, H. *Biochim. Biophys. Acta* **1986**, *874*, 174−180.
(107) Bradic, Z.; Conrad, R.; Wilkins, R. G. *J. Biol. Chem.* **1977**, *252*, 6069−6075.
(108) Fuseya, M.; Ichimura, K.; Yamamura, T.; Tach'iri, Y.; Satake, K.; Amemiya, Y.; Kihara, H. *J. Biochem.* **1989**, *105*, 293−298.
(109) Raner, G. M.; Martins, L. J.; Ellis, W. R., Jr. *Biochemistry* **1997**, *36*, 7037−7043.
(110) Farmer, C. S.; Kurtz, D. M., Jr.; Liu, Z. J.; Wang, B. C.; Rose, J.; Ai, J. Y.; Sanders-Loehr, J. *J. Biol. Inorg. Chem.* **2001**, *6*, 418−429.
(111) Kaminaka, S.; Takizawa, H.; Handa, T.; Kihara, H.; Kitagawa, T. *Biochemistry* **1992**, *31*, 6997−7002.
(112) Springborg, J.; Wilkins, P. C.; Wilkins, R. G. *Acta Chem. Scand.* **1989**, *43*, 967−974.
(113) Harrington, P. C.; Wilkins, R. G. *J. Inorg. Biochem.* **1983**, *19*, 339−344.
(114) Armstrong, G. D.; Sykes, A. G. *Inorg. Chem.* **1986**, *25*, 3514−3516.
(115) Zhang, B.-J.; Andrew, C. R.; Tomkinson, N. P.; Sykes, A. G. *Biochim. Biophys. Acta* **1992**, *1102*, 245−252.
(116) Bradic, Z.; Harrington, P. C.; Wilkins, R. G. Oxygen and hydrogen peroxide promoted interconversion of iron(II) and iron(III) in hemerythrin. In *Biochemical and clinical aspects of oxygen*; Caughey, W. S., Ed.; Academic Press: New York, 1979; pp 557−571.
(117) Behrouzian, B.; Buist, P. H. *Curr. Opin. Chem. Biol.* **2002**, *6*, 577−582.
(118) Sazinsky, M. H.; Bard, J.; Di Donato, A.; Lippard, S. J. *J. Biol. Chem.* **2004**, *279*, 30600−30610.
(119) Shanklin, J.; Whittle, E. *FEBS Lett.* **2003**, *545*, 188−192.
(120) Fox, B. G.; Borneman, J. G.; Wackett, L. P.; Lipscomb, J. D. *Biochemistry* **1990**, *29*, 6419−6427.
(121) Lee, S.-K.; Nesheim, J. C.; Lipscomb, J. D. *J. Biol. Chem.* **1993**, *268*, 21569−21577.
(122) Nesheim, J. C.; Lipscomb, J. D. *Biochemistry* **1996**, *35*, 10240−10247.
(123) Lee, S.-K.; Lipscomb, J. D. *Biochemistry* **1999**, *38*, 4423−4432.
(124) Wallar, B. J.; Lipscomb, J. D. *Biochemistry* **2001**, *40*, 2220−2233.
(125) Brazeau, B. J.; Lipscomb, J. D. *Biochemistry* **2000**, *39*, 13503−13515.
(126) Brazeau, B. J.; Wallar, B. J.; Lipscomb, J. D. *J. Am. Chem. Soc.* **2001**, *123*, 10421−10422.
(127) Brazeau, B. J.; Austin, R. N.; Tarr, C.; Groves, J. T.; Lipscomb, J. D. *J. Am. Chem. Soc.* **2001**, *123*, 11831−11837.
(128) Liu, K. E.; Valentine, A. M.; Qiu, D.; Edmondson, D. E.; Appelman, E. H.; Spiro, T. G.; Lippard, S. J. *J. Am. Chem. Soc.* **1995**, *117*, 4997−4998.
(129) Valentine, A. M.; Stahl, S. S.; Lippard, S. J. *J. Am. Chem. Soc.* **1999**, *121*, 3876−3887.
(130) Coufal, D. E.; Tavares, P.; Pereira, A. S.; Hyunh, B. H.; Lippard, S. J. *Biochemistry* **1999**, *38*, 4504−4513.
(131) Ambundo, E. A.; Friesner, R. A.; Lippard, S. J. *J. Am. Chem. Soc.* **2002**, *124*, 8770−8771.
(132) Muthusamy, M.; Ambundo, E. A.; George, S. J.; Lippard, S. J.; Thorneley, R. N. F. *J. Am. Chem. Soc.* **2003**, *125*, 11150−11151.
(133) Baldwin, J.; Krebs, C.; Ley, B. A.; Edmondson, D. E.; Huynh, B. H.; Bollinger, J. M., Jr. *J. Am. Chem. Soc.* **2000**, *122*, 12195−12206.
(134) Baldwin, J.; Voegtli, W. C.; Khidekel, N.; Moënne-Loccoz, P.; Krebs, K.; Pereira, A. S.; Ley, B. A.; Huynh, B. H.; Loehr, T. M.; Riggs-Gelasco, P. J.; Rozenzweig, A. C.; Bollinger, J. M., Jr. *J. Am. Chem. Soc.* **2001**, *123*, 7017−7030.
(135) Bollinger, J. M., Jr.; Edmondson, D. E.; Huynh, B. H.; Filley, J.; Norton, J. R.; Stubbe, J. *Science* **1991**, *253*, 292−298.
(136) Bollinger, J. M., Jr.; Tong, W. H.; Ravi, N.; Huynh, B. H.; Edmondson, D. E.; Stubbe, J. *J. Am. Chem. Soc.* **1994**, *116*, 8015−8023.
(137) Bollinger, J. M., Jr.; Tong, W. H.; Ravi, N.; Huynh, B. H.; Edmondson, D. E.; Stubbe, J. *J. Am. Chem. Soc.* **1994**, *116*, 8024−8032.
(138) Bollinger, J. M., Jr.; Chen, S. X.; Parkin, S. E.; Mangravite, L. M.; Ley, B. A.; Edmondson, D. E.; Huynh, B. H. *J. Am. Chem. Soc.* **1997**, *119*, 5976−5977.
(139) Bollinger, J. M., Jr.; Krebs, C.; Vicol, A.; Chen, S. X.; Ley, B. A.; Edmondson, D. E.; Huynh, B. H. *J. Am. Chem. Soc.* **1998**, *120*, 1094−1095.
(140) Katterle, B.; Sahlin, M.; Schmidt, P. P.; Potsch, S.; Logan, D. T.; Graslund, A.; Sjoberg, B. M. *J. Biol. Chem.* **1997**, *272*, 10414−10421.
(141) Krebs, C.; Chen, S. X.; Baldwin, J.; Ley, B. A.; Patel, U.; Edmondson, D. E.; Huynh, B. H.; Bollinger, J. M., Jr. *J. Am. Chem. Soc.* **2000**, *122*, 12207−12219.
(142) Liu, A.; Leese, D. N.; Swarts, J. C.; Sykes, A. G. *Inorg. Chim. Acta* **2002**, *337*, 83−90.
(143) Miller, M. A.; Gobena, F. T.; Kauffmann, K.; Münck, E.; Que, L., Jr.; Stankovich, M. T. *J. Am. Chem. Soc.* **1999**, *121*, 1096−1097.
(144) Moënne-Loccoz, P.; Baldwin, J.; Ley, B. A.; Loehr, T. M.; Bollinger, J. M., Jr. *Biochemistry* **1998**, *37*, 14659−14663.
(145) Ravi, N.; Bollinger, J. M., Jr.; Huynh, B. H.; Edmondson, D. E.; Stubbe, J. *J. Am. Chem. Soc.* **1994**, *116*, 8007−8014.
(146) Riggs-Gelasco, P. J.; Shu, L. J.; Chen, S. X.; Burdi, D.; Huynh, B. H.; Que, L., Jr.; Stubbe, J. *J. Am. Chem. Soc.* **1998**, *120*, 849−860.
(147) Tong, W. H.; Chen, S.; Lloyd, S. G.; Edmondson, D. E.; Huynh, B. H.; Stubbe, J. *J. Am. Chem. Soc.* **1996**, *118*, 2107−2108.
(148) Abad, J. L.; Camps, F.; Fabrias, G. *Angew. Chem., Int. Ed.* **2000**, *39*, 3279−3281.
(149) Broadwater, J. A.; Ai, J.; Loehr, T. M.; Sanders-Loehr, J.; Fox, B. G. *Biochemistry* **1998**, *37*, 14664−14671.
(150) Broadwater, J. A.; Achim, C.; Münck, E.; Fox, B. G. *Biochemistry* **1999**, *38*, 12197−12204.
(151) Lyle, K. S.; Haas, J. A.; Fox, B. G. *Biochemistry* **2003**, *42*, 5857−5866.
(152) Pereira, A. S.; Small, W.; Krebs, C.; Tavares, P.; Edmondson, D. E.; Theil, E. C.; Huynh, B. H. *Biochemistry* **1998**, *37*, 9871−9876.
(153) Hwang, J.; Krebs, C.; Huynh, B. H.; Edmondson, D. E.; Theil, E. C.; Penner-Hahn, J. E. *Science* **2000**, *287*, 122−125.
(154) Jameson, G. N. L.; Jin, W.; Krebs, C.; Perreira, A. S.; Tavares, P.; Liu, X.; Theil, E. C.; Huynh, B. H. *Biochemistry* **2002**, *41*, 13435−13443.
(155) Emerson, J. P.; Coulter, E. D.; Cabelli, D. E.; Phillips, R. S.; Kurtz, D. M., Jr. *Biochemistry* **2000**, *41*, 4348−4357.
(156) Emerson, J. P.; Coulter, E. D.; Phillips, R. S.; Kurtz, D. M., Jr. *J. Biol. Chem.* **2003**, *278*, 39662−39668.

(157) Pikus, J. D.; Mitchell, K. H.; Studts, J. M.; McClay, K.; Steffan, R. J.; Fox, B. G. *Biochemistry* **2000**, *39*, 791−799.
(158) Kopp, D. A.; Lippard, S. J. *Curr. Opin. Chem. Biol.* **2002**, *6*, 568−576.
(159) Broadwater, J. A.; Haas, J. A.; Fox, B. G. *Fett/Lipid* **1998**, *100*, 103−113.
(160) Du Bois, J.; Mizoguchi, T. J.; Lippard, S. J. *Coord. Chem. Rev.* **2000**, *200−202*, 443−485.
(161) Suzuki, M.; Furutachi, H.; Okawa, H. *Coord. Chem. Rev.* **2000**, *200−202*, 105−129.
(162) Pierre, J. L.; Fontecave, M. *Biometals* **1999**, *12*, 195−199.
(163) Fontecave, M.; Ménage, S.; Duboc-Toia, C. *Coord. Chem. Rev.* **1998**, *178−180*, 1555−1572.
(164) Que, L., Jr. *J. Chem. Soc., Dalton Trans.* **1997**, 3933−3940.
(165) Que, L., Jr.; Dong, Y. *Acc. Chem. Res.* **1996**, *29*, 190−196.
(166) Busch, D. H.; Alcock, N. W. *Chem. Rev.* **1994**, *94*, 585−623.
(167) Girerd, J.-J.; Banse, F.; Simaan, A. J. *Struct. Bonding (Berlin)* **2000**, *97*, 145−177.
(168) Feig, A. L.; Lippard, S. J. *J. Am. Chem. Soc.* **1994**, *116*, 8410−8411.
(169) Ménage, S.; Brennan, B. A.; Juarez-Garsia, C.; Münck, E.; Que, L., Jr. *J. Am. Chem. Soc.* **1990**, *112*, 2.
(170) Dong, Y.; Yan, S.; Young, V. G., Jr.; Que, L., Jr. *Angew. Chem., Int. Ed.Engl.* **1996**, *35*, 618−620.
(171) Ookubo, T.; Sugimoto, H.; Nagayama, T.; Masuda, H.; Sato, T.; Tanaka, K.; Maeda, Y.; Okawa, H.; Hayashi, Y.; Uehara, A.; Suzuki, M. *J. Am. Chem. Soc.* **1996**, *118*, 701−702.
(172) Kim, K.; Lippard, S. J. *J. Am. Chem. Soc.* **1996**, *118*, 4914−4915.
(173) Feig, A. L.; Becker, M.; Schindler, S.; van Eldik, R.; Lippard, S. J. *Inorg. Chem.* **1996**, *35*, 2590−2601.
(174) Feig, A. L.; Masschelein, A.; Bakac, A.; Lippard, S. J. *J. Am. Chem. Soc.* **1997**, *119*, 334−342.
(175) Herold, S.; Lippard, S. J. *J. Am. Chem. Soc.* **1997**, *119*, 145−156.
(176) Sugimoto, H.; Nagayama, T.; Maruyama, S.; Fujinami, S.; Yasuda, Y.; Suzuki, M.; Uehara, A. *Bull. Chem. Soc. Jpn.* **1998**, *71*, 2267−2279.
(177) LeCloux, D. D.; Barrios, A. M.; Mizoguchi, T. J.; Lippard, S. J. *J. Am. Chem. Soc.* **1998**, *120*, 9001−9014.
(178) LeCloux, D. D.; Barrios, A. M.; Lippard, S. J. *Bioorg. Med. Chem.* **1999**, *7*, 763−772.
(179) Hagadorn, J. R.; Que, L., Jr.; Tolman, W. B. *J. Am. Chem. Soc.* **1998**, *120*, 13531−13532.
(180) Than, R.; Schrodt, A.; Westerheide, L.; van Eldik, R.; Krebs, B. *Eur. J. Inorg. Chem.* **1999**, 1537−1543.
(181) Zhang, X.; Furutachi, H.; Fujinami, S.; Nagamoto, S.; Maeda, Y.; Watanabe, Y.; Kitagawa, T.; Suzuki, M. *J. Am. Chem. Soc.* **2005**, *127*, 826−827.
(182) Selke, M.; Sisemore, M. F.; Valentine, J. S. *J. Am. Chem. Soc.* **1996**, *118*, 2008−2012.
(183) Selke, M.; Sisemore, M. F.; Ho, R. Y. N.; Wertz, D. L.; Valentine, J. S. *J. Mol. Catal. A* **1997**, *117*, 71−82.
(184) Neese, F.; Solomon, E. I. *J. Am. Chem. Soc.* **1998**, *120*, 12829−12848.
(185) Ho, R. Y. N.; Roelfes, G.; Hermant, R.; Hage, R.; Feringa, B. L.; Que, L., Jr. *Chem. Commun.* **1999**, 2161−2162.
(186) Roelfes, G.; Lubben, M.; Chen, K.; Ho, R. Y. N.; Meetsma, A.; Genseberger, S.; Hermant, R. M.; Hage, R.; Mandal, S. K.; Young, V. G., Jr.; Zang, Y.; Kooijman, H.; Spek, A. L.; Que, L., Jr.; Feringa, B. L. *Inorg. Chem.* **1999**, *38*, 1929−1936.
(187) Goto, Y.; Wada, S.; Morishima, I.; Watanabe, Y. *J. Inorg. Biochem.* **1998**, *69*, 241−247.
(188) Kryatov, S. V.; Chavez, F. A.; Reynolds, A. M.; Rybak-Akimova, E. V.; Que, L., Jr.; Tolman, W. B. *Inorg. Chem.* **2004**, *43*, 2141−2150.
(189) Carson, E. C.; Lippard, S. J. *J. Am. Chem. Soc.* **2004**, *126*, 3412−3413.
(190) Grapperhaus, C. A.; Mienert, B.; Bill, E.; Weyhermüller, T.; Wieghardt, K. *Inorg. Chem.* **2000**, *39*, 5306−5317.
(191) Lim, M. H.; Rohde, J.-U.; Stubna, A.; Bukowski, M. R.; Costas, M.; Ho, R. Y. N.; Münck, E.; Nam, W.; Que, L., Jr. *Proc. Natl. Acad. Sci. U.S.A.* **2003**, *100*, 3665−3670.
(192) Kaizer, J.; Costas, M.; Que, L., Jr. *Angew. Chem., Int. Ed.* **2003**, *42*, 3671−3673.
(193) Kaizer, J.; Klinker, E. J.; Oh, N. Y.; Rohde, J.-U.; Song, W. J.; Stubna, A.; Kim, J.; Münck, E.; Nam, W.; Que, L., Jr. *J. Am. Chem. Soc.* **2004**, *126*, 472−473.
(194) Balland, V.; Charlot, M.-F.; Banse, F.; Girerd, J.-J.; Mattioli, T. A.; Bill, E.; Bartoli, J.-F.; Battioni, P.; Mansuy, D. *Eur. J. Inorg. Chem.* **2004**, 301−308.
(195) Dong, Y.; Fujii, H.; Hendrich, M. P.; Leising, R. A.; Pan, G.; Randall, C. R.; Wilkinson, E. C.; Zang, Y.; Que, L., Jr.; Fox, B. G.; Kauffmann, K.; Münck, E. *J. Am. Chem. Soc.* **1995**, *117*, 1169−1170.
(196) Dong, Y.; Zang, Y.; Shu, L.; Wilkinson, E. C.; Que, L., Jr. *J. Am. Chem. Soc.* **1997**, *119*, 12683−12684.
(197) Hsu, H.-F.; Dong, Y. H.; Shu, L.; Young, V. G., Jr.; Que, L., Jr. *J. Am. Chem. Soc.* **1999**, *121*, 5230−5237.
(198) Skulan, A. J.; Hanson, M. A.; Hsu, H.-F.; Dong, Y.; Que, L., Jr.; Solomon, E. I. *Inorg. Chem.* **2003**, *42*, 6489−6496.
(199) Skulan, A. J.; Hanson, M. A.; Hsu, H.-F.; Que, L., Jr.; Solomon, E. I. *J. Am. Chem. Soc.* **2003**, *125*, 7344−7356.
(200) Lee, D.; Du Bois, J.; Petasis, D.; Hendrich, M. P.; Krebs, C.; Huynh, B. H.; Lippard, S. J. *J. Am. Chem. Soc.* **1999**, *121*, 9893−9894.
(201) Lee, D.; Pierce, B.; Krebs, C.; Hendrich, M. P.; Huynh, B. H.; Lippard, S. J. *J. Am. Chem. Soc.* **2002**, *124*, 3993−4007.
(202) Slep, L. D.; Mijovilovich, A.; Meyer-Klaucke, W.; Weyhermüller, T.; Bill, E.; Bothe, E.; Neese, F.; Wieghardt, K. *J. Am. Chem. Soc.* **2003**, *125*, 15554−15570.
(203) Jüstel, T.; Müller, M.; Weyhermüller, T.; Kressl, C.; Bill, E.; Hildebrandt, P.; Lengen, M.; Grodzicki, M.; Trautwein, A. X.; Nuber, B.; Wieghardt, K. *Chem.−Eur. J.* **1999**, *5*, 793−810.
(204) Costas, M.; Rohde, J.-U.; Stubna, A.; Ho, R. Y. N.; Quaroni, L.; Münck, E.; Que, L., Jr. *J. Am. Chem. Soc.* **2001**, *123*, 12931−12932.
(205) Ghosh, A.; Tangen, E.; Gonzalez, E.; Que, L., Jr. *Angew. Chem., Int. Ed.* **2004**, *43*, 834−838.
(206) Ghosh, A.; Tiago de Oliveira, F.; Yano, T.; Nishioka, T.; Beach, E. S.; Kinoshita, I.; Münck, E.; Ryabov, A. D.; Horwitz, C. P.; Collins, T. J. *J. Am. Chem. Soc.* **2005**, *127*, 2505−2513.
(207) White, M. C.; Doyle, A. G.; Jacobsen, E. N. *J. Am. Chem. Soc.* **2001**, *123*, 7194−7195.
(208) Costas, M.; Tipton, A. K.; Chen, K.; Jo, D.-H.; Que, L., Jr. *J. Am. Chem. Soc.* **2001**, *123*, 6722−6723.
(209) Fujita, M.; Que, L., Jr. *Adv. Synth. Catal.* **2004**, *346*, 190−194.
(210) Dubois, G.; Murphy, A.; Stack, T. D. P. *Org. Lett.* **2003**, *5*, 2469−2472.
(211) Duban, E. A.; Bryliakov, K. P.; Talsi, E. P. *Mendeleev Commun.* **2005**, 12−14.
(212) Ryu, J. Y.; Kim, J.; Costas, M.; Chen, K.; Nam, W.; Que, L., Jr. *Chem. Commun.* **2002**, 1288−1289.
(213) Chen, K.; Costas, M.; Kim, J.; Tipton, A. K.; Que, L., Jr. *J. Am. Chem. Soc.* **2002**, *124*, 3026−3035.
(214) Fujita, M.; Costas, M.; Que, L., Jr. *J. Am. Chem. Soc.* **2003**, *125*, 9912−9913.
(215) Foster, T. L.; Caradonna, J. P. *J. Am. Chem. Soc.* **2003**, *125*, 3678−3679.
(216) Mukerjee, S.; Stassinopoulos, A.; Caradonna, J. P. *J. Am. Chem. Soc.* **1997**, *119*, 8097−8098.
(217) Roth, J. P.; Yoder, J. C.; Won, T.-J.; Mayer, J. M. *Science* **2001**, *294*, 2524−2526.
(218) Yoder, J. C.; Roth, J. P.; Gussenhoven, E. M.; Larsen, A. S.; Mayer, J. M. *J. Am. Chem. Soc.* **2003**, *125*, 2629−2640.
(219) Mader, E. A.; Larsen, A. S.; Mayer, J. M. *J. Am. Chem. Soc.* **2004**, *126*, 8066−8067.
(220) Meyer, T. J.; Huynh, M. H. V. *Inorg. Chem.* **2003**, *42*, 8140−8160.
(221) Chang, C. J.; Chang, M. C. Y.; Damrauer, N. H.; Nocera, D. G. *Biochim. Biophys. Acta* **2004**, *1655*, 13−28.
(222) Mayer, J. M.; Rhile, R. J. *Biochim. Biophys. Acta* **2004**, *1655*, 51−58.
(223) Weiss, J. *Experientia* **1953**, *9*, 61−62.
(224) Purmal, A. P.; Skurlatov, Y. I.; Travin, S. O. *Izv. Akad. Nauk SSSR, Ser. Khim.* **1980**, 492−497.
(225) Hashimoto, K.; Nagatomo, S.; Fujinami, S.; Furutachi, H.; Ogo, S.; Suzuki, M.; Uehare, A.; Maeda, Y.; Watanabe, Y.; Kitagawa, T. *Angew. Chem., Int. Ed.* **2002**, *41*, 1202−1204.
(226) Mairata i Payeras, A.; Ho, R. Y. N.; Fujita, M.; Que, L., Jr. *Chem.−Eur. J.* **2004**, *10*, 4944−4953.
(227) Logager, T.; Holcman, J.; Sehested, K.; Pedersen, T. *Inorg. Chem.* **1992**, *31*, 3523−3529.
(228) Pestovsky, O.; Bakac, A. *J. Am. Chem. Soc.* **2004**, *126*, 13757−13764.
(229) Jacobsen, F.; Holcman, J.; Sehested, K. *Int. J. Chem. Kinet.* **1997**, 17−24.
(230) Jacobsen, F.; Holcman, J.; Sehested, K. *Int. J. Chem. Kinet.* **1998**, *30*, 215−221.
(231) Mártire, D. O.; Caregnato, P.; Furlong, J.; Allegretti, P.; Gonzalez, M. C. *Int. J. Chem. Kinet.* **2002**, *34*, 488−494.
(232) Collins, T. J.; Kostka, K. L.; Münck, E.; Uffelman, E. S. *J. Am. Chem. Soc.* **1990**, *112*, 5637−5639.
(233) Cummins, C. C.; Schrock, R. R. *Inorg. Chem.* **1994**, *33*, 395−396.
(234) Betley, T. A.; Peters, J. C. *J. Am. Chem. Soc.* **2004**, *126*, 6252−6254.
(235) Zang, V.; van Eldik, R. *Inorg. Chem.* **1990**, *29*, 1705−1711.
(236) Seibig, S.; van Eldik, R. *Inorg. Chem.* **1997**, *36*, 4115−4120.
(237) Bull, C.; McClune, G. J.; Fee, J. A. *J. Am. Chem. Soc.* **1983**, *105*, 5290−5300.
(238) Borggard, O. K.; Farver, O.; Andersen, V. S. *Acta Chem. Scand.* **1971**, *25*, 3541−3543.
(239) Seibig, S.; van Eldik, R. *Eur. J. Inorg. Chem.* **1999**, 447−454.
(240) Seibig, S.; van Eldik, R. *Inorg. React. Mech.* **1999**, *1*, 91−105.
(241) Schneppensieper, T.; Wanat, A.; Stochel, G.; van Eldik, R. *Inorg. Chem.* **2002**, *41*, 2565−2573.

(242) Schneppensieper, T.; Wanat, A.; Stochel, G.; Goldstein, S.; Meyerstein, D.; van Eldik, R. *Eur. J. Inorg. Chem.* **2001**, 2317−2325.
(243) Schneppensieper, T.; Finkler, S.; Czap, A.; van Eldik, R.; Heus, M.; Nieuwenhuizen, P.; Wreesmann, C.; Abma, W. *Eur. J. Inorg. Chem.* **2001**, 491−501.
(244) Ilan, Y.; Czapski, G. *Biochim. Biophys. Acta* **1977**, *498*, 386-394.
(245) Butler, J.; Halliwell, B. *Arch. Biochem. Biophys.* **1982**, *218*, 174−178.
(246) Cheng, K. L.; Lott, P. F. *Anal. Chem.* **1956**, *28*, 462−465.
(247) Horner, O.; Jeandey, C.; Oddou, J.-L.; Bonville, P.; Latour, J.-M. *Eur. J. Inorg. Chem.* **2002**, 1186−1189.
(248) Ahmad, S.; McCallum, J. D.; Shiemke, A. K.; Appelman, E. H.; Loehr, T. M.; Sanders-Loehr, J. *Inorg. Chem.* **1988**, *27*, 2230−2233.
(249) Brausam, A.; van Eldik, R. *Inorg. Chem.* **2004**, *43*, 5351−5359.
(250) Walling, C. *Acc. Chem. Res.* **1975**, *8*, 125−131.
(251) Francis, K. C.; Cummins, D.; Oakes, J. *J. Chem. Soc., Dalton Trans.* **1985**, 493−501.
(252) van Eldik, R.; Klarner, F.-G. *High-Pressure Chemistry: Synthetic, Mechanistic, and Supercritical Applications*; Wiley-VCH: Weinheim, Germany, 2003.
(253) *High-Pressure Chemistry*; van Eldik, R., Klärner, F.-G., Eds.; Wiley-VCH: Weinheim, Germany, 2002.
(254) Stochel, G.; van Eldik, R. *Coord. Chem. Rev.* **1999**, *187*, 329−374.
(255) Macyk, J.; van Eldik, R. *Biochim. Biophys. Acta* **2002**, *1595*, 283−296.
(256) Schneppensieper, T.; Seibig, S.; Zahl, A.; Tregloan, P.; van Eldik, R. *Inorg. Chem.* **2001**, *40*, 3570−3676.
(257) Swaddle, T. W.; Merbach, A. E. *Inorg. Chem.* **1981**, *20*, 4212−4216.
(258) Grant, M.; Jordan, R. B. *Inorg. Chem.* **1981**, *20*, 55−60.
(259) Ivanovic-Burmazovic, I.; Hamza, M. S. A.; van Eldik, R. *Inorg. Chem.* **2002**, *41*, 5150−5161.
(260) Sharma, V. K.; Millero, F. J.; Hommonay, Z. *Inorg. Chim. Acta* **2004**, *357*, 3583−3587.
(261) Schrodt, A.; van Eldik, R. *Inorg. React. Mech.* **1998**, *1*, 57−64.
(262) Kimura, E.; Kodama, M.; Machida, R.; Ishizu, K. *Inorg. Chem.* **1982**, *21*, 595−602.
(263) Nam, W.; Ho, R. Y. N.; Valentine, J. S. *J. Am. Chem. Soc.* **1991**, *113*, 7052−7054.
(264) Nam, W.; Kim, H. J.; Kim, S. H.; Ho, R. Y. N.; Valentine, J. S. *Inorg. Chem.* **1996**, *35*, 1045−1049.
(265) Mountford, H. S.; Spreer, L. O.; Otvos, J. W.; Calvin, M.; Brewer, K. J.; Richter, M.; Scott, B. *Inorg. Chem.* **1992**, *31*, 717−718.
(266) Suh, M. P.; Kong, G.-Y.; Kim, I.-S. *Bull. Korean Chem. Soc.* **1993**, *14*, 439−444.
(267) Chan, P.-K.; Poon, C.-K. *J. Chem. Soc., Dalton Trans.* **1976**, 858−862.
(268) Kist, L. T.; Trujillo, J. F.; Szpoganicz, B.; Manez, M. A.; Basallote, M. G. *Polyhedron* **1997**, *16*, 3827−3833.
(269) Buchalova, M.; Busch, D. H.; van Eldik, R. *Inorg. Chem.* **1998**, *37*, 1116−1120.
(270) Buchalova, M.; Warburton, P. A.; van Eldik, R.; Busch, D. H. *J. Am. Chem. Soc.* **1997**, *119*, 5867−5876.
(271) Buchalova, M. Ph.D., University of Kansas, 1997.
(272) Busch, D. H.; Zimmer, L. L.; Grzybowski, J. J.; Olszanski, D. J.; Jackels, S. C.; Callahan, R. C.; Christoph, G. G. *Proc. Natl. Acad. Sci. U.S.A.* **1981**, *78*, 5919.
(273) Gibson, Q. H.; Smith, M. H. *Proc. R. Soc.* **1965**, *163*, 206.
(274) Collman, J. P.; Herrmann, P. C.; Fu, L.; Eberspacher, T. A.; Eubanks, M.; Boitrel, B.; Hayoz, P.; Zhang, X.; Brauman, J. I.; Day, V. W. *J. Am. Chem. Soc.* **1997**, *119*, 3481.
(275) Zhang, X.; Zhang, D.; Busch, D. H.; van Eldik, R. *J. Chem. Soc., Dalton Trans.* **1999**, 2751−2758.
(276) Rush, J. D.; Koppenol, W. H. *J. Am. Chem. Soc.* **1988**, *110*, 4957−4963.
(277) Szulbinski, W. S.; Warburton, R.; Busch, D. H. *Inorg. Chem.* **1993**, *32*, 5368−5376.
(278) Szulbinski, W. S.; Busch, D. H. *Inorg. Chim. Acta* **1995**, *234*, 143−148.
(279) Seo, M. S.; In, J.-H.; Kim, S. O.; Oh, N. Y.; Hong, J.; Kim, J.; Que, L., Jr.; Nam, W. *Angew. Chem., Int. Ed.* **2004**, *43*, 2417−2420.
(280) Berndou, J.; Fabiano, A.-S.; Robert, A.; Meunier, B. *J. Am. Chem. Soc.* **1994**, *116*, 9375−9376.
(281) Funabiki, T.; Mizoguchi, A.; Suigimoto, T.; Tada, S.; Tsugi, M.; Sakamoto, H.; Yoshida, S. *J. Am. Chem. Soc.* **1986**, *108*, 2921−2932.
(282) Dei, A.; Gatteschi, D.; Pardi, L. *Inorg. Chem.* **1993**, *32*, 1389−1395.
(283) Ito, M.; Que, L., Jr. *Angew. Chem., Int. Ed.* **1997**, *36*, 1342−1344.
(284) Lin, G.; Reid, G.; Bugg, T. D. H. *Chem. Commun.* **2000**, 1119−1120.
(285) Lin, G.; Reid, G.; Bugg, T. D. H. *J. Am. Chem. Soc.* **2001**, *123*, 5030−5039.
(286) Koch, W. O.; Krüger, H.-J. *Angew. Chem., Int. Ed. Engl.* **1995**, *34*, 2671−2674.
(287) Koch, W. O.; Schünemann, V.; Gerdan, M.; Trautwein, A. X.; Krüger, H.-J. *Chem.—Eur. J.* **1998**, *4*, 1255−1265.
(288) Raffard, N.; Carina, R.; Simaan, A. J.; Sainton, J.; Riviere, E.; Tchertanov, L.; Bourcier, S.; Bouchoux, G.; Delroisse, M.; Banse, F.; Girerd, J.-J. *Eur. J. Inorg. Chem.* **2001**, 2249−2254.
(289) Ménage, S.; Wilkinson, E. C.; Que, L., Jr.; Fontecave, M. *Angew. Chem., Int. Ed. Engl.* **1995**, *34*, 203−205.
(290) Ménage, S.; Vincent, J. M.; Lambeaux, C.; Chottard, G.; Grand, A.; Fontecave, M. *Inorg. Chem.* **1993**, *32*, 4766−4773.
(291) Ménage, S.; Vincent, J. M.; Lambeaux, C.; Fontecave, M. *J. Chem. Soc., Dalton Trans.* **1994**, 2081−2084.
(292) Sobolev, A. P.; Babushkin, D. E.; Talsi, E. P. *J. Mol. Catal. A* **2000**, *159*, 233−245.
(293) Legros, J.; Bolm, C. *Angew. Chem., Int. Ed.* **2004**, *43*, 4225−4228.
(294) Kitajima, N.; Fukui, H.; Moro-oka, Y.; Mizutani, Y.; Kitagawa, T. J. *J. Am. Chem. Soc.* **1990**, *112*, 6402−6403.
(295) Kitajima, N.; Tamura, N.; Amagai, H.; Fukui, H.; Moro-oka, Y.; Mizutani, Y.; Kitagawa, T.; Mathur, R.; Heerwegh, K.; Reed, C. A.; Randall, C. R.; Que, L., Jr.; Tatsumi, K. *J. Am. Chem. Soc.* **1994**, *116*, 9071−9085.
(296) Mehn, M. P.; Fujisawa, K.; Hegg, E. L.; Que, L., Jr. *J. Am. Chem. Soc.* **2003**, *125*, 7828−7842.
(297) Ha, E. H.; Ho, R. Y. N.; Kisiel, J. F.; Valentine, J. S. *Inorg. Chem.* **1995**, *34*, 2265−2266.
(298) Hikichi, S.; Ogihara, T.; Fujisawa, K.; Kitajima, N.; Akita, M.; Moro-oka, Y. *Inorg. Chem.* **1997**, *36*, 4539−4547.
(299) Hegg, E. L.; Ho, R. Y. N.; Que, L., Jr. *J. Am. Chem. Soc.* **1999**, *121*, 1972−1973.
(300) Sivasubramanian, V. K.; Ganesan, M.; Rajagopal, S.; Ramaraj, R. *J. Org. Chem.* **2002**, *67*, 1506−1514.
(301) Bryliakov, K. P.; Talsi, E. P. *Angew. Chem., Int. Ed.* **2004**, *43*, 5228−5230.
(302) Arai, T.; Shinozuka, K.; Sawai, H. *Bull. Chem. Soc. Jpn.* **1998**, *71*, 1159−1169.
(303) Jang, H. G.; Cox, D. D.; Que, L., Jr. *J. Am. Chem. Soc.* **1991**, *113*, 9200−9204.
(304) Paskali, M.; Duda, M.; Schweppe, F.; Zurlinden, K.; Müller, F. K.; Krebs, B. *J. Chem. Soc., Dalton Trans.* **2001**, 828−837.
(305) Duda, M.; Pascaly, M.; Krebs, B. *J. Chem. Soc., Chem. Commun.* **1997**, 835−836.
(306) Merkel, M.; Schnieders, D.; Baldeau, S. M.; Krebs, B. *Eur. J. Inorg. Chem.* **2004**, 783−790.
(307) Velusami, M.; Mayilmurugan, R.; Palaniandavar, M. *Inorg. Chem.* **2004**, *43*, 6284−6293.
(308) Cox, D. D.; Que, L., Jr. *J. Am. Chem. Soc.* **1988**, *110*, 8085−92.
(309) Merkel, M.; Pascaly, M.; Krebs, B.; Astner, J.; Foxon, S. P.; Schindler, S. *Inorg. Chem.*, submitted.
(310) Foxon, S. P.; Walter, O.; Schindler, S. *Eur. J. Inorg. Chem.* **2002**, 111−121.
(311) Schatz, M.; Becker, M.; Thaler, F.; Hampel, F.; Schindler, S.; Jacobson, R. R.; Tyeklar, Z.; Murthy, N. N.; Ghosh, P.; Chen, Q.; Zubieta, J.; Karlin, K. D. *Inorg. Chem.* **2001**, *40*, 2312−2322.
(312) Funabiki, T.; Yamazaki, T.; Fukui, A.; Tanaka, T.; Yoshida, S. *Angew. Chem., Int. Ed.* **1998**, *37*, 513−515.
(313) Jo, D.-H.; Chiou, Y.-M.; Que, L., Jr. *Inorg. Chem.* **2001**, *40*, 3181−3190.
(314) Chiou, Y.-M.; Que, L., Jr. *J. Am. Chem. Soc.* **1995**, *117*, 3999−4013.
(315) Kim, J.; Zang, Y.; Costas, M.; Harrison, R. G.; Wilkinson, E. C.; Que, L., Jr. *J. Biol. Inorg. Chem.* **2001**, *6*, 275−284.
(316) Jensen, M. P.; Lange, S. J.; Mehn, M. P.; Que, E. L.; Que, L., Jr. *J. Am. Chem. Soc.* **2003**, *125*, 2113−2128.
(317) Kim, C.; Chen, K.; Que, L., Jr. *J. Am. Chem. Soc.* **1997**, *119*, 5964−5965.
(318) Lobanova, M. V.; Bryliakov, K. P.; Duban, E. A.; Talsi, E. P. *Mendeleev Commun.* **2003**, 175−177.
(319) Weitzer, M.; Schindler, S.; Brehm, G.; Schneider, S.; Hoermann, E.; Jung, B.; Kaderli, S.; Zuberbuehler, A. D. *Inorg. Chem.* **2003**, *42*, 1800−1806.
(320) Schatz, M.; Raab, V.; Foxon, S. P.; Brehm, G.; Schneider, S.; Reiher, M.; Holthausen, M. C.; Sundermeyer, J.; Schindler, S. *Angew. Chem., Int. Ed.* **2004**, *43*, 4360−4363.
(321) MacBeth, C. E.; Golombek, A. P.; Young, V. G., Jr.; Yang, C.; Kuczera, K.; Hendrich, M. P.; Borovik, A. S. *Science* **2000**, *289*, 938−941.
(322) Gupta, R.; Borovik, A. S. *J. Am. Chem. Soc.* **2003**, *125*, 13234−13242.
(323) Mandel, J. B.; Maricondi, C.; Douglas, B. E. *Inorg. Chem.* **1988**, *27*, 2990−2996.
(324) Weitzer, M.; Schatz, M.; Hampel, F.; Heinemann, F. W.; Schindler, S. *J. Chem. Soc., Dalton Trans.* **2002**, 686−694.
(325) Schatz, M.; Leibold, M.; Foxon, S. P.; Weitzer, M.; Heinemann, F. W.; Hampel, F.; Walter, O.; Schindler, S. *J. Chem. Soc., Dalton Trans.* **2003**, 1480−1487.

(326) Horner, O.; Anxolabehere-Mallart, E.; Charlot, M.-F.; Tchertanov, C. L.; Guilhem, J.; Mattioli, T. A.; Boussac, A.; Girerd, J.-J. *Inorg. Chem.* **1999**, *38*, 1222−1232.
(327) Hazell, A.; McKenzie, C. J.; Nielsen, L. P.; Schindler, S.; Weitzer, M. *J. Chem. Soc., Dalton Trans.* **2002**, 310−317.
(328) Bernal, I.; Jensen, I. M.; Jensen, K. B.; McKenzie, C. J.; Toftlund, H.; Tuchagues, J.-P. *J. Chem. Soc., Dalton Trans.* **1995**, 3667−3675.
(329) Jensen, K. B.; McKenzie, C. J.; Nielsen, L. P.; Pedersen, J. Z.; Svendsen, H. M. *J. Chem. Soc., Chem. Commun.* **1999**, 1313−1314.
(330) Simaan, A. J.; Dopner, S.; Banse, F.; Bourcier, S.; Bouchoux, G.; Boussac, A.; Hildebrandt, P.; Girerd, J.-J. *Eur. J. Inorg. Chem.* **2000**, 1627−1633.
(331) Simaan, A. J.; Banse, F.; Mialane, P.; Boussac, A.; Un, S.; Kargar-Grisel, T.; Bouchoux, G.; Girerd, J.-J. *Eur. J. Inorg. Chem.* **1999**, 993−996.
(332) Horner, O.; Jeandey, C.; Oddou, J.-L.; Bonville, P.; McKenzie, C. J.; Latour, J.-M. *Eur. J. Inorg. Chem.* **2002**, 3278−3283.
(333) Balland, V.; Banse, F.; Anxolabehere-Mallart, E.; Chiladi, M.; Mattioli, T. A.; Philouze, C.; Blondin, G.; Girerd, J.-J. *Inorg. Chem.* **2003**, *42*, 2470−2477.
(334) Shearer, J.; Scarrow, R. C.; Kovacs, J. A. *J. Am. Chem. Soc.* **2002**, *124*, 11709−11717.
(335) Roelfes, G.; Lubben, M.; Hage, R.; Que, L., Jr.; Feringa, B. L. *Chem.*−*Eur. J.* **2000**, *6*, 2152−2159.
(336) van den Berg, T. A.; de Boer, J. W.; Browne, W. R.; Roelfes, G.; Feringa, B. L. *Chem. Commun.* **2004**, 2550−2551.
(337) Roelfes, G.; Vrajmasu, V.; Chen, K.; Ho, R. Y. N.; Rohde, J.-U.; Zondervan, C.; la Crois, R. M.; Schudde, E. P.; Lutz, M.; Spek, A. L.; Hage, R.; Feringa, B. L.; Münck, E.; Que, L., Jr. *Inorg. Chem.* **2003**, *42*, 2639−2653.
(338) Bukowski, M. R.; Comba, P.; Limberg, C.; Merz, M.; Que, L., Jr.; Wistuba, T. *Angew. Chem., Int. Ed.* **2004**, *116*, 1283−1287.
(339) Payne, S. C.; Hagen, K. S. *J. Am. Chem. Soc.* **2000**, *122*, 6399−6410.
(340) Chavez, F. A.; Ho, R. Y. N.; Pink, M.; Young, V. G., Jr.; Kryatov, S. V.; Rybak-Akimova, E. V.; Andres, H.; Münck, E.; Que, L., Jr.; Tolman, W. B. *Angew. Chem., Int. Ed.* **2002**, *41*, 149−152.
(341) He, C.; Barrios, A. M.; Lee, D.; Kuzelka, J.; Davydov, R. M.; Lippard, S. J. *J. Am. Chem. Soc.* **2000**, *122*, 12683−12690.
(342) Mizoguchi, T. J.; Kuzelka, J.; Spingler, B.; DuBois, J. L.; Davydov, R. M.; Hedman, B.; Hodgson, K. O.; Lippard, S. J. *Inorg. Chem.* **2001**, *40*, 4662−4673.
(343) Duboc-Toia, C.; Ménage, S.; Ho, R. Y. N.; Que, L., Jr.; Lambeaux, C.; Fontecave, M. *Inorg. Chem.* **1999**, *38*, 1261−1268.
(344) Mekmouche, Y.; Hummel, H.; Ho, R. Y. N.; Que, L., Jr.; Schunemann, V.; Thomas, F.; Trautwein, A. X.; Lebrun, C.; Gorgy, K.; Lepretre, J. C.; Collomb, M. N.; Deronzier, A.; Fontecave, M.; Ménage, S. *Chem.*−*Eur. J.* **2002**, *8*, 1196−1204.
(345) Costas, M.; Cady, C. W.; Kryatov, S. V.; Ray, M.; Ryan, M. J.; Rybak-Akimova, E. V.; Que, L., Jr. *Inorg. Chem.* **2003**, *42*, 7519−7530.
(346) Kryatov, S. V.; Rybak-Akimova, E. A. *J. Chem. Soc., Dalton Trans.* **1999**, 3335−3336.
(347) MacMurdo, V. L.; Zheng, H.; Que, L., Jr. *Inorg. Chem.* **2000**, *39*, 2254−2255.
(348) Westerheide, L.; Müller, F. K.; Than, R.; Krebs, B.; Dietrich, J.; Schindler, S. *Inorg. Chem.* **2001**, *40*, 1951−1961.
(349) Yoon, S.; Lippard, S. J. *Inorg. Chem.* **2003**, *42*, 8606−8608.
(350) Kuzelka, J.; Mukhopadhyay, S.; Spingler, B.; Lippard, S. J. *Inorg. Chem.* **2003**, *42*, 6447−6457.
(351) Kryatov, S. V.; Taktak, S.; Korendovych, I. V.; Rybak-Akimova, E. V.; Kaizer, J.; Stéphane Torelli, S.; Shan, X.; Mandal, S.; MacMurdo, V.; Mairata i Payeras, A.; Que, L., Jr. *Inorg. Chem.* **2005**, *44*, 85−99.
(352) Reynolds, R. A.; Dunham, W. R.; Coucouvanis, D. *Inorg. Chem.* **1998**, *37*, 1232−1241.
(353) Dong, Y.; Ménage, S.; Brennan, B. A.; Elgren, T. E.; Jang, H. G.; Pearce, L. L.; Que, L., Jr. *J. Am. Chem. Soc.* **1993**, *115*, 1851−1859.
(354) Hayashi, Y.; Suzuki, M.; Uehara, A.; Mizutani, Y.; Kitagawa, T. *Chem. Lett.* **1992**, 91−94.
(355) Brennan, B. A.; Chen, Q.; Juarez-Garsia, C.; True, A. E.; O'Connor, C. J.; Que, L., Jr. *Inorg. Chem.* **1991**, *30*, 1937−1943.
(356) Watton, S. P.; Masschelein, A.; Rebek, J., Jr.; Lippard, S. J. *J. Am. Chem. Soc.* **1994**, *116*, 5196−5205.
(357) Lee, D.; Lippard, S. J. *J. Am. Chem. Soc.* **1998**, *120*, 12153−12154.
(358) Lee, D.; Lippard, S. J. *Inorg. Chem.* **2002**, *41*, 2704−2719.
(359) Yoon, S.; Lippard, S. J. *J. Am. Chem. Soc.* **2004**, *126*, 2666−2667.
(360) Lee, D.; Krebs, C.; Huynh, B. H.; Hendrich, M. P.; Lippard, S. J. *J. Am. Chem. Soc.* **2000**, *122*, 5000−5001.
(361) Lee, D.; Lippard, S. J. *Inorg. Chem.* **2002**, *41*, 827−837.
(362) Moreira, R. F.; Tshuva, E. Y.; Lippard, S. J. *Inorg. Chem.* **2004**, *43*, 4427−4434.
(363) Tshuva, E. Y.; Lee, D.; Bu, W. M.; Lippard, S. J. *J. Am. Chem. Soc.* **2002**, *124*, 2416−2417.
(364) Wilkinson, E. C.; Dong, Y.; Zang, Y.; Fujii, H.; Fraczkiewicz, R.; Fraczkiewicz, G.; Czernuszewicz, R. S.; Que, L., Jr. *J. Am. Chem. Soc.* **1998**, *120*, 955−962.
(365) Kryatov, S. V.; Rybak-Akimova, E. V.; MacMurdo, V. L.; Que, L., Jr. *Inorg. Chem.* **2001**, *40*, 2220−2228.
(366) Peover, M. E.; White, B. S. *J. Chem. Soc., Chem. Commun.* **1965**, 183−184.
(367) Ruiz, J.; Astruc, D. *C. R. Acad. Sci., Ser. IIc* **1998**, *1*, 21−27.
(368) Mizuta, T.; Wang, J.; Miyoshi, K. *Inorg. Chim. Acta* **1995**, *230*, 119−125.
(369) Brunold, T. C.; Tamura, N.; Kitajima, N.; Moro-oka, Y.; Solomon, E. I. *J. Am. Chem. Soc.* **1998**, *120*, 5674−5690.
(370) Kryatov, S. V.; Nazarenko, A. Y.; Robinson, P. D.; Rybak-Akimova, E. V. *Chem. Commun.* **2000**, 921−922.
(371) Kim, C.; Dong, Y.; Que, L., Jr. *J. Am. Chem. Soc.* **1997**, *119*, 3635−3636.
(372) Leising, R. A.; Brennan, B. A.; Que, L., Jr.; Fox, B. G.; Münck, E. *J. Am. Chem. Soc.* **1991**, *113*, 3988−3990.
(373) Rybak-Akimova, E. V.; Kryatov, S. V.; Herrera, A. M. *J. Inorg. Biochem.* **2001**, *86*, 414.
(374) Kodera, M.; Taniike, Y.; Itoh, M.; Tanahashi, Y.; Shimakoshi, H.; Kano, K.; Hirota, S.; Lijima, S.; Ohba, M.; Okawa, H. *Inorg. Chem.* **2001**, *40*, 4821−4822.
(375) Hummel, H.; Mekmouche, Y.; Duboc-Toia, C.; Ho, R. Y. N.; Que, L., Jr.; Schünemann, V.; Thomas, F.; Trautwein, A. X.; Lebrun, C.; Fontecave, M.; Ménage, S. *Angew. Chem., Int. Ed.* **2002**, *41*, 617−620.
(376) van Eldik, R. *Inorg. Chem.* **2004**, *43*, 2756−2758.
(377) Schmid, R.; Sapunov, V. N. *Nonformal Kinetics*; Verlag Chemie: Weinheim, 1982.
(378) Wilkins, R. G. *Kinetics and mechanisms of reactions of transition metal complexes*; VCH Publishers: Weinheim, 1991.
(379) Basolo, F.; Pearson, R. G. *Mechanisms of Inorganic Reactions*, 2nd ed.; Wiley: New York, 1967.
(380) Brown, S. B.; Jones, P.; Suggett, A. *Prog. Inorg. Chem.* **1970**, *13*, 159−204.
(381) Chaffee, E.; Edwards, J. O. *Prog. Inorg. Chem.* **1970**, *13*, 205−242.
(382) Langford, C. H.; Gray, H. B. *Ligand Substitution Processes*; W. A. Benjamin, Inc.: New York, 1965.
(383) Taube, H. *Prog. Inorg. Chem.* **1986**, *34*, 607−625.
(384) van Eldik, R. *Coord. Chem. Rev.* **1999**, *182*, 373−410.
(385) Jordan, R. B. *Reaction Mechanisms of Inorganic and Organometallic Systems*; Oxford University Press: New York, 1991.
(386) Atwood, J. D. *Inorganic and Organometallic Reaction Mechanisms*; VCH: New York, 1997.
(387) Tobe, M. L.; Burgess, J. *Inorganic Reaction Mechanisms*; Longman: Harlow, Essex, England, 1999.
(388) Schindler, S.; Hubbard, C. D.; van Eldik, R. *Chem. Soc. Rev.* **1998**, *27*, 387−393.
(389) Kim, J. H.; Dong, Y. H.; Larka, E.; Que, L., Jr. *Inorg. Chem.* **1996**, *35*, 2369−2372.
(390) Lane, B. S.; Burgess, K. *J. Am. Chem. Soc.* **2001**, *123*, 2933−2934.
(391) *Oxygen and Ozone*; Battino, R., Ed.; Pergamon Press: New York, 1981; Vol. 7.
(392) Battino, R.; Clever, H. L. *Chem. Rev.* **1966**, *66*, 395−463.
(393) Kretschmer, C. B.; Nowakowska, J.; Wiebe, R. *Ind. Eng. Chem.* **1946**, *38*, 506−509.
(394) Klinman, J. P. *J. Biol. Inorg. Chem.* **2001**, *6*, 1−13.
(395) *CRC Handbook of Chemistry and Physics*, 79th ed.; Lide, D. R., Ed.; CRC Press: New York, 1998.
(396) Karlin, K. D.; Nasir, M. S.; Cohen, B. I.; Cruse, R. W.; Kaderli, S.; Zuberbühler, A. D. *J. Am. Chem. Soc.* **1994**, *116*, 1324−1336.
(397) Sinn, E.; Matthes, K.; Naumann, E. *Wiss. Z.*−*Friedrich-Shiller-Univ. Jena, Math.-Naturwiss. Reiche* **1967**, *16*, 523−529.
(398) Lühring, P.; Schumpe, A. *J. Chem. Eng. Data* **1989**, *34*, 250−252.
(399) Sawyer, D. T.; Chieriacato, G., Jr.; Angelis, C. T.; Nanni, E. J., Jr.; Tsuchiya, T. *Anal. Chem.* **1982**, *54*, 1720−1724.
(400) Achord, J. M.; Hussey, C. L. *Anal. Chem.* **1980**, *52*, 601−602.
(401) Karlin, K. D.; Wei, N.; Jung, B.; Kaderli, S.; Niklaus, P.; Zuberbühler, A. D. *J. Am. Chem. Soc.* **1993**, *115*, 9506−9514.
(402) Mahapatra, S.; Kaderli, S.; Llobet, A.; Neuhold, Y.-M.; Palanché, T.; Halfen, J. A.; Young, V. G., Jr.; Kaden, T.; Que, L., Jr.; Zuberbühler, A. D.; Tolman, W. B. *Inorg. Chem.* **1997**, *36*, 6343−6356.

CR030709Z